

**The *Rhizobium leguminosarum* Norway -  
*Lotus burtii* interaction as a model for  
studying how rhizobia enter plant cells**

---

Dissertation zur Erlangung des Doktorgrades der Naturwissenschaften  
Doctor rerum naturalium (Dr. rer. nat.) an der Fakultät für Biologie der  
Ludwig-Maximilians-Universität München

---

**Juan Liang**  
München, July 2020



---

1. Gutachter: Dr. Macarena Marín

2. Gutachter: Prof. Dr. Heinrich Jung

Tag der Abgabe: 21.07.2020

Tag der mündlichen Prüfung: 16.11.2020

---



## **Eidesstattliche Versicherung**

Hiermit versichere ich an Eides statt, dass die vorliegende Dissertation von mir selbstständig und ohne unerlaubte Hilfe angefertigt ist.

München, den 21.07.2020

---

Juan Liang

## **Erklärung**

Hiermit erkläre ich, dass die Dissertation nicht ganz oder in wesentlichen Teilen einer anderen Prüfungskommission vorgelegt worden ist. Ich habe nicht versucht, anderweitig eine Dissertation einzureichen oder mich einer Doktorprüfung zu unterziehen.

München, den 21.07.2020

---

Juan Liang

## Table of contents

<b>Publications originating from this work</b> .....	<b>1</b>
<b>Declaration of contribution as co-author</b> .....	<b>2</b>
<b>Abbreviations</b> .....	<b>3</b>
<b>Summary</b> .....	<b>5</b>
<b>General introduction</b> .....	<b>7</b>
<b>1. Overview of root nodule symbiosis</b> .....	<b>7</b>
<b>2. Surface colonisation of legume roots</b> .....	<b>9</b>
2.1 Chemotaxis and motility in the rhizosphere.....	9
2.2 Biofilms and root attachment.....	10
<b>3. Rhizobia signals in symbiotic interaction</b> .....	<b>11</b>
3.1 Nod factors .....	11
3.2 Extracellular polysaccharides.....	14
3.3 Type three secreted effectors.....	16
<b>4. Host perception and downstream signalling</b> .....	<b>16</b>
4.1 Nod factor signalling and the Common Symbiotic Pathway.....	17
4.2 Other symbiotic signalling .....	18
<b>5. Nodule organogenesis</b> .....	<b>18</b>
<b>6. Infection</b> .....	<b>20</b>
6.1 Infection thread-dependent mechanism .....	20
6.2 Alternative Infection mechanisms.....	21
6.3 Requirement of rhizobia signals in infection.....	22
<b>7. Natural diversity of rhizobia and legume interaction</b> .....	<b>23</b>
<b>Aims of the thesis</b> .....	<b>25</b>
<b>Results</b> .....	<b>26</b>
<b>Publication I:</b> .....	<b>26</b>
Complete genome of <i>Rhizobium leguminosarum</i> Norway, an ineffective <i>Lotus</i> micro-symbiont.....	26
Supplementary materials.....	38
<b>Publication II:</b> .....	<b>42</b>
A subcompatible <i>Rhizobium</i> strain reveals infection duality in <i>Lotus</i> .....	42
Supplementary materials.....	54
<b>General discussion</b> .....	<b>65</b>
<b>1. Infection thread-independent mechanisms</b> .....	<b>65</b>
<b>2. The internalisation process of <i>RI</i> Norway</b> .....	<b>67</b>
<b>3. Approaches to identify rhizobial genes involved in the internalisation process</b> 69	
<b>4. Nodulation incompatibility on <i>L. japonicus</i> Gifu</b> .....	<b>70</b>
<b>5. Synergistic effect of dual species root colonisation</b> .....	<b>72</b>
<b>6. General Conclusion</b> .....	<b>75</b>
<b>Appendix</b> .....	<b>76</b>

<b>Supplementary figures .....</b>	<b>76</b>
<b>Supplementary results .....</b>	<b>77</b>
1. <i>RI</i> Norway co-colonised <i>L. japonicus</i> Gifu nodules in the presence of <i>Mn</i> 10.2.2 .....	77
2. Co-colonisation by <i>RI</i> Norway and <i>Mn</i> 10.2.2 does not impair the growth of the host.....	78
3. <i>RI</i> Norway hitchhikes in the nodule independent of the infection thread.....	80
4. Co-inoculation of <i>Mn</i> 10.2.2 and <i>RI</i> Norway promotes root colonisation by both strains .....	83
5. Co-inoculation of <i>Mn</i> 10.2.2 and <i>RI</i> Norway promotes root colonisation of <i>L. japonicus</i> Gifu by both strains from a distal spot .....	86
6. <i>RI</i> Norway promotes motility of <i>Mn</i> 10.2.2 on a surface polysaccharide-dependent manner ..	88
7. <i>RI</i> Norway and <i>Mn</i> 10.2.2 can form mixed biofilms <i>in vitro</i> .....	90
<b>Supplementary materials and methods .....</b>	<b>94</b>
1. Bacterial strains and growth conditions.....	94
2. Plant growth and inoculation conditions .....	94
3. Bacteria isolation from nodules .....	96
4. Conjugation .....	96
5. Generation of the <i>pssA</i> and <i>exo5</i> gene deletion mutants .....	96
6. Biofilms quantification by 24-well plate .....	97
7. Biofilms quantification by glass chamber slide.....	97
8. Swarming assay.....	99
9. Histological staining and microscopy .....	99
10. Statistics and data visualisation .....	100
<b>References.....</b>	<b>101</b>
<b>List of figures .....</b>	<b>116</b>
<b>Acknowledgements .....</b>	<b>117</b>
<b>Curriculum vitae.....</b>	<b>119</b>





## Publications originating from this work

- **Liang J\***, Hoffrichter A\*, Brachmann A, Marín M (2018). Complete genome of *Rhizobium leguminosarum* Norway, an ineffective *Lotus* micro-symbiont, *Stand Genomic Sci*, 13:36

\* These authors contributed equally to the work

- **Liang J**, Klingl A, Lin Y, Boul E, Thomas-Oates J, Marín M. (2019). A subcompatible *Rhizobium* strain reveals infection duality in *Lotus*, *J Exp Bot*, 70, pp. 1903-1913
- Venado RE, **Liang J**, Marín M (2020). Chapter Four - Rhizobia infection, a journey to the inside of plant cells. In *Adv Bot Res*, eds. Frendo P, Frugier F, Masson-Boivin C (ed.) *Regulation of Nitrogen-Fixing Symbioses in Legumes*, 94, pp. 97-118, Academic Press

## Declaration of contribution as co-author

### Publication I:

**Liang J\***, Hoffrichter A\*, Brachmann A, Marín M (2018). Complete genome of *Rhizobium leguminosarum* Norway, an ineffective *Lotus* micro-symbiont, *Stand Genomic Sci*, 13:36

\* These authors contributed equally to the work

In this publication, Brachmann A sequenced and annotated the genome of the strain. Hoffrichter A conducted the genome assembly and comparisons and presented the results in Fig 3, Fig 4, Fig S2, Table 3, Table 4, Table 5, Table S2. Marín M conducted the phylogenetic analysis and manual inspection of the annotation. I performed the imaging, chemotaxonomic analysis, DNA extraction and plant phenotype. I presented the results in Fig. 1, Fig. S1, Table S1.

### Publication II:

**Liang J**, Klingl A, Lin Y, Boul E, Thomas-Oates J, Marín M. (2019). A subcompatible *Rhizobium* strain reveals infection duality in *Lotus*, *J Exp Bot*, 70, pp. 1903–1913

In this publication, Klingl A performed the TEM imaging. Boul E conducted the structural analysis of the Nod factors. Lin Y and I conducted the qRT-PCR. Marín M and I conducted the root hair phenotyping and wrote the manuscript. I performed the plant phenotyping, mutation generation, data quantification. I presented the results in Fig. 1, Fig. 2e, f, Fig. 3, Fig. 4, Fig. 6, Fig. S1 - S4.

Signature of supervisor

---

Dr. Macarena Marín

Signature of student

---

Juan Liang

## Abbreviations

°C	Degree(s) celsius
3D	Three dimensional
ALA	5-aminolevulinic acid
ASL	Asymmetric leaves 2-like
bp	Base pair
bv.	Biovar
CCaMK	Calcium calmodulin dependent kinase
CLSM	Confocal laser scanning microscopy
dpi	Days post-inoculation
DsRed	<i>Discosoma sp.</i> red fluorescent protein
EPR3	Exopolysaccharide receptor 3
EPS	Exopolysaccharide
ERN1	Ethylene responsive factor required for nodulation 1
ETI	Effector-triggered immunity
GFP	Green fluorescent protein
GlcNAc	$\beta$ -1,4-linked N-acetyl glucosamine
GUS	$\beta$ -glucuronidase
GWAS	Genome-wide association study
KPS	Capsular polysaccharides
LB	Luria-Bertani broth
LBD	Lateral organ boundaries domain
LPS	Lipopolysaccharides
LYK3	Lysin motif receptor-like kinase 3
LysM	Lysin motif
MAMP	Microbe-associated molecular pattern
MAPK	Mitogen-activated protein kinase
<i>Mn</i>	<i>Mesorhizobium norvegicum</i>
NGS	Next generation sequencing
NFP	Nod factor perception
NFR1	Nod factor receptor 1
NFR5	Nod factor receptor 5

NIN	Nodule inception
Nod	Nodulation
Nops	Nodulation outer proteins
NPL	Nodulation pectate lyase
NUP	Nucleoporin
OD	Optical density
PHB	Poly- $\beta$ -hydroxybutyrate
qRT-PCR	Quantitative reverse transcription polymerase chain reaction
R protein	Resistance protein
Raps	Rhizobia adhering proteins
<i>Rl</i>	<i>Rhizobium leguminosarum</i>
ROS	Reactive oxygen species
SD	Standard deviation
SEM	Scanning electron microscopy
SYMREM1	Symbiotic remorin 1
SYMRK	Symbiosis receptor-like kinase
T1SS	Type 1 secretion system
T3Es	Type 3 secreted effectors
T3SS	Type 3 secretion system
T4SS	Type 4 secretion system
T5SS	Type 5 secretion system
T6SS	Type 6 secretion system
TCA	Tricarboxylic acid
TEM	Transmission electron microscopy
Tnseq	Transposon insertion sequencing
TY	Tryptone yeast
wpi	Week post-inoculation
$\Delta$	Delta
$\mu$	Micro

## Summary

Nitrogen-fixing rhizobia bacteria engage in a mutualistic symbiosis with legume plants. One of the defining features of this symbiosis is the formation of organs called nodules on the roots of the hosts. Establishment of an efficient interaction requires sophisticated and bidirectional communication between the host and the microsymbiont. The perception of the rhizobial signals by the host leads to the internalisation of rhizobia on the growing root nodule after the epidermal penetration and cortical spreading steps. The perception of rhizobial signal in the early stages has been extensively explored, however, the internalisation mechanism is still under investigation. This is caused by the lack of genetically amenable systems to study. Plant made tubular like structures, called infection threads are formed during rhizobia infection of host cells. A system that can uncouple infection thread formation and host cell infection will be suitable to uncover the mechanism of the internalisation process. To identify a suitable system to study this mechanism, a natural isolate *Rhizobium leguminosarum* Norway that infects *Lotus* was explored. Confocal and electron microscopy uncovered that *Rl* Norway invades the root nodule of *Lotus burtii* without using infection threads. Strikingly, *Rl* Norway is directly internalised from the apoplast into the host cell via “peg”-like structures. The expression of symbiotic genes involved in the infection process induced by *Rl* Norway is delayed and decreased in comparison to the response induced by a strain utilising an infection thread-dependent mode. These results revealed that *Rl* Norway uses an alternative infection strategy to colonise *Lotus* cells. Furthermore, a mutant impaired in the biosynthesis of the Lipochitooligosaccharides, known as Nodulation (Nod) factors, failed to induce “peg”-like structures during the internalisation process. This indicates that the formation of “peg”-like structures depends on the Nod factors and reinforces the previous hypothesis that there is signal perception before rhizobia are internalised.

In addition to the signalling exchanges with the host, the rhizobia root colonisation is a prerequisite for the establishment of the root nodule symbiosis. However, the root colonisation of the microbe community is a complex process. The interaction between rhizobia, including competition and cooperation, is hypothesised to influence the root colonisation, which is so far not well examined. *Rl* Norway was co-isolated with *Mesorhizobium norvegicum* 10.2.2 from the same nodule. Interestingly, the microscopic quantification of root colonisation revealed increasing colonisation of *Rl* Norway and *Mn* 10.2.2 in the co-inoculation compared with the single inoculation. To understand the mechanism underlying the increased root colonisation, rhizobia behaviours related to the root colonisation were determined. A swarming assay showed that the motility of *Mn* 10.2.2 is increased in the presence of *Rl* Norway. In addition,

biofilms were quantified *in vitro*. *R/* Norway formed biofilms alone, while *Mn* 10.2.2 did not. Interestingly, co-culture of *R/* Norway and *Mn* 10.2.2 enabled *Mn* 10.2.2 to form mixed biofilms together with *R/* Norway. To investigate the role of the surface polysaccharides of *R/* Norway during mixed biofilms formation, the biofilms of a mutant, with impaired surface polysaccharides biosynthesis was analysed. The structure of the biofilms formed by this mutant was altered under the single- and co-inoculation condition in comparison with the wild type strain. This indicates that the structure of the biofilms is determined by the surface polysaccharides of *R/* Norway. Overall, this thesis concludes that the two strains exhibit synergism, which could possibly contribute to the increased root colonisation.

# General introduction

## 1. Overview of root nodule symbiosis

The legume family (Leguminosae) is among the most important plant taxa, because of the role of its members in both ecological and agricultural systems all over the world (Sprent, Ardley and James 2017). Legumes, such as soybean (*Glycine max*), pea (*Pisum sativum*), peanut (*Arachis hypogaea*), and broad bean (*Vicia Faba*), are used as important protein sources for human and livestock consumption (Foyer et al. 2016, Considine, Siddique and Foyer 2017). Legumes mutualistically associate with nitrogen-fixing bacteria collectively called rhizobia. Legumes host rhizobia inside root organs called nodules, where symbiont reduce dinitrogen into ammonium. This form can be assimilated by the host. In return, the intracellularly accommodated rhizobia receive dicarboxylates. This mutualistic interaction is called root nodule symbiosis (Downie 2014). Nitrogen fixed by legumes contribute to a large part of the biological nitrogen fixation. Up to 30% of the nitrogen fixed by legumes returns to the soil (Walley et al. 1996, Frankow-Lindberg and Dahlin 2013). The intercropping and rotation of legumes with cereals and other non-leguminous crops in the field can also increase the yield of them (Foyer et al. 2016). This largely reduces the need for synthetic nitrogenous fertilisers, which are produced industrially via the energy consuming Haber–Bosch process (Gilchrist and Benjamin 2017).

The signal exchange between rhizobia and the host plays a fundamental role for the establishment of an efficient root nodule symbiosis (Oldroyd 2013, Roy et al. 2020). Legume roots secrete chemical compounds to recruit rhizobia from the rhizosphere to colonise the root surface (Fig. 1a, b, c) (Liu and Murray 2016, Downie 2010). In response, rhizobia secrete symbiotic molecules, which are perceived by the host (Fig. 1a).

This initiates two simultaneous processes: nodule organogenesis (Patriarca et al. 2004) and its controlled rhizobial infection (Fig. 1d, e, f) (Gage 2004). These two processes are dominantly controlled by the host via the stringent perception of symbiotic molecules (Oldroyd et al. 2011, Roy et al. 2020). The perception of symbiotic molecules is mainly known to be involved in the early stages; however, their role in later stages has not been well elucidated. The reason for this is that a suitable system to study this is not available. The aim of this work was to find a suitable system to investigate the perception in the later stages by exploring the natural diversity of *Lotus* plants.

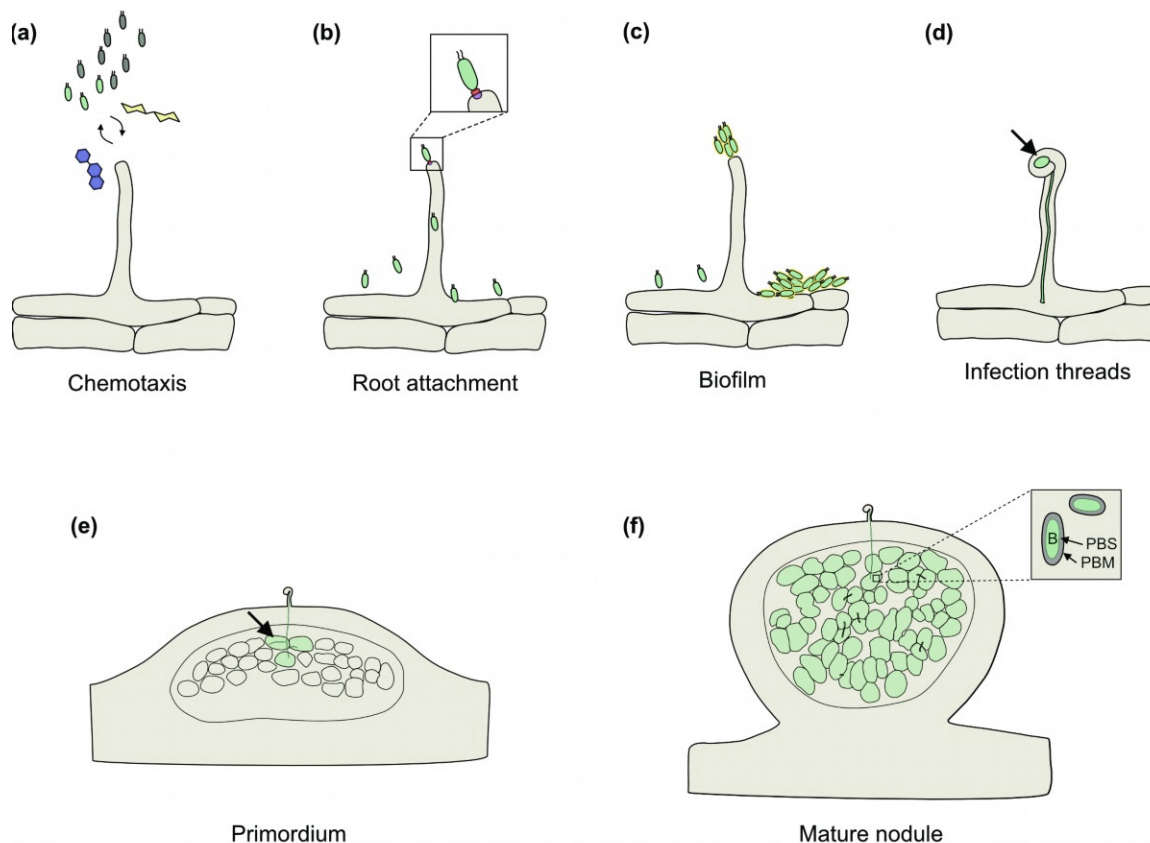


**Figure 1: Overview of the different steps in the root nodule symbiosis.**

(a) Rhizobia are attracted toward roots via chemoattraction by a chemical gradient of root exudates. Flavonoids (depicted as blue coloured structures) secreted from legume roots induce the expression of rhizobia *nod* genes that mediate the synthesis of Lipochitooligosaccharides, so called Nodulation (Nod) factors (depicted as yellow-coloured structures). (b) Glucomannans (red) on the rhizobia surface bind to plant lectins (purple) presented on the cell surface. (c) Rhizobia adhere firmly on root hairs and the root surface via biofilms. (d) Rhizobia are entrapped in a curled hair deformed into a “Shepherd crook” and form a microcolony (arrow) on the root tip. Rhizobia induce the formation of an inward growing infection thread, which encloses and guides them to reach the bottom of the epidermis. (e) The infection thread (arrow) arrives and ramifies in the cortex of the dividing nodule primordium. Green colour in cortex cells depicts infection. (f) Primordium develops into mature nodule with enlarged cells filled with bacteroids (Zoom in view: B: bacteroids. PBM: Peribacteroid membrane. PBS: Peribacteroid space). Scheme is illustrated based on the interaction between *Mesorhizobium loti* MAFF 303099 with *Lotus japonicus* Gifu (Poole, Ramachandran and Terpolilli 2018, Liang et al. 2019).



## 2. Surface colonisation of legume roots

### 2.1 Chemotaxis and motility in the rhizosphere

The soil area influenced by the plant roots is known as the rhizosphere (York et al. 2016). The root exudates shape the environment of the rhizosphere so that it can accommodate a wide range of microbes. Root exudates are primary and secondary metabolites, such as sugars, amino acids, organic acids, enzymes, fatty acids, phenolic compounds, etc., secreted from the roots into the soil (Canarini et al. 2019). Sugars (e.g. sucrose, glucose), amino acids (e.g. glycine, glutamate), and organic acids (e.g. malate, citrate) can be directly used by rhizobia as nutrients (Canarini et al. 2019). This makes the rhizosphere a nourishing spot in the soil. Besides, root exudates can act as chemotactic signals, attracting rhizobia to move along chemical gradients and colonise the root. Transcriptomic analyses of different rhizobia in the presence of root exudates have shown that chemotactic genes actively respond to the secreted compounds. For example, root exudates from soybean induce upregulation of chemotaxis genes in *Bradyrhizobium diazoefficiens* strains (Liu et al. 2017). Chemotaxis via root exudates can be used by the host to recruit and repel specific rhizobia (Baetz and Martinoia 2014). For instance, milk vetch (*Astragalus*) root exudates specifically attract *Sinorhizobium meliloti* 102F51 and 102F66, among the six strains that were tested, whereas root exudates from alsike clover (*Trifolium hybridum*) can attract all six strains (Currier and Strobel 1976).

Flavonoids are among the most prominent root exudates, as they have a variety of functions, which include antimicrobial activity (Parniske, Ahlborn and Werner 1991, Ulanowska et al. 2006), chemotaxis and induction of symbiotic response of rhizobia (Fig. 1a) (Begum et al. 2001, Bolaños-Vásquez and Werner 1997). The basic flavonoid structure is composed by a flavan nucleus with 15 carbon atoms arranged in three rings (Reddy et al. 2007). A variety of flavonoids are released from specific leguminous plants. For instance, *Glycine max* secretes daizein, genistein, coumestrol, and isoliquiritigenin, *Trifolium repens* secretes geraldone, dihydroxyflavone, and methoxyflavone (Liu and Murray 2016). The flavonoids released from roots provide a gradient that acts as a chemotactic stimuli for rhizobia (Poole et al. 2018).

The motility of rhizobia allows them to move up the flavonoid gradient, ultimately resulting in the colonisation of the root (Cooper 2004). Rhizobia exhibit different types of motility depending on external appendages and living environments (Mitchell and Kogure 2006, Gordon and Wang 2019). The best studied types of motility in rhizobia are swimming and swarming, which both utilise the rotation of the flagella for propulsion (Tambalo, Yost and Hynes 2010, Vicario, Dardanelli and Giordano 2015, Braeken et al. 2008). Swimming occurs in liquid environments,

while swarming allows bacteria to spread across semi-solid and solid surfaces (Lowe, Meister and Berg 1987, Kearns 2010). The motility is crucial for rhizobia to colonise the root in the early stage. For instance, a motility impaired *Rhizobium tropici* CIAT899 strain presents decreased root colonisation (Ormeño-Orrillo et al. 2008). In addition, the impairment of flagella dependent motility in *Mesorhizobium tianshanense* decreases its root colonisation capacity (Zheng et al. 2015).

## 2.2 Biofilms and root attachment

After arriving at the root surface, rhizobia apply primary and secondary attachment mechanisms (Wheatley and Poole 2018). Different molecules of rhizobia contribute to the primary attachment. Rhicadhesin of *Rhizobium leguminosarum* (*Rl*) biovar (bv.) *viciae* mediates calcium dependent binding to the root (Smit et al. 1991). Glucomannan is another molecule predicted to be required for lectin-mediated attachment under acidic conditions (Fig 1. b). A glucomannan defective mutant of *Rl* bv. *viciae* 3841 is incapable of attaching on root hairs (Williams et al. 2008).

After the primary attachment, aggregation of rhizobia embedded in biofilms strengthen the root colonisation (Fig. 1c) (Downie 2010). Biofilms are bacteria structures composed of a matrix of hydrated extracellular polymeric substances containing polysaccharides, lipids, proteins, among other components (Flemming and Wingender 2010). Formation of mature biofilms on roots requires extracellular polysaccharides, such as exopolysaccharide (EPS), cellulose fibrils and glycans. For example, reducing EPS and linear mixed-linkage  $\beta$ -glucan production in *Rl* bv. *viciae* 3841 and *S. meliloti* 8530 decrease the biofilm formation and root attachment, respectively (Williams et al. 2008, Russo et al. 2006, Rinaudi and González 2009, Meneses, Mendoza-Hernández and Encarnación 2010). Cellulose fibrils synthesised by *Rl* 248, *Rl* RBL5523 and *Rl* bv. *trifolii* ANU843 enable tight attachment of rhizobia cells to root hairs (Smit, Kijne and Lugtenberg 1987, Laus, van Brussel and Kijne 2005, Robledo et al. 2012). In addition to polysaccharides, the *Rhizobium*-adhering proteins (Raps) are likely to mediate the biofilm formation (Ausmees, Jacobsson and Lindberg 2001, Abdian et al. 2013). One common feature of Rap proteins is that they contain one or more rhizobia binding domains, which were proposed to confer adhesion via protein-protein interactions (Abdian et al. 2013). For instance, calcium binding protein RapA1 of *Rl* bv. *trifolii* R200 was proposed to function as an agglutinin meditating auto aggregates of cells (Abdian et al. 2013, Vozza et al. 2016). RapA2 directly binds to acidic EPS and capsular polysaccharides (KPS) in a calcium-dependent manner

(Abdian et al. 2013, Vozza et al. 2016). Rap proteins may aid adhesion to the EPS and facilitate biofilm maturation.

Overall, biofilm-mediated rhizobia root attachment requires: i) binding of the microbes to the root surface, ii) different types of extracellular polysaccharides that act as a matrix to immobilise rhizobia, iii) and proteins to strengthen the structure. This leads to a cohesive interaction between the microbes and host interface. Although the ability to form biofilm is not essential for the formation of nodules (Smit et al. 1987, Mongiardini et al. 2008), it is probably crucial for competitiveness of microbes in the context of the complex soil environment (Williams et al. 2008, Ormeño-Orrillo et al. 2008).

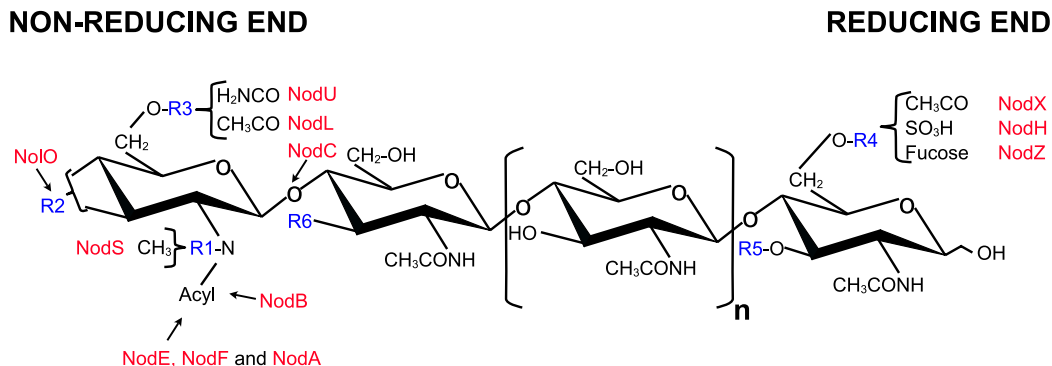
### **3. Rhizobia signals in symbiotic interaction**

Although a broad range of bacteria can colonise the root, leguminous hosts normally only establish efficient symbiotic interactions with specific groups of rhizobia. To distinguish specific symbionts from other microbes, hosts need to recognise the intricate species-specific structures of rhizobial molecules (Downie 2010).

#### **3.1 Nod factors**

Plant exuded flavonoids act as signals to induce symbiotic gene expression in rhizobia. Different strains respond to different flavonoids. For instance, *RI* pJ1477 induces higher symbiotic gene expression in the presence of naringenin and hesperetin from the root exudates of *Pisum sativum* L. and *Lens culinaris* L. (Begum et al. 2001). While *RI* bv. *phaseoli* responds to coumestrol, naringenin, and daidzein from the root exudates of *Phaseolus vulgaris* (Bolaños-Vásquez and Werner 1997). Flavonoids accumulate in the cytoplasmic membrane of rhizobia (Recourt et al. 1989) and are perceived by the NodD protein (D'Haese and Holsters 2002). NodD is a transcription factor that binds to so called *nod* boxes, which are conserved DNA motives in the promoters of nodulation loci. Although there is no evidence showing the direct physical binding of NodD to flavonoids, the presence of flavonoids enhances binding of NodD to *nod* boxes, for example in *Azorhizobium caulinodans* ORS571 and in *S. meliloti* 1021 (Goethals, Van Montagu and Holsters 1992, Peck, Fisher and Long 2006). NodD regulates the expression of *nod* genes involved in the biosynthesis of the Nod factors (Fisher et al. 1988).

**Table 1: Nod factors and the substituents**



Strains	Acyl	R1	R2	R3	R4	R5	R6	n	Ref
<i>M. loti</i> E1R	C <sub>18:1</sub> , C <sub>18:0</sub>	Me	Cb	H	AcFuc	H	OH	2	(Poinsot et al. 2001)
<i>M. loti</i> R7A	C <sub>16:0</sub> , C <sub>18:0</sub> , C <sub>18:1</sub> C <sub>22:0-OH</sub>	Me	Cb	H	AcFuc	H	OH	0	(Rodpothong et al. 2009)
<i>M. huakuii</i> Ra5	C <sub>18:4</sub> , C <sub>18:1</sub>	Me	OH	H	S	H	OH	0, 1, 2	(Yang et al. 1999)
<i>Rl</i> bv. <i>viciae</i> RBL5560	C <sub>18:1</sub> , C <sub>18:4</sub> , C <sub>18:0</sub>	H	OH	Ac	H	H	OH	1,2	(Spaink et al. 1991)
<i>Rl</i> bv. <i>trifolii</i> LPR5045	C <sub>18:0</sub> , C <sub>18:1</sub> , C <sub>20:3</sub> , C <sub>20:4</sub>	H	OH	Ac	H	H	OH	2	(van der Drift et al. 1996)
<i>S. meliloti</i> 2011	C <sub>16:1</sub> , C <sub>16:2</sub> , C <sub>16:3</sub>	H	OH	H, Ac	S	H	OH	1,2	(Ardourel et al. 1994, Lerouge et al. 1990)
<i>S. fredii</i> HH103	C <sub>16:0</sub> , C <sub>16:1</sub> , C <sub>18:0</sub> , C <sub>18:1</sub>	H	H	H	AcFuc, Fuc	H	OH	0, 1,2	(Gil-Serrano et al. 1997)

Abbreviations: Ac, acetyl; Cb, carbamoyl; AcFuc, acetylfucosyl; Fuc, fucosyl; H, hydrogen; Me, methyl; S, sulphate; OH, hydroxy. R1-R6 indicate substituents of Nod factors. *nod* genes involved in the synthesis of substituents are indicated in red colour. Scheme of the Nod factors structure is modified from (Perret, Staehelin and Broughton 2000).

The Nod factors are lipochitooligosaccharides that act as primary symbiotic signals. Their backbone is made up of three to five  $\beta$ -1,4-linked N-acetyl glucosamine (GlcNAc) residues, which vary in different rhizobia species (Table 1) (D'Haeze and Holsters 2002, Kamst et al. 1997). The core of Nod factors is synthesised by enzymes encoded by the *nodABC* genes (D'Haeze and Holsters 2002). The N-acetylglucosaminyltransferase encoded by *nodC* is responsible for adding the GlcNAc to the non-reducing end of the backbone (Kamst et al. 1997). The *nodB* gene encodes a deacetylase responsible for removing the N-acetyl moiety from the non-reducing end of the GlcNAc. This allows the *nodA* encoded acyltransferase to acetylate the acetyl free non-reducing end (John et al. 1993, Debelle et al. 1996). The fatty acids in the non-reducing end vary from saturated, monounsaturated to highly unsaturated in different rhizobia species (D'Haeze and Holsters 2002). In addition, other *nod* genes encode enzymes responsible for specific substituents at the different ends of Nod factor molecules, which also vary in different rhizobia species. These can be fucosyl, sulphuryl, acetyl, methyl, carbamoyl, and arabinosyl groups (Downie 1998). For instance, Nod factors of *Rl* bv. *viciae* RBL 5560, and *Rl* bv. *trifolii* LPR 5045 have an O-acetyl substituent, which is added by the acetyl transferase enzyme encoded by the *nodL* gene (Table 1 R3) (van der Drift et al. 1996, Ardourel et al. 1994, Lerouge et al. 1990). By contrast, *Mesorhizobium loti* E1R has a methyl substituent in the non-reducing end, which is added by the enzyme encoded in the *nodS* locus (Table 1 R1) (Poinsot et al. 2001).

In the reducing end, acetyl fucose substituents are added by the acetyl transferase encoded by *nodZ* in *M. loti* E1R and *Sinorhizobium fredii* HH103 (Table 1 R4) (Poinsot et al. 2001, Gil-Serrano et al. 1997). NodH acts as the sulfotransferase that attaches a sulphate group in the non-reducing end, for example in *S. meliloti* 2011 and *Mesorhizobium huakuii* Ra5 (Table 1 R4) (Yang et al. 1999, Lerouge et al. 1990). NodIJ are responsible for exporting the Nod factors (Vázquez, Santana and Quinto 1993).

The *nod* genes are often organised in clusters located in mobile genetic elements, such as symbiotic islands in the genus *Mesorhizobium* and *Bradyrhizobium* (Sullivan et al. 2002, Gottfert et al. 2001) or in symbiotic plasmids such as in *Rl* and different *Sinorhizobium* strains (Young et al. 2006, Wang et al. 2018). A diverse range of Nod factors are generated by different rhizobia species. It has been proposed that the different substituents mediate specific recognition by the host and contribute to signalling specificity (Downie 2010).

### 3.2 Extracellular polysaccharides

In addition to Nod factors, different types of extracellular polysaccharides are important for an efficient root nodule symbiosis. Rhizobia produce a variety of extracellular polysaccharides, including EPS, LPS, KPS, and other glycans (Downie 2010). They do not only provide a protective capsule and are the backbone of biofilms, but also can be recognised as signals by the host. Among these extracellular polysaccharides, the EPS is better characterised in rhizobia in terms of components and structure. EPS molecules produced by rhizobia display species-specific structures. Such structures can be composed of linear or branched repeating units containing monosaccharides and substituents with non-carbohydrate moieties (e.g., acetyl, pyruvyl, succinyl, and 3-hydroxybutanoyl groups) (Marczak et al. 2017). For example, *Rl* strains that belong to different biovars have a very similar basic EPS structure with a polymer of a decorated octamer containing pyruvyl, O-acetyl, and O-(3-hydroxybutanoyl) substituents (Fig. 2a) (Robertson et al. 1981, O'Neill, Darvill and Albersheim 1991). The EPS of *S. meliloti* 2011 is composed of succinoglycan (EPS I) with acetyl, pyruvyl and succinate substituents, and galactoglucan with acetyl and pyruvyl substituents (EPS II) (Fig. 2b) (Becker et al. 2002). While the EPS of *M. loti* R7A is composed of D-galactose, D-glucuronic acid and riburonic acid, with only O-acetyl modifications (Fig. 2c) (Muszyński et al. 2016).

The synthesis of EPS requires the coordinated activity of enzymes at different levels. The required enzymes are involved in the following steps: sugar precursor synthesis, unit assembly, polymerisation, and export of the EPS chain onto the cell surface (Skorupska et al. 2006, Janczarek 2011). A set of *exo* genes and *pss* genes have been identified as being responsible for EPS synthesis in different stages, but they are highly divergent across rhizobia species (Janczarek 2011). The *exo5* and *exoB* genes have been identified to be involved in the synthesis of sugar precursors in *Rl* and *Mesorhizobium* (Canter Cremers et al. 1990, Sánchez-Andújar et al. 1997, Kelly et al. 2013). The *exo5* gene encodes a UDP-glucose dehydrogenase, which is responsible for the conversion of UDP-glucose to UDP-glucuronic acid in *Rl* but has not been identified in *M. loti* (Laus et al. 2004, Muszynski et al. 2011, Kelly et al. 2013). In *Rl*, the first step in the synthesis of the octasaccharide unit is accomplished by a glucosyl-IP-transferase, which is encoded by the *pssA* gene (Latchford, Borthakur and Johnston 1991). The *exoA* gene in *M. loti* R7A and *S. meliloti* strains encodes the first glycosyltransferase in the pathway (Kelly et al. 2013, Becker et al. 1993). In the later stages, the repeating units are assembled to further form mature EPS. For more information refer to the following reviews (Skorupska et al. 2006, Janczarek 2011, Marczak et al. 2017).



### 3.3 Type three secreted effectors

Rhizobia secrete effector proteins into the host cytoplasm to modulate the symbiotic signalling pathway via the type three secretion system (T3SS) (Miwa and Okazaki 2017, Teulet et al. 2019). This system was initially identified in pathogenic bacteria, which employ it to suppress the immune system of the host. T3SSs were later identified in several rhizobia, including *S. fredii* NGR234 (Freiberg et al. 1997), *Bradyrhizobium elkanii* USDA61 (Okazaki et al. 2009), *M. loti* MAFF303099 (Kaneko et al. 2000, Okazaki et al. 2010), and *S. fredii* USDA257 (Meinhardt et al. 1993), USDA191 (Bellato et al. 1997), and HH103 (Bellato et al. 1997).

The T3SS acts as a nanomachine embedded in the double membrane of bacteria to deliver effector proteins to the host cell (Costa et al. 2015). Components of the T3SS construct a needle complex or also termed the injectosome that serves as a translocator on the plasma membrane (Marlovits et al. 2004). The cocktail of secreted proteins is named type three secreted effectors (T3Es) (Miwa and Okazaki 2017, Marie, Broughton and Deakin 2001). There are more than 30 T3Es identified in *Bradyrhizobium japonicum* USDA110 and approximately 15 in *S. fredii* NGR234 (Kimbrel et al. 2013). Proteins secreted by some rhizobia are designated Nodulation outer proteins (Nops) (Marie et al. 2001). These Nops have a very diverse range of functions. NopM from *S. fredii* NGR234 has E3 ubiquitin ligase activity (Xin et al. 2012). It inhibits microbe-associated molecular pattern (MAMP) induced ROS production and mitogen-activated protein kinase (MAPK) signalling (Xin et al. 2012). NopT from *S. fredii* NGR234 (Dai et al. 2008) and BEL2-5 from *B. elkanii* USDA61 (Faruque et al. 2015) function as cysteine proteases. Besides, calcium binding motif containing NopE has been identified in *B. japonicum* USDA110. NopE executes self-cleavage in a calcium dependent manner (Wenzel et al. 2010).

## 4. Host perception and downstream signalling

Highly diverse and species-specific extracellular molecules are synthesised and released from rhizobia, which are perceived by a sophisticated system from the host. The perception of Nod factors and the signalling mediated by Nod factors induce cytoplasmic calcium influx in the cytoplasm and calcium oscillations in the nucleus (Cárdenas et al. 2008, Ehrhardt, Wais and Long 1996, Shaw and Long 2003). The decoding of the nuclear calcium oscillations activates a downstream transcription factor network that transcriptionally reprograms cells to regulate nodule organogenesis and infection (Roy et al. 2020). In addition, perception of EPS and



effectors are also involved in inducing downstream symbiotic signalling (Kawaharada et al. 2017, Teulet et al. 2019).

#### **4.1 Nod factor signalling and the Common Symbiotic Pathway**

The host symbiotic signalling pathway has been studied in depth in two model legumes, *Medicago truncatula* and *Lotus japonicus*. Here, I mainly focus on *L. japonicus*, which is more relevant to this thesis. Nod factors released by rhizobia are perceived by Nod Factor Receptor 1 (NFR1) and NFR5 located on the plasma membrane of the root epidermal cells (Madsen et al. 2003, Radutoiu et al. 2003). These receptors form complexes with the leucine-rich repeat Symbiosis Receptor Kinase (SYMRK) (Stracke et al. 2002, Endre et al. 2002, Antolin-Llovera et al. 2014, Ried, Antolin-Llovera and Parniske 2014). Perception of Nod factors induces accumulation of calcium on the root hair, which triggers calcium influx in the cytoplasm and later calcium oscillations in the nucleus (Shaw and Long 2003).

The cytoplasmic calcium influx is generated from the movement of calcium across the plasma membrane (Cárdenas et al. 2008) and correlates with a reactive oxygen species (ROS) burst in the root hair (Cárdenas et al. 2008). This burst occurs within seconds upon Nod factors treatment, last for around three minutes, and is involved in early infection (Cárdenas et al. 2008, Montiel Gonzalez et al. 2016). For a detailed review of ROS refer to (Damiani et al. 2016).

Calcium oscillations in the root-hair nucleus occurs after approximately 10 minutes of Nod factors application (Ehrhardt et al. 1996). Nuclear envelope located calcium channels CASTOR and POLLUX (Charpentier et al. 2008, Kim et al. 2019) and the nucleoporins (NUP)133, NUP85, and NENA have been shown to mediate the calcium oscillations (Kanamori et al. 2006, Saito et al. 2007, Groth et al. 2010). It has been proposed that the calcium- and calmodulin-dependent protein kinase (CCaMK) decodes this signal in the nucleus (Tirichine et al. 2006b, Lévy et al. 2004, Oldroyd and Downie 2006). CCaMK interacts with and phosphorylates a coiled-coil domain containing transcription factor named Cyclops (Yano et al. 2008). The phosphorylation of specific residues on Cyclops leads to its activation (Singh et al. 2014). GRAS-domain-type transcription factors Nodulation Signalling Pathway 1 (NSP1) and NSP2 are positioned downstream of CCaMK, which are required for infection and nodule organogenesis (Heckmann et al. 2006). The CCaMK/Cyclops complex binds to the Nodule Inception (NIN) promoter and activates NIN transcription (Singh et al. 2014). NIN is a transcription factor that targets more than 100 downstream genes involved in nodule organogenesis and infection (Liu et al. 2019a). In addition, the transcription factor ERF

Required for Nodulation 1 (ERN1) is also a target of the CCaMK/Cyclops complex and regulates infection related genes (Cerri et al. 2017, Liu et al. 2019a). The perception of Nod factors and downstream signalling elicit the gene reprogramming required for the nodule organogenesis and infection processes.

## 4.2 Other symbiotic signalling

In addition to Nod factor-mediated signalling, other rhizobia molecules have been described to be perceived by the host, although their mechanisms of action remain to be fully understood. In *L. japonicus*, EPS molecules are perceived by the LysM receptor kinase Exopolysaccharide Receptor 3 (EPR3) (Kawaharada et al. 2015). The expression of the *epr3* gene depends on the perception of Nod factors (Kawaharada et al. 2015). Further studies showed that the expression of the *epr3* is integrated in the common symbiotic pathway, and the genetic requirement for *epr3* expression in the epidermis and interior nodule tissue is different (Kawaharada et al. 2017). The ortholog of the EPR3 protein from *M. truncatula*, a LysM receptor-like kinase (LYK10), is not responsible for the recognition of the deficient EPS in *S. melilot* 1021 (Maillet et al. 2020). This suggests that the perception of the EPS is involved in the infection process, but the mechanism varies between different leguminous hosts.

Some leguminous hosts perceive T3Es as signals to control the root nodule symbiosis in a Nod factor-independent manner (Giraud et al. 2007, Okazaki et al. 2015). They instead use T3Es that are capable of bypassing Nod factors signalling by a still unknown mechanism.

Overall, perception of species-specific Nod factors and other symbiotic signals is a finely tuned process, which is crucial to initiate the root nodule symbiosis. The following sections will illustrate the crucial genes involved in the nodule organogenesis process and the highly diverse infection routes employed by rhizobia.

## 5. Nodule organogenesis

Cell divisions are initiated downstream of Nod-factor mediated signalling, which give rise to a new organ, the nodule. Nod factor treatment in the absence of rhizobia is sufficient to initiate nodule organogenesis in *Medicago sativa* (Truchet et al. 1991). Moreover, the *snf1-1* gain of function mutant of CCaMK induces spontaneous nodule formation in the absence of rhizobia (Tirichine et al. 2006a). Nod-factor induced signalling is also interlinked with hormone homeostasis at different levels. Nod factors induce the expression of cytokinin biosynthesis genes and the accumulation of cytokinin in the root (van Zeijl et al. 2015). Cytokinin is a

phytohormone involved in plant development and morphogenesis (Kieber and Schaller 2018). Exogenous application of cytokinin is sufficient to trigger cell divisions in the cortex (Bauer et al. 1996). Lotus histidine kinase (LHK) functions as cytokinin receptor, which is essential for nodule organogenesis (Gonzalez-Rizzo, Crespi and Frugier 2006, Murray et al. 2007, Held et al. 2014). The *snf2* gain of function mutation of this receptor induces spontaneous nodule formation in the absence of rhizobia (Tirichine et al. 2007). Cytokinin signalling has been shown to be involved in the regulation of the transcription factor NIN. Cytokinin-responsive elements in the NIN promoter are required for NIN expression in the pericycle, which is essential for nodule primordium formation (Liu et al. 2019b).

Downstream targets of NIN are Nuclear Factor Y (NF-Y) subunit genes *NF-YA1* and *NF-YB1*, which are responsible for promoting cell divisions (Soyano et al. 2013). Another target of NIN sufficient for cell divisions is *Asymmetric Leaves 2-Like/Lateral Organ Boundaries domain 16a* (*ASL18/LBD16a*) (Soyano et al. 2019). Interestingly, orthologs of *ASL18/LBD16a* are required for formation of lateral root primordium in nonlegume plants. Transcriptional analysis revealed that gene expression of both the lateral root and nodule primordium formation highly overlap (Schiessl et al. 2019). This suggests that co-option of the lateral root initiation with nodule organogenesis are induced downstream of NIN. The promoter of *ASL18/LBD16a* responds to another important phytohormone, auxin, which accumulates in the cortex during nodule development (reviewed in (Kohlen et al. 2018)).

These programs are conserved in different legumes (Shen et al. 2020). However, the nodule morphology is highly diverse across leguminous plants (Sprent et al. 2017). *Glycine max* and *Lotus* species induce spherical determinate nodules without persistent meristem. Indeterminate nodule with persistent meristem presents an elongated shape, which are best characterised in *Medicago* species (Xiao et al. 2014) and *Pisum sativum* (Hirsch 1992). The semi-aquatic species *Sesbania rostrata* forms nodules on the stem and nodules associated with lateral root are found in plants from the *Aeschynomene* genus (Ndoye et al. 1994, Bonaldi et al. 2011). *Lupinus* genus plants form very unique lupinoid type of nodule, which forms around the subtending root (Gonzalez-Sama et al. 2004). The common feature of these diverse types of nodules is that mature nodules contain enlarged cells filled with rhizobia (Fig. 1f). This is controlled by a distinct, but interlinked process, the infection.

## 6. Infection

Rhizobia embark on an elaborate infection route to colonise primordium that develop on the root of the host. Similar to the contrastive nodule morphologies induced across leguminous plants (Sprent et al. 2017), diverse infection modes are observed in legume and rhizobia interactions (Ibanez, Wall and Fabra 2017, Venado, Liang and Marín 2020). They share three steps: 1) crossing of epidermis, 2) cortical spreading, and 3) intracellular uptake of rhizobia. A tube-like structure, termed infection thread, although widely employed by hosts to guide rhizobia entering the root, it is not the only existing path of infection. This section will describe infection thread-dependent and alternative mechanisms.

### 6.1 Infection thread-dependent mechanism

The infection thread-dependent mechanism has been extensively studied in the Papilionoideae subfamily including *Lotus*, *Medicago*, and *Pisum* (Sprent 2007). In members of these genera, the epidermis of the root is penetrated by rhizobia via infection threads formed in root hairs (Murray 2011). The formation and progression of these structures require massive cell biological remodelling (Oldroyd et al. 2011, van Spronsen et al. 2001).

The infection initiates when rhizobia attach on the root hair. Nod factors induce membrane polarisation (Ehrhardt, Atkinson and Long 1992) and cytoskeleton rearrangement (de Ruijter, Bisseling and Emons 1999), which leads to root hair deformation and branching (Knight et al. 1986, Heidstra et al. 1994, Miwa et al. 2006). The cytoskeleton rearrangement occurs within 3 to 10 minutes after Nod factors treatment (Timmers et al. 1998). The root hair deforms into a “shepherd’s crook” in order to entrap bacteria in a pocket between appressed cell walls. Bacteria continuously divide and form a microcolony (Fig. 1d) (Gage 2002). Thereafter, accumulation of Nod factors occurs, which leads to cellular reprogramming inducing cell wall remodelling and plasma membrane invagination in the root hair cell. This results in the formation of the infection thread (Fig. 1d) (Jordan, Grinyer and Coulter 1963, Rae, Bonfante-Fasolo and Brewin 1992). This structure encloses dividing rhizobia within a matrix containing glycoproteins (Rae et al. 1992).

Infection thread grow inward and reach the bottom of the root hair. In response to the epidermal infection, cytoplasm and nuclei of the sublayer of cortical cells align in the radial direction with the infection thread, forming a cytoplasmic bridge (van Brussel et al. 1992). The bridge contains the cytoplasm and endomembrane localising on the outer side and amyloplasts in the inner side. These bridge structures are called pre-infection threads and have been observed in *Vicia*, *Medicago*, and *Lotus* (van Brussel et al. 1992, van Spronsen et al. 2001). At the bottom

of the root hair cell, local cell wall remodelling releases rhizobia (Gage 2004, Gage 2002, van Spronsen et al. 1994). Cortical infection threads (Fig. 1e arrow) enclosing rhizobia continue from cell to cell and form an infection thread network (Gage 2004, Monahan-Giovanelli, Pinedo and Gage 2006). Consequently, rhizobia spread into the dividing primordium, where rhizobia are released into the host cell from unwallied infection droplets (Jordan et al. 1963, Goodchild and Bergersen 1966).

## 6.2 Alternative Infection mechanisms

Mechanisms that do not use infection threads to cross the epidermis are classified depending on the differences in the three steps listed above.

The epidermis can alternatively be penetrated via two infection thread-independent modes: “crack-entry” and intercellular infection. In “crack-entry”, rhizobia enter the root through fissures formed in lateral root emergence sites or through natural root wounds. This mode of infection has been widely recruited by leguminous plants from the Genistoid and Dalbergioid clades. In plants from these two clades, the “crack-entry” site is dominantly associated with axillary root hairs in the lateral root emergence site (Boogerd and van Rossum 1997). *A. hypogaea* and *Aeschynomene* spp. are often penetrated through the junctions between root hairs in the lateral root axils (Chandler 1978, Bonaldi et al. 2011). With few examples in the rest of the Papilionoideae subfamily, rhizobia use the “crack-entry” mechanism, however, root hairs are not obviously engaged in the infection process. For instance, *S. rostrata* growing under waterlogged conditions can be infected via the “crack-entry” independent of root hair (Ndoye et al. 1994). Similarly, no root hairs grow on aquatic legume *Neptunia natans* under the water culture condition, while rhizobia enter the junction between lateral and main root (James et al. 1992, Subbarao et al. 1995).

Another mode to penetrate the epidermis is the intercellular infection through the middle lamella between root epidermal cells. This infection strategy is prevalent among Actinorhizal plants of the orders Rosales, Fagales, and Cucurbitales (Pawlowski and Demchenko 2012), which has only been reported in few leguminous hosts. The epidermis of *L. albus* is penetrated via this intercellular infection process (Gonzalez-Sama et al. 2004). *M. scabrella* is another example that is invaded between intact epidermal cells (de Faria, Hay and Sprent 1988).

After crossing the first barrier of the root, rhizobia need to spread in the sub-epidermal and cortex layer of the primordium. Some leguminous plants can still recruit the infection threads program. For example, in *S. rostrata*, after entering the outer cortex, bacteria proliferate in intercellular space and kill a few of the outer cortex cells to form an “infection pocket” (Ndoye

et al. 1994). Cortical infection threads derived from the “infection pocket” can form intra- and inter-cellular infection threads (Ndoye et al. 1994). However, spreading of rhizobia can be fully independent of infection threads and can vary between different species (reviewed in (Ibanez et al. 2017, Venado et al. 2020)). For instance, *Stylosanthes* spp. and *A. indica* are invaded from plant cells that die and collapse after infection (Chandler, Date and Roughley 1982, Bonaldi et al. 2011). In *Chamaecytisus proliferus*, the neighbouring cells collapse after being infected by rhizobia via the intercellular space of nodules (Vega-Hernández et al. 2000). *A. hypogaea* is colonised intercellularly by rhizobia via separation of the middle lamella, which do not induce cell death (Chandler 1978, Boogerd and van Rossum 1997, Uheda, Daimon and Yoshizako 2001). *L. albus* directly internalise its symbiont *Bradyrhizobium* sp. ISLU16 into the host cell after epidermal crossing (Gonzalez-Sama et al. 2004). *M. scabrella* nodules are infected via primary wall layers and intercellular space (de Faria et al. 1988).

The internalisation of rhizobia also varies between different plants. However, in all cases described so far, at the sites of infection bacteria are embedded in an electron-dense material. This material is proposed to act against the turgor pressure from the plant cell (Rae et al. 1992, Parniske 2018). Sometimes this structure, often called “peg”-like structure, resembles a poorly defined infection thread and is often detected when bacteria are directly internalised from the apoplast. As in the infection thread dependent mechanism, the invagination in these alternative modes of infection requires cellular rearrangements (Yokota et al. 2009). However, the detailed mechanism of “peg”-like structures formation has not been elucidated.

### **6.3 Requirement of rhizobia signals in infection**

The formation of infection structures is mainly controlled by the host in response to the perception of rhizobia signals, such as Nod factors and extracellular polysaccharides (Downie 2010). For example, Nod factor-induced signalling plays a fundamental role in the formation of infection threads. Infection threads are only efficiently induced when the Nod factors structures are compatible for the specific host. The specific substituents in both the reducing and non-reducing ends of the Nod factors produced by different rhizobia are crucial. For example, in *S. meliloti* 2011, a *nodF* and *nodL* double mutant producing Nod factors lacking a glucosamine residue and an O-acetyl group in the non-reducing end are unable to induce infection thread formation on *M. truncatula* (Ardourel et al. 1994). The fucosyl residues of Nod factors produced by *M. loti* R7A are pivotal for infection thread formation in *Lotus*. The infection threads induced by a *nodZ* mutant, which lacks a fucosyl residue, are largely reduced in *L. japonicus* and almost completely abolished in *L. corniculatus* (Rodpothong et al. 2009).

Extracellular polysaccharides also contribute to infection threads development in different symbioses. A *M. loti* R7A *exoU* mutant, which forms truncated EPS, aborts the elongation of the infection thread almost completely (Kelly et al. 2013, Kawaharada et al. 2015). A *pssZ* mutant of *Ri* bv. *trifolii* RT24.2 and a *pssD* mutant of *Ri* bv. *trifolii* TA1 display abnormally enlarged cortical infection threads and defective intracellular colonisation of the bacteria (Lipa et al. 2018, Król et al. 1998). In addition, the formation of elongated infection threads is impaired in the *epr3-10* and *epr3-11* mutants in comparison to wild type *L. japonicus* Gifu plants (Kawaharada et al. 2015). Other extracellular polysaccharides are also involved in the efficient formation of infection threads, although the host perception mechanism is still unknown. For example, a *lps-212* mutant in *S. melitoli* 1021 that producing an LPS lacking a sulphate modification forms aborted infection threads and inefficient nodules (Keating, Willits and Long 2002).

These studies reinforce the fundamental role of the rhizobia signals in the establishment of efficient infection. The final goal of the infection is the internalisation of the rhizobia into the host cell. The internalisation is pivotal for the nitrogen fixation, because the host cell provides a suitable environment for rhizobia to fix nitrogen via the nitrogenase. However, the perception of rhizobia signals has been mainly addressed on the epidermis, and the perception mechanisms in later steps are currently not clear.

## 7. Natural diversity of rhizobia and legume interaction

Legumes are the third largest flowering family with approximately 751 genera and 19,500 species (Sprent et al. 2017, LPWG 2017). Rhizobia are composed of 11 genera of alphaproteobacteria (*Rhizobium*, *Bradyrhizobium*, *Sinorhizobium*, *Mesorhizobium*, etc.) and three genera of betaproteobacteria (*Paraburkholderia*, *Cupriavidus*, *Trinickia*) (Laranjo, Alexandre and Oliveira 2014). This suggests that legumes and rhizobia are widely diverse in nature. The diversity of the root nodule symbiosis is reflected by the contrastive infection mechanisms and nodule organogenesis induced by rhizobia (Sprent 2007).

However, current studies of the genetic basis of root nodule symbiosis mainly build on the compatible interaction between *Medicago-Sinorhizobium* and *Lotus-Mesorhizobium* due to the genetic amenability. Forward and reverse genetic screens have been widely applied to determine genes engaged in the nodule organogenesis and the early stages of the infection (Roy et al. 2020). However, the genes involved in the later stages of the infection are poorly

elucidated, because of the lack of the proper system to uncouple epidermal infection from the later steps.

Gossmann et al. carried a study to investigate the natural variations of *Lotus* (Gossmann et al. 2012). Rhizobia were isolated from *Lotus* nodules sampled from 30 spots across Europe. A *Rl* strain (*Rl* Norway) was isolated from a *Lotus corniculatus* nodule together with a *Mesorhizobium norvegicum* (*Mn*) strain (*Mn* 10.2.2) (Gossmann et al. 2012, Kabdullayeva, Crosbie and Marín 2020). *Mn* 10.2.2 induces nitrogen-fixing nodules on *L. corniculatus*, while *Rl* Norway cannot. This suggests that *Rl* Norway can hitchhike onto nodules induced by *Mn* 10.2.2. Co-colonisation with the compatible symbiont in the nodule has been proposed to be used as a protective niche for the inefficient symbionts (Westhoek et al. 2017, Mendoza-Suárez et al. 2020, Checcucci et al. 2016, Friesen and Mathias 2010). Although *Rl* Norway cannot nodulate *L. corniculatus*, it can nodulate a broad range of other *Lotus* species, which are not typical hosts of *Rl* (Gossmann et al. 2012). However, in all cases the plants display nitrogen-starvation symptoms and develop fully infected nodules that do not fix nitrogen (Gossmann et al. 2012). Besides, *Rl* Norway induces  $\beta$ -glucuronidase (GUS) activity in the *L. japonicus* Gifu T90 GUS line, which is responsive to rhizobia and Nod factors (Gossmann et al. 2012, Webb et al. 2000). However, no nodules are induced by *Rl* Norway on *L. japonicus* Gifu (Gossmann et al. 2012).

Notably, in *Lotus burtii* and *L. japonicus* MG-20, *Rl* Norway can colonise intracellularly but epidermal infection threads are not observed (Gossmann et al. 2012). In addition, *Rl* Norway colonises only between the cells in the bumps of *L. japonicus* Nepal. These infection phenotypes suggest that *Rl* Norway may use an alternative infection thread independent mechanism.



# Aims of the thesis

From the infection phenotypes observed on *Lotus* species, we hypothesised that *RI* Norway induces an alternative infection mode on *Lotus* instead of the infection thread-dependent infection mechanism. The lack of infection threads in the cortex can uncouple the infection threads formation with the internalisation process, which is amenable to uncover the mechanism in the internalisation step. However, to further address this question, we need to characterise the strain and to deeply delineate the phenotypes.

The first aim of my thesis was **to characterise the genome of *RI* Norway and symbiotic genes of the strain**. To approach this, we sequenced the genome of *RI* Norway and analysed its phylogeny. We compared it with its close relative *RI* bv. *viciae* 3841, which is a nitrogen-fixing symbiont of *Vicia* plants. In addition, we characterised traits of *RI* Norway, including the colony morphology, the bacterial shape, and the carbon source utilisation.

The second aim of this study was **to investigate the infection mechanism that *RI* Norway employs to infect *Lotus***. The preliminary study indicates that *RI* Norway induced a larger number of nodules on *L. burtii* in comparison with other *Lotus* hosts. The infection process on *L. burtii* was studied by different microscopic approaches. To further investigate the host response to *RI* Norway, the expression of symbiotic marker genes involved in the infection upon *RI* Norway inoculation were determined by quantitative reverse transcription polymerase chain reaction (qRT-PCR). Furthermore, to study the role of Nod factors in the infection, a *nodC* mutant was generated by homologous recombination mutagenesis method. To investigate the role of Nod factors in the internalisation process, transgenic roots overexpressing SYMRK and forming spontaneous nodules were inoculated with the *nodC* mutant. Confocal microscopy was used to inspect the intracellular colonisation of the *nodC* mutant on the nodule.

Root colonisation is a prerequisite for the establishment of root nodule symbiosis. As *RI* Norway was co-isolated together with *Mn* 10.2.2, it is hypothesised that there are interactions between these two strains. The third aim of this thesis was **to study how does the interaction of *RI* Norway and *Mn* 10.2.2 affect the root colonisation**. The root colonisation of *RI* Norway and *Mn* 10.2.2 in both single and co-inoculation conditions was quantified. Later, the bacterial interactions required for root colonisation, including the swarming motility and *in vitro* biofilm formation, were examined with single- and co-cultures of rhizobia. Furthermore, to address the role of surface polysaccharides in the swarming motility and biofilm formation, mutants with impaired genes involved in the biosynthesis of the surface polysaccharides were investigated.

# Results

## Publication I:

Complete genome of *Rhizobium leguminosarum* Norway, an ineffective *Lotus* micro-symbiont

EXTENDED GENOME REPORT

Open Access



# Complete genome of *Rhizobium leguminosarum* Norway, an ineffective *Lotus* micro-symbiont

Juan Liang<sup>†</sup>, Anne Hoffrichter<sup>†</sup>, Andreas Brachmann and Macarena Marín\* 

## Abstract

Rhizobia bacteria engage in nitrogen-fixing root nodule symbiosis, a mutualistic interaction with legume plants in which a bidirectional nutrient exchange takes place. Occasionally, this interaction is suboptimal resulting in the formation of ineffective nodules in which little or no atmospheric nitrogen fixation occurs. *Rhizobium leguminosarum* Norway induces ineffective nodules in a wide range of *Lotus* hosts. To investigate the basis of this phenotype, we sequenced the complete genome of *RI* Norway and compared it to the genome of the closely related strain *R. leguminosarum* bv. *viciae* 3841. The genome comprises 7,788,085 bp, distributed on a circular chromosome containing 63% of the genomic information and five large circular plasmids. The functionally classified bacterial gene set is distributed evenly among all replicons. All symbiotic genes (*nod*, *fix*, *nif*) are located on the pRLN3 plasmid. Whole genome comparisons revealed differences in the metabolic repertoire and in protein secretion systems, but not in classical symbiotic genes.

**Keywords:** Symbiosis, *Rhizobium*, Legume, Ineffective nodulation, Genome

## Introduction

Legume crops are central to sustainable agricultural practices and food security [1, 2]. They have a low need for synthetic nitrogen fertilizers input, as they engage in a symbiosis with a group of diazotrophic bacteria collectively known as rhizobia. This symbiotic interaction is initiated by a molecular crosstalk between rhizobia and their cognate legume host. Upon recognition of specific signals, legume plants intracellularly accommodate rhizobia inside root organs called nodules, where they engage in a bidirectional nutrient exchange [3]. Occasionally, suboptimal interactions establish between the symbiotic partners. These lead to the formation of ineffective nodules in which limited to no nitrogen fixation occurs. These ineffective symbiotic associations are characterized by the formation of small white nodules, which results in reduced or no plant growth promotion [4].

Ineffective nitrogen-fixing symbioses have been described after introduction of crop legumes into areas where previously native legumes grew. The soil microbiota

associated to native species can often outcompete inoculant strains [5]. For instance, ineffective nitrogen fixation occurs in fields where perennial and annual clovers co-exist [6, 7]. In field trials, inoculant strains were unable to completely overcome indigenous *R. leguminosarum* bv. *trifolii* strains and occupied on average 50% of the nodules [8]. In extreme cases, it has been shown that endogenous rhizobia can completely block the nodulation of introduced rhizobia. For example, the nodulation of pea cultivars Afghanistan and Iran by rhizobial inoculants is suppressed in natural soils by the presence of a non-nodulating strain [9]. However, although ineffective nodulation is a limiting factor for sustainable agriculture, the molecular basis underlying it remains largely unknown [10].

*Rhizobium leguminosarum* (*RI*) strains are cognate micro-symbionts of legumes, including *Pisum*, *Lens*, *Lathyrus*, *Vicia*, *Phaseolus* and *Trifolium* [11]. However, a *R. leguminosarum* strain isolated from a *Lotus corniculatus* nodule in Norway exhibits a different compatibility range that includes several *Lotus* species and ecotypes. *RI* Norway does not induce effective nodules in any *Lotus* species tested so far [12]. Strikingly, there are host genotype specific differences in the nodulation phenotypes

\* Correspondence: [m.marin@biologie.uni-muenchen.de](mailto:m.marin@biologie.uni-muenchen.de)

<sup>†</sup>Juan Liang and Anne Hoffrichter contributed equally to this work.  
Institute of Genetics, Faculty of Biology, Ludwig-Maximilians-University Munich, Munich, Germany



induced by *Rl* Norway, as it cannot induce nodules on *L. japonicus* Gifu, but induces bumps on *L. japonicus* Nepal, and white nodules on *L. burttii* and *L. japonicus* MG-20. This is in contrast to compatible *Mesorhizobium* strains that induce monomorphic phenotypes in the same plant ecotypes [12].

The striking diversity of ineffective nodulation phenotypes induced by *Rl* Norway in *Lotus* motivated us to sequence and annotate its complete genome, and to compare it to the published genome of *R. leguminosarum* bv. *viciae* 3841 (*Rlv* 3841), a well-characterised *R. leguminosarum* strain. Here, we show that the genomes are largely conserved. There are no major differences in the *nif* and *fix* clusters required for nitrogen fixation and in the *nod* cluster essential for the production of nodulation factor. However, differences were observed in terms of metabolic and protein secretion system genes.

## Organism information

### Classification and features

*Rl* Norway is a Gram-negative strain in the order *Rhizobiales* of the class *Alphaproteobacteria* (Table 1). Cells are rod-shaped and have dimensions of  $0.84 \pm 0.11 \mu\text{m}$  in width and  $1.43 \pm 0.31 \mu\text{m}$  in length (Fig. 1a). This strain is fast growing and forms colonies after 3 days in TY medium at 28 °C. Colonies on TY are circular and slightly domed, their surface is shiny and smooth, and their texture is moderately mucoid (Fig. 1b).

The phylogenetic relationship of *Rl* Norway was inferred based on a concatenated tree of the *dnaK*, *recA*, and *rpoB* house-keeping genes (Fig. 2). Based on this phylogeny *Rl* Norway is placed within the *R. leguminosarum* group. The 16S rRNA gene of *Rl* Norway shows more than 99.9% identity with its orthologs in other *R. leguminosarum* strains, such as

**Table 1** Classification and general features of *Rl* Norway in accordance to the MIGS recommendations [46] published by the Genome Standards Consortium [47]

MIGS ID	Property	Term	Evidence code <sup>a</sup>
	Classification	Domain Bacteria	TAS [48]
		Phylum <i>Proteobacteria</i>	TAS [49]
		Class <i>Alphaproteobacteria</i>	TAS [50, 51]
		Order <i>Rhizobiales</i>	TAS [50, 52]
		Family <i>Rhizobiaceae</i>	TAS [53–55]
		Genus <i>Rhizobium</i>	TAS [55–57]
		Species <i>Rhizobium leguminosarum</i>	TAS [55, 57–59]
	Gram stain	Negative	IDA
	Cell shape	Rod	IDA
	Motility	Motile	IDA
	Sporulation	Non-sporulating	NAS
	Temperature range	Mesophile	NAS
	Optimum temperature	28 °C	NAS
	pH range; Optimum	Not reported	
	Carbon source	Carbon sources sustaining growth are indicated in Figure S1	IDA
MIGS-6	Habitat	Soil, root nodule of <i>Lotus corniculatus</i>	TAS [12]
MIGS-6.3	Salinity	Not reported	
MIGS-22	Oxygen requirement	Aerobic	NAS
MIGS-15	Biotic relationship	Free-living/symbiotic	TAS [12]
MIGS-14	Pathogenicity	Non-pathogen	NAS
MIGS-4	Geographic location	Norway	TAS [12]
MIGS-5	Sample collection	17. August 2006	TAS [12]
MIGS-4.1	Latitude	61°10'54.6"	TAS [12]
MIGS-4.2	Longitude	08°57'54.5"	TAS [12]
MIGS-4.4	Altitude	Not available	

<sup>a</sup>Evidence codes - IDA Inferred from Direct Assay, TAS Traceable Author Statement (i.e., a direct report exists in the literature), NAS Non-traceable Author Statement (i.e., not directly observed for the living, isolated sample, but based on a generally accepted property for the species, or anecdotal evidence). These evidence codes are from the Gene Ontology project [60]

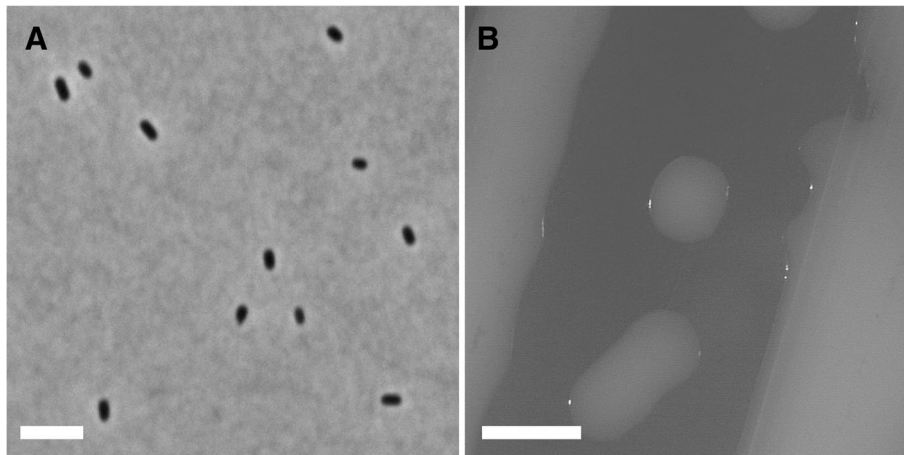


**Fig. 1** Morphological characterisation of *Rl* Norway. **a** Phase contrast micrograph of *Rl* Norway grown in liquid TY medium. Scale bar: 1  $\mu$ m. **b** Photomicrograph of the colony morphology of *Rl* Norway grown on TY medium. Scale bar: 1 mm

*Rlv* 3841 and *Rl* biovar *trifolii* WSM1325, WSM2304, and CB782.

The metabolic fingerprinting of *Rl* Norway was conducted with the Biolog GN2 MicroPlate. *Rl* Norway grew in multiple organic compounds as sole carbon source, these included Adonitol, L-Arabinose, D-Arabitol, D-Cellobiose, D-Fructose, and Glycerol, among others (Additional file 1: Figure S1). The metabolic fingerprinting of this strain was similar to the pattern described for other *R. leguminosarum* strains, but it was clearly distinct from the pattern of *Rlv* 3841 (Additional file 1: Figure S1) [13].

#### Symbiotaxonomy

*Rl* Norway was originally co-isolated from a *L. corniculatus* nodule together with two *Mesorhizobium* strains, but does not induce nodules in *L. corniculatus* or *L. japonicus*

Gifu, when inoculated alone [12]. However, it induces bumps on *L. japonicus* Nepal, and ineffective nodules on *L. burtii* and *L. japonicus* MG-20 [12]. This polymorphic nodulation phenotype is not observed, when these hosts are inoculated with *Mesorhizobium* strains [12]. *Rl* Norway induces ineffective nodules in *Pisum*, and *Latyrus*. The nodulation and symbiotic characteristics of *Rl* Norway are summarized in Additional file 2: Table S1.

#### Genome sequencing information

##### Genome project history

*Rl* Norway was selected for sequencing, because of the striking diversity of ineffective nodulation phenotypes that it induces in *Lotus*, a host that belongs to a different cross-inoculation group. The complete genome sequencing was performed at the Genomics Service Unit (LMU Biocenter, Munich). The nucleotide sequences reported



**Fig. 2** Phylogenetic tree showing the relationship between *Rl* Norway and other Rhizobia. The tree was constructed by maximum likelihood using the concatenated sequences of *recA*, *dnaK*, and *rpoB*. The calculated bootstrap values are indicated at the nodes. *Rl* Norway is highlighted in bold grey. Type strains are indicated with superscript <sup>T</sup>. *B. japonicum* USDA6 was used as an out-group

in this study have been deposited in the GenBank database under accession numbers CP025012.1, CP025013.1, CP025014.1, CP025015.1, CP025016.1, and CP025017.1. The data is summarized in Table 2.

#### Growth conditions and genomic DNA preparation

*Rl* Norway was grown at 28 °C and 180 rpm for 2 days in TY medium. Genomic DNA was isolated from 30 ml of a bacterial suspension ( $OD_{600} = 1.0$ ) using the CTAB method [14]. The DNA quality was determined by nanodrop and gel electrophoresis.

#### Genome sequencing and assembly

The genome was sequenced using a combination of Illumina and MinION sequencing technologies. Library construction and sequencing were performed at the Genomics Service Unit (LMU Biocenter, Munich). For whole genome sequencing a short read DNA library was generated with the Nextera Kit (Illumina) according to manufacturer's instructions. Sequencing ( $2 \times 150$  bp, v2 chemistry) was performed on a MiSeq sequencer (Illumina) yielding around 15 Mio paired reads and 2.3 Gb of primary sequence. A long read library was prepared with the 1D Genomic DNA Sequencing Kit (Oxford Nanopores) according to manufacturer's instructions. MinION (Oxford Nanopores) sequencing resulted in around 180,000 sequences with a total of 670 Mb primary sequence (mean length 3.8 kb). Hybrid genome assembly with Unicycler v0.4.0 [15] using default settings resulted in six circular contigs. The average base coverage of the genome is 380x.

#### Genome annotation

Genome annotation was performed with RAST 2.0 [16, 17] and MicroScope [18]. Clusters of orthologous groups (COGs) of proteins were predicted using the COGNiTOR

software [19], signal peptides were detected using the SignalP 4.1 server [20], and Pfam domains were predicted using the Pfam batch sequence search from EMBL-EBI [21]. Transmembrane predictions and CRISPR repeats were determined using the TMHMM Server v. 2.0 [22] and CRISPRFinder [23], respectively. All genes discussed in the text were manually inspected.

#### Genome properties

The genome of *Rl* Norway consists of 7,788,085 bp, distributed on a circular chromosome containing 63% of the genomic information and five large circular plasmids ranging from 280 to 1098 kb (Fig. 3). The complete genome and the chromosome are comparable in size to other *R. leguminosarum* strains [13, 24]. The chromosome contains three identical rRNA operons and 54 tRNA genes, none of which are found on any of the five plasmids (Table 3 and Fig. 3). In total 7866 protein-encoding genes were identified. BUSCO analysis [25] confirmed complete presence of the core bacteria dataset. The six replicons have a comparable mix of functional classes (Additional file 3: Figure S2A). However, all genes from the BUSCO core bacteria dataset are located on the chromosome, with only a few additional gene duplications on the plasmid replicons.

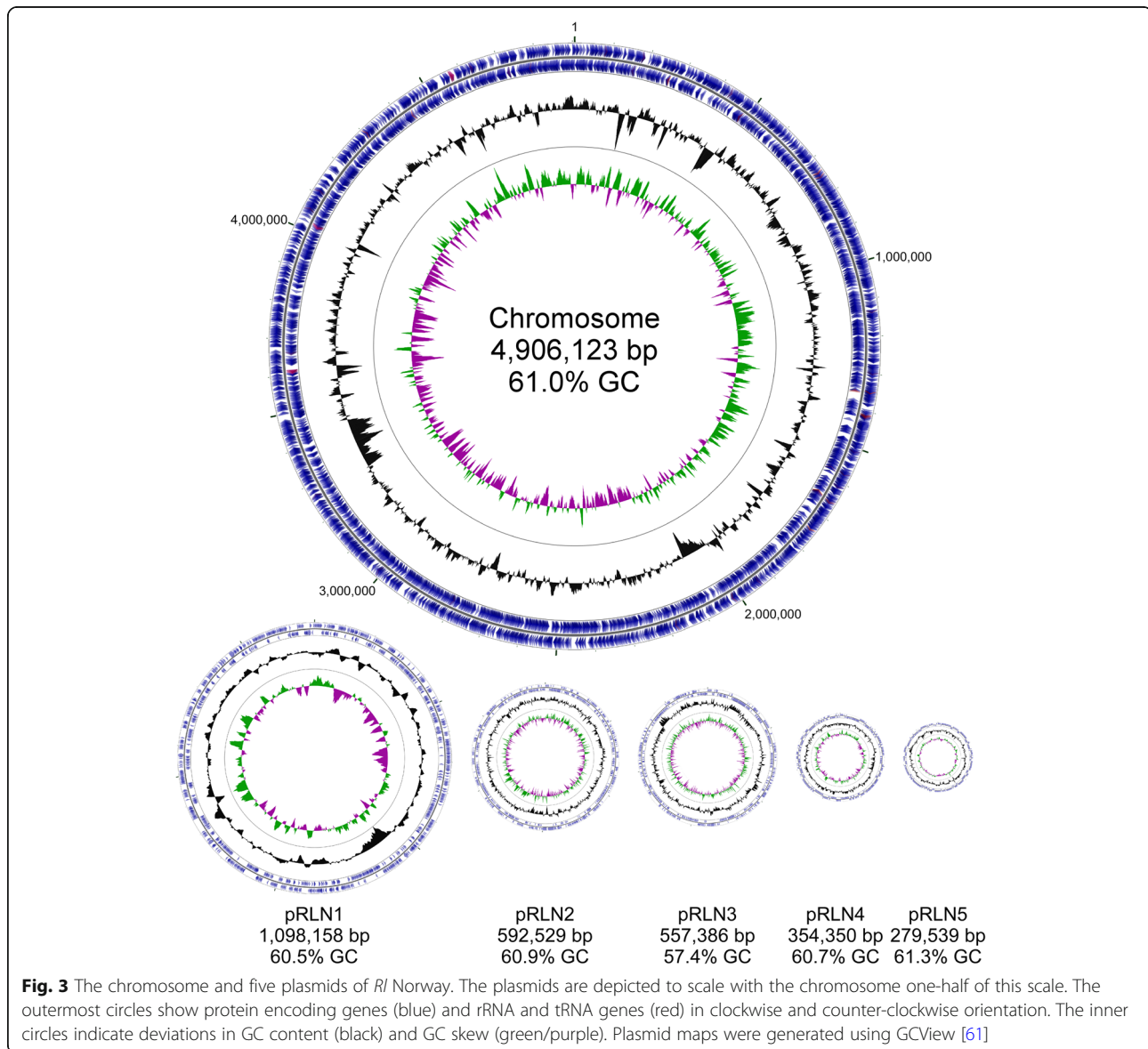
#### Insights from the genome sequence

##### Extended insights

The genomes of *Rl* Norway and *Rlv* 3841 have a very similar relative occurrence of functional protein encoding genes (Additional file 3: Figure S2B) and do not show any gross genomic alterations. Interestingly, although *Rl* Norway contains more protein encoding genes than *Rlv* 3841 (7866 vs. 7263 genes), the number of genes for which a functional annotation could be retrieved is almost identical (6106 vs. 6105 genes). Hence, the major difference

**Table 2** Genome sequencing project information for *Rl* Norway

MIGS ID	Property	Term
MIGS 31	Finishing quality	Finished
MIGS-28	Libraries used	Paired-end (Illumina); 1D Genomic (Nanopore)
MIGS 29	Sequencing platforms	Illumina MiSeq; Nanopore MinION
MIGS 31.2	Fold coverage	380x
MIGS 30	Assemblers	Unicycler v0.4.0
MIGS 32	Gene calling method	MicroScope
	Locus Tag	CUJ84
	Genbank ID	CP025012.1, CP025013.1, CP025014.1, CP025015.1, CP025016.1, and CP025017.1
	GenBank Date of Release	31. January 2018
	BIOPROJECT	<a href="https://bioproject.ncbi.nlm.nih.gov/submitter/PRJNA417364">PRJNA417364</a>
MIGS 13	Project relevance	Agriculture, root nodule symbiosis
	Source Material Identifier	<i>Rhizobium leguminosarum</i> Norway



lies in the number of not functionally classifiable genes (1760 vs. 1158 genes) (Table 4).

#### Plasmid repertoire and genospecies classification

The five plasmids contain one set of putative *repABC* replication system genes each [26]. Comparative analysis of the Rep proteins from *Rl* Norway with those from *Rlv* 3841 revealed high identity between plasmids pRLN1 and pRL12, between pRLN2 and pRL11, and between pRLN5 and pRL10 (Fig. 4a). Gene content comparison and synteny analysis supported this result. Although large portions of pRLN4 and pRL9 are similar (Fig. 4b, and c), the RepABC proteins encoded in pRLN4 are more similar to their orthologs in pRL32503.

Plasmid pRLN3 is slightly different than the other replicons of *Rl* Norway (Additional file 3: Figure S2A). It

does not exhibit significant similarity to *Rlv* 3841 (Fig. 4b, and c), has a slightly lower GC content and a lower proportion of protein encoding sequences (Additional file 4: Table S2), and has a higher proportion of putative encoded proteins without known homologs (Additional file 3: Figure S2A). In addition, it is the only plasmid containing potentially active transposons (2 copies) and several incomplete and therefore most likely inactivated transposon copies. The pRLN3 RepABC proteins share high similarity to their orthologs in pRL1.

For genospecies classification, we compared the *Rl* Norway genome to representatives of the five proposed genospecies (gsA-gsE) [13]. Typically, genomes are regarded to belong to the same species if the ANI values are above 95%. The two highest average nucleotide identity (ANI) scores (*Rl* CC278f: 96.34%; *Rl* SM51: 95.59%)

**Table 3** Genome statistics for *Rl* Norway

Attribute	Value	%of Total
Genome size (bp)	7,788,085	100.00
DNA coding (bp)	6,859,686	88.08
DNA G + C (bp)	4,659,466	59.83
DNA scaffolds	6	100.00
Total genes	8079	100.00
Protein coding genes	7866	97.36
RNA genes	73	0.90
Pseudo genes	150	1.86
Genes in internal clusters	Not determined	Not determined
Genes with function prediction	6147	76.09
Genes assigned to COGs	6106	75.58
Genes with Pfam domains	6295	77.92
Genes with signal peptides	619	7.66
Genes with transmembrane helices	1656	20.50
CRISPR repeats	0	0.00

were found with members of the genospecies gsD. All other comparisons resulted in ANI scores below 95% (Table 5). The ANI score between *Rl* Norway and *Rlv* 3841, which belongs to gsB, is only 93.26%. Although genospecies gsA and *Rl* CC278f in gsD are not yet well supported [13], the results indicate that *Rl* Norway belongs to genospecies gsD. This also fits well with *Rl* Norway having a plasmid subtype combination typical for gsD strains ([13]& personal communication Peter Young).

#### Central metabolism

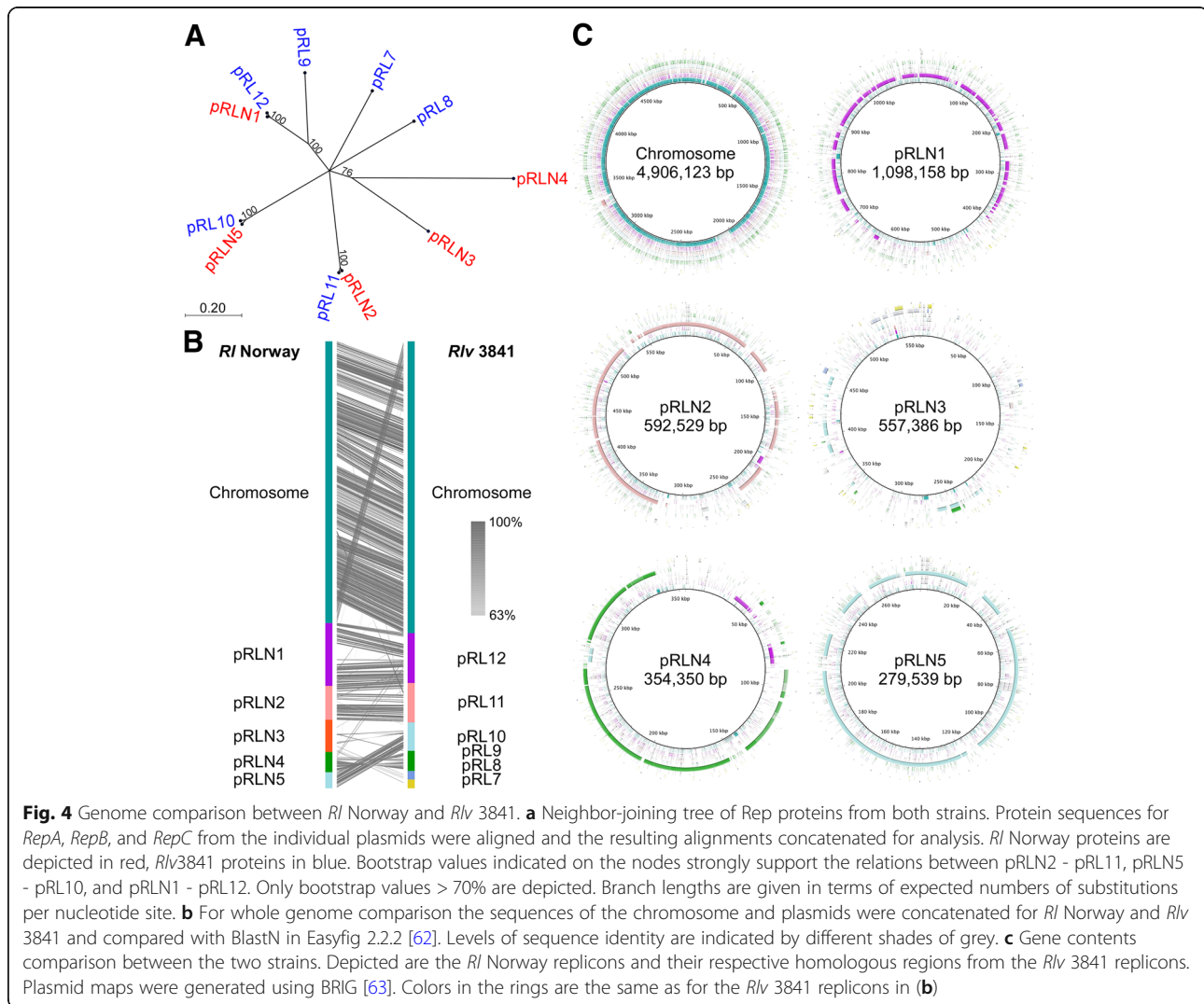
In terms of central metabolic genes *Rl* Norway resembles *Rlv* 3841. Both strains harbour genes encoding enzymes of the tricarboxylic acid (TCA) cycle required for aerobic respiration and energy production [27], of the pentose phosphate pathway required for the oxidation of glucose and the synthesis of nucleotides [28], and of the Entner-Doudoroff pathway for the catabolism of glucose to pyruvate [29]. Both strains lack a gene encoding the phosphofructokinase, an essential enzyme of the Embden-Meyerhof-Parnas glycolysis. These genetic similarities were reflected in a similar growth

**Table 4** Number of genes associated with general COG functional categories

Code	Value	%age	Description
J	210	2.67	Translation, ribosomal structure and biogenesis
A	0	0	RNA processing and modification
K	686	8.72	Transcription
L	219	2.78	Replication, recombination and repair
B	2	0.03	Chromatin structure and dynamics
D	40	0.51	Cell cycle control, Cell division, chromosome partitioning
V	74	0.94	Defense mechanisms
T	415	5.28	Signal transduction mechanisms
M	334	4.25	Cell wall/membrane biogenesis
N	92	1.17	Cell motility
U	106	1.35	Intracellular trafficking and secretion
O	199	2.53	Posttranslational modification, protein turnover, chaperones
C	342	4.35	Energy production and conversion
G	709	9.01	Carbohydrate transport and metabolism
E	831	10.56	Amino acid transport and metabolism
F	117	1.49	Nucleotide transport and metabolism
H	210	2.67	Coenzyme transport and metabolism
I	270	3.43	Lipid transport and metabolism
P	318	4.04	Inorganic ion transport and metabolism
Q	206	2.62	Secondary metabolites biosynthesis, transport and catabolism
R	905	11.51	General function prediction only
S	630	8.01	Function unknown
–	1760	22.37	Not in COGs

The total is based on the total number of protein coding genes in the genome





pattern in different carbon sources using Biolog GN2 MicroPlates (Additional file 1: Figure S1) [13].

A noticeable difference in the Biolog assay was the assimilation of amino acids such as D- and L-alanine, L-serine and L-proline, and nucleosides. However, no major differences were observed in the genes mediating their metabolism. The only clear exceptions were that *Rf*

**Table 5** Genome comparison of *Rf* Norway with members of the five genospecies and the respective ANI scores

	Norway vs	One-way ANI 1	One-way ANI 2	Two-way ANI
(gsA)	WSM1325	93.45%	93.52%	93.70%
gsB	3841	93.01%	93.06%	93.26%
gsC	TA1	93.75%	93.80%	93.94%
gsD	SM51	95.40%	95.40%	95.59%
(gsD)	CC278f	96.11%	96.19%	96.34%
gsE	128C53	94.66%	94.75%	94.84%

Norway lacks a putative D-serine deaminase required for the conversion of D-serine to pyruvate, but contains two putative aspartate ammonia-lyases (CUJ84\_pRLN3000095, CUJ84\_pRLN3000303) and two putative asparagine synthetases (CUJ84\_pRLN3000485, CUJ84\_pRLN3000155). In terms of amino acid transport, two ABC-type broad specificity amino-acid transporters have been characterized in *Rlv* 3841, Aap (AapJQMP) and Bra (BraDEFGC) [30]. The *bra* (CUJ84\_Ch003782–3787) and *aap* (CUJ84\_Ch001810–1813) clusters are highly conserved in *Rf* Norway. Another interesting difference concerned the metabolism of butanoate. In contrast to *Rlv* 3841, *Rf* Norway did not grow on  $\gamma$ -hydroxybutyric acid (Additional file 1: Figure S1). This is supported by the lack of a gene cluster (pRL100133–138 in *Rlv* 3841) associated to  $\gamma$ -hydroxybutyrate utilisation [13]. Furthermore, *Rf* Norway harbours an ortholog to the *phbC1* gene (CUJ84\_Ch001779), but lacks *phbC2*.

These genes encode type I and type III poly- $\beta$ -hydroxybutyrate (PHB) synthases, which are required for free-living and bacteroid PHB biosynthesis, respectively [31].

### Secretion systems

Gram-negative bacteria secrete a suite of proteins via macromolecular complexes that have been classified as type 1–6 secretion systems in addition to the *sec* and *tat* transport systems [32]. A survey of the *Rl* Norway genome indicates that this strain contains a large repertoire of secretion systems that is distinct from the repertoire of *Rlv* 3841 (Table 6). *Rl* Norway harbours five putative type 1 secretion systems (T1SS; Table 6). T1SSa, T1SSb and T1SSc are unique to *Rl* Norway. Interestingly, the genes encoding the T1SSa and T1SSc systems form operons with two large genes encoding putative repeats-in-

toxin (RTX) toxins. The proteins forming the T1SSd and T1SSe have orthologs with more than 90% identity in *Rlv* 3841. For instance, the T1SSd proteins are orthologous to the PrsD and PrsE proteins of *Rlv* 3841 that are required for biofilm formation [33]. Like *Rlv* 3841, *Rl* Norway lacks T2SS and T3SS, but harbours T4SS and T6SS [34].

*Bacteria* utilize T3SS, T4SS and/or T6SS to inject effector proteins directly into eukaryotic host cells or into other bacteria [35–37]. In rhizobia, these effectors can mediate compatibility with the host [38]. *Rl* Norway harbours a putative T4SS that is distinct from the T4SS from *Rlv* 3841. The respective T4SS encoding *virB* operons are not syntenic and the encoding genes share on average less than 30% identity. The T4SS of *Rl* Norway is encoded in the pRLN1 plasmid and is predicted to translocate proteins and not DNA, as *Rl* Norway lacks a VirD2 relaxase [39]. In addition, it has the peculiarity that the *virB11* gene is partially duplicated and two genes are located in-between the duplication.

*Rl* Norway and *Rlv* 3841 harbour syntenic *imp* (*tss*) and *hcp* clusters encoding type (i) T6SS. In both cases the *imp* cluster is lacking orthologs to the *evpJ* and *tssJ* genes. However, a comparison to *Agrobacterium tumefaciens* C58 revealed that these genes are also absent in the corresponding *imp* and *hcp* operons (atu4330-atu4352). In addition, all essential genes for protein secretion are conserved [40].

T5SS are structures in which the cargo protein translocates itself across the plasma membrane. These are classified into auto-transporters (translocator and cargo encoded in the same gene) and two-partner systems (translocator and cargo are encoded by two separate genes) [41]. *Rl* Norway harbours two T5SS auto-transporters. However, T5SSb is split into two genes and it is probably not a bona fide T5SS. *Rl* Norway also has one two-partner system, in which the cargo protein is a putative filamentous hemagglutinin (Table 6). In contrast, *Rlv* 3841 contains three auto-transporters, but no two-partner system [34].

### Symbiotic gene repertoire

Plasmid pRLN3 harbours all symbiotic genes in *Rl* Norway. The *nod* genes that are required for the synthesis and export of the nodulation factor, a key determinant in compatibility, are organised in one cluster (CUJ84\_pRLN3000416–426) comprising the *nodJICBADFELMN* genes. They have the same organisation as the *nod* cluster in *Rlv* 3841 [24], and the encoded proteins share at least 93.6% identity with their *Rlv* 3841 orthologs. However, in contrast to *Rlv* 3841, *Rl* Norway lacks *nodO* and *nodT* orthologs in the proximity of the *nod* cluster. Interestingly, genes encoding putative transposases flank the *Rl* Norway *nod* cluster. The genes required for nitrogen fixation are

**Table 6** Secretion system repertoire in *Rl* Norway

Secretion system	Location	Mandatory genes (gene identifier)
Type 1 secretion system (T1SS)		
T1SSa	Chromosome	<i>hlyD</i> (CUJ84_Ch000199), <i>hlyB</i> (CUJ84_Ch000200)
T1SSb	Chromosome	<i>hlyD</i> (CUJ84_Ch000279), <i>hlyB</i> (CUJ84_Ch000280)
T1SSc	Chromosome	<i>hlyD</i> (CUJ84_Ch002330), <i>hlyB</i> (CUJ84_Ch002331)
T1SSd	Chromosome	<i>prsE</i> (CUJ84_Ch003677), <i>prsD</i> (CUJ84_Ch003678)
T1Sse	Chromosome	<i>hlyD</i> (CUJ84_Ch004833), <i>hlyB</i> (CUJ84_Ch004834)
T4SSa	pRLN1	<i>virB1</i> (CUJ84_pRLN1000390), <i>virB2</i> (CUJ84_pRLN1000391), <i>virB3</i> (CUJ84_pRLN1000392), <i>virB4</i> (CUJ84_pRLN1000393), <i>virB5</i> (CUJ84_pRLN1000394), <i>virB6</i> (CUJ84_pRLN1000396), <i>virB8</i> (CUJ84_pRLN1000398), <i>virB9</i> (CUJ84_pRLN1000399), <i>virB10</i> (CUJ84_pRLN1000400)
Type 5 secretion system (T5SS)		
T5SSa	Chromosome	<i>autB</i> (CUJ84_Ch000739)
T5SSb	Chromosome	Partial <i>autB</i> (CUJ84_Ch002323)
T5SSc	pRLN2	<i>tpsA</i> (CUJ84_pRLN2000298), <i>tpsB</i> (CUJ84_pRLN2000297)
Type 6 secretion system (T6SS)		
T6SS	pRLN1	<i>tssB</i> (CUJ84_pRLN1000762), <i>tssC</i> (CUJ84_pRLN1000760, CUJ84_pRLN1000761), <i>tssD</i> (CUJ84_pRLN1000765), <i>tssE</i> (CUJ84_pRLN1000758), <i>tssF</i> (CUJ84_pRLN1000757), <i>tssG</i> (CUJ84_pRLN1000756), <i>tssH</i> (CUJ84_pRLN1000764), <i>tssI</i> (CUJ84_pRLN1000767), <i>tssK</i> (CUJ84_pRLN1000754), <i>tssL</i> (CUJ84_pRLN1000753), <i>tssM</i> (CUJ84_pRLN1000752)

located in proximity. The *fixABCX* (CUJ84\_pRLN3000397–400) and the *nifAB* genes (CUJ84\_pRLN3000401–402) are located almost directly downstream *nodJ*, whereas *nifNEKDH* (CUJ84\_pRLN3000271–275), *fixSIHG* (CUJ84\_pRLN3000258–261) and *fixPQON* (CUJ84\_pRLN3000263–266) are located approximately 137.5 kb downstream of *nodJ*. The three subunits of the nitrogenase encoded by the *nifHDK* genes share 99.7, 93.5, and 96.3% identity to their respective *Rlv* 3841 orthologs. A noteworthy difference between both strains is that *Rl* Norway harbours a single *fixNOQP* operon encoding the essential *cbb<sub>3</sub>* terminal oxidase, whereas *Rlv* 3841 contains two copies [24]. Furthermore, *Rl* Norway lacks genes encoding the FixK and FixL transcriptional regulators, which together with FnrN control the expression of the nitrogen fixation genes in other rhizobia strains [42]. Instead, *Rl* Norway harbours two putative *fmrN* genes (CUJ84\_Chrom002641, CUJ84\_pRLN3000544) that are located in the chromosome and in the pRLN3 symbiotic plasmid. This is reminiscent of *R. leguminosarum* bv. *viciae* UPM791, in which FnrN is the global regulator of the fix genes. In this strain, FnrN is regulated by micro-aerobic conditions and binds a palindromic element called anaerobox [43, 44]. Putative anaerobox sequences were found upstream of *fmrN1* (CUJ84\_Chrom002641) and the *fixNOQP* and *fixGHIS* operons, which suggest that FnrN might regulate their expression in *Rl* Norway. However, no anaerobox was found upstream of *fmrN2* (CUJ84\_pRLN3000544). Interestingly, *fmrN2* is approximately 16.5 kb upstream of a putative uptake hydrogenase cluster comprising 18 genes (CUJ84\_pRLN3000511–528). The cluster organisation resembles the *hup* and *hyp* genes from *Rlv* UPM791 [45]. Notably, *Rlv* 3841 lacks such a hydrogenase cluster.

## Conclusions

Although detrimental in agriculture, ineffective nitrogen-fixing symbiosis remains poorly investigated. In this regard, *Rl* Norway is an interesting strain as it exhibits a parasitic behaviour in a wide range of hosts. Comparative genomic analyses with other *R. leguminosarum* strains have the potential to reveal novel factors mediating symbiotic compatibility and efficiency.

## Additional files

**Additional file 1: Figure S1.** *Rl* Norway substrate utilization pattern determined by Biolog. In blue and yellow are indicated substrates only utilized by *Rl* Norway and *Rlv* 3841, respectively. Green indicates substrates used by both strains, whereas white depicts conditions in which both strains did not grow. *Rlv* 3841 utilization pattern was extracted from [1]. (TIF 9702 kb)

**Additional file 2: Table S1.** Nodulation phenotypes of *Rl* Norway on selected hosts. (DOCX 68 kb)

**Additional file 3: Figure S2.** Distribution of functional classes of protein encoding genes within the *Rl* Norway genome. (A) Functional class distribution across the six *Rl* Norway replicons. (B) Comparison

of the relative occurrence of functionally classified protein encoding genes between the *Rl* Norway and *Rlv* 3841 genomes. Functional annotation (COG) was performed on WebMGA server [1]. (TIF 10046 kb)

**Additional file 4: Table S2.** Genome statistics for *Rl* Norway. (DOCX 47 kb)

## Abbreviations

COGs: Clusters of orthologous groups; CTAB: Cetyl trimethylammonium bromide; DAMPs: Damage associated molecular patterns; PHB: Poly-β-hydroxybutyrate; *Rl*: *Rhizobium leguminosarum*; RTX: Repeats-in-toxin; T1SS: Type 1 secretion system; TCA: Tricarboxylic acid

## Acknowledgements

We thank Martin Parniske for providing the *Rl* Norway strain and critical reading of the manuscript, Moritz Thomas for expert technical assistance in MinION library preparation and sequencing, and Marion Cerri for insightful discussions and reading the manuscript. We specially thank Peter Young for sharing unpublished sequences and fruitful discussions.

## Funding

This work was funded by the German research foundation (DFG-grant: MA7269–1).

## Authors' contributions

JL performed the imaging, the chemotaxonomic analyses, and extracted the genomic DNA. AB conducted the genome sequencing and annotation. AH conducted the genome assembly and comparisons. MM conducted the phylogenetic analysis and the manual inspection of the annotation. MM and AB conceived the experiments and wrote the manuscript. All authors read and approved the final manuscript.

## Competing interests

The authors declare that they have no competing interests.

## Publisher's Note

Springer Nature remains neutral with regard to jurisdictional claims in published maps and institutional affiliations.

Received: 9 February 2018 Accepted: 10 November 2018

Published online: 05 December 2018

## References

1. Stagnari F, Maggio A, Galieni A, Pisante M. Multiple benefits of legumes for agriculture sustainability: an overview. *Chem Biol Technol Agric*. 2017;4(1):2.
2. Rubiales D, Mikic A. Introduction: legumes in sustainable agriculture. *Crit Rev Plant Sci*. 2015;34(1–3):2–3.
3. Oldroyd GE, Murray JD, Poole PS, Downie JA. The rules of engagement in the legume-rhizobial symbiosis. *Annu Rev Genet*. 2011;45:119–44.
4. Westhoek A, Field E, Rehling F, Mulley G, Webb I, Poole PS, Turnbull LA. Policing the legume-*Rhizobium* symbiosis: a critical test of partner choice. *Sci Rep*. 2017;7(1):1419.
5. Streeter JG. Failure of inoculant rhizobia to overcome the dominance of indigenous strains for nodule formation. *Can J Microbiol*. 1994;40(7):513–22.
6. Parker DT, Allen ON. The nodulation status of *Trifolium ambiguum*. *Soil Sci Soc Am Pro*. 1952;16(4):350–3.
7. Howieson JG, Yates RJ, O'Hara GW, Ryder M, Real D. The interactions of *Rhizobium leguminosarum* biovar *trifolii* in nodulation of annual and perennial *Trifolium* spp. from diverse centres of origin. *Aust J Exp Agric*. 2005;45(3):199–207.
8. Amesgottfred NP, Christie BR. Competition among strains of *Rhizobium leguminosarum* biovar *trifolii* and use of a diallel analysis in assessing competition. *Appl Environ Microb*. 1989;55(6):1599–604.
9. Winarno R, Lie TA. Competition between *Rhizobium* strains in nodule formation - interaction between nodulating and non-nodulating strains. *Plant Soil*. 1979;51(1):135–42.
10. Bohlool BB, Ladha JK, Garrity DP, George T. Biological nitrogen fixation for sustainable agriculture - a perspective. *Plant Soil*. 1992;141(1–2):1–11.
11. Fred EB, Baldwin IL, McCoy E. Root nodule bacteria and leguminous plants; 1932.

12. Gossmann JA, Markmann K, Brachmann A, Rose LE, Parniske M. Polymorphic infection and organogenesis patterns induced by a *Rhizobium leguminosarum* isolate from *Lotus* root nodules are determined by the host genotype. *New Phytol.* 2012;196(2):561–73.
13. Kumar N, Lad G, Giuntini E, Kaye ME, Udomwong P, Shamsani NJ, Young JPW, Bailly X. Bacterial genospecies that are not ecologically coherent: population genomics of *Rhizobium leguminosarum*. *Open Biol.* 2015;5(1):140133.
14. Murray MG, Thompson WF. Rapid isolation of high molecular-weight plant DNA. *Nucleic Acids Res.* 1980;8(19):4321–5.
15. Wick RR, Judd LM, Gorrie CL, Holt KE. Unicycler: Resolving bacterial genome assemblies from short and long sequencing reads. *PLoS Comput Biol.* 2017;13(6):e1005595.
16. Overbeek R, Olson R, Pusch GD, Olsen GJ, Davis JJ, Disz T, Edwards RA, Gerdes S, Parrello B, Shukla M, et al. The SEED and the rapid annotation of microbial genomes using subsystems technology (RAST). *Nucleic Acids Res.* 2014;42(D1):D206–14.
17. Aziz RK, Bartels D, Best AA, DeJongh M, Disz T, Edwards RA, Formsma K, Gerdes S, Glass EM, Kubal M, et al. The RAST server: rapid annotations using subsystems technology. *BMC Genomics.* 2008;9(1):75.
18. Vallenet D, Calteau A, Cruveiller S, Gachet M, Lajus A, Josso A, Mercier J, Renaux A, Rollin J, Rouy Z, et al. microScope in 2017: an expanding and evolving integrated resource for community expertise of microbial genomes. *Nucleic Acids Res.* 2017;45(D1):D517–28.
19. Tatusov RL, Koonin EV, Lipman DJ. A genomic perspective on protein families. *Science.* 1997;278:631–7.
20. Petersen TN, Brunak S, von Heijne G, Nielsen H. SignalP 4.0: discriminating signal peptides from transmembrane regions. *Nat Methods.* 2011;8:785.
21. Finn RD, Coghill P, Eberhardt RY, Eddy SR, Mistry J, Mitchell AL, Potter SC, Punta M, Qureshi M, Sangrador-Vegas A, et al. The Pfam protein families database: towards a more sustainable future. *Nucleic Acids Res.* 2016;44(D1):D279–85.
22. Krogh A, Larsson B, von Heijne G, Sonnhammer EL. Predicting transmembrane protein topology with a hidden Markov model: application to complete genomes. *J Mol Biol.* 2001;305:567–80.
23. Grissa I, Vergnaud G, Pourcel C. CRISPRFinder: a web tool to identify clustered regularly interspaced short palindromic repeats. *Nucleic Acids Res.* 2007;35:W52–7.
24. Young JP, Crossman LC, Johnston AW, Thomson NR, Ghazoui ZF, Hull KH, Wexler M, Curson AR, Todd JD, Poole PS, et al. The genome of *Rhizobium leguminosarum* has recognizable core and accessory components. *Genome Biol.* 2006;7(4):R34.
25. Simão FA, Waterhouse RM, Ioannidis P, Kriventseva EV, Zdobnov EM. BUSCO: assessing genome assembly and annotation completeness with single-copy orthologs. *Bioinformatics.* 2015;31(19):3210–2.
26. Ramírez-Romero MA, Soberón N, Pérez-Oseguera A, Téllez-Sosa J, Cevallos MA. Structural elements required for replication and incompatibility of the *Rhizobium etli* symbiotic plasmid. *J Bacteriol.* 2000;182(11):3117–24.
27. Dunn MF. Tricarboxylic acid cycle and anaplerotic enzymes in rhizobia. *FEMS Microbiol Rev.* 1998;22(2):105–23.
28. Stincone A, Prigione A, Cramer T, Wamelink MMC, Campbell K, Cheung E, Olin-Sandoval V, Gruning NM, Kruger A, Alam MT, et al. The return of metabolism: biochemistry and physiology of the pentose phosphate pathway. *Biol Rev.* 2015;90(3):927–63.
29. Conway T. The Entner-Doudoroff pathway - history, physiology and molecular biology. *FEMS Microbiol Lett.* 1992;103(1):1–28.
30. Hosie AHF, Allaway D, Galloway CS, Dunsby HA, Poole PS. *Rhizobium leguminosarum* has a second general amino acid permease with unusually broad substrate specificity and high similarity to branched-chain amino acid transporters (bra/LIV) of the ABC family. *J Bacteriol.* 2002;184(15):4071–80.
31. Terpolilli JJ, Masakapalli SK, Karunakaran R, Webb IUC, Green R, Watmough NJ, Kruger NJ, Ratcliffe RG, Poole PS. Lipogenesis and redox balance in nitrogen-fixing pea bacteroids. *J Bacteriol.* 2016;198(20):2864–75.
32. Green E, Meccas J. Bacterial secretion systems: an overview. In: Kudva I, Cornick N, Plummer P, Zhang Q, Nicholson T, Bannantine J, Bellaire B, editors. *Virulence mechanisms of bacterial pathogens*, Fifth Edition. Washington, DC: ASM Press; 2016. p. 215–39. <https://doi.org/10.1128/microbiolspec.VMBF-0012-2015>.
33. Russo DM, Williams A, Edwards A, Posadas DM, Finnie C, Dankert M, Downie JA, Zorreguieta A. Proteins exported via the PrsD-PrsE type I secretion system and the acidic exopolysaccharide are involved in biofilm formation by *Rhizobium leguminosarum*. *J Bacteriol.* 2006;188(12):4474–86.
34. Krehenbrink M, Downie JA. Identification of protein secretion systems and novel secreted proteins in *Rhizobium leguminosarum* bv. *viciae*. *BMC Genomics.* 2008;9(1):55.
35. Cianfanelli FR, Monlezun L, Coulthurst SJ. Aim, load, fire: the type VI secretion system, a bacterial nanoweapon. *Trends Microbiol.* 2016;24(1):51–62.
36. Ding ZY, Atmakuri K, Christie PJ. The outs and ins of bacterial type IV secretion substrates. *Trends Microbiol.* 2003;11(11):527–35.
37. Deng WY, Marshall NC, Rowland JL, McCoy JM, Worrall LJ, Santos AS, Strynadka NCJ, Finlay BB. Assembly, structure, function and regulation of type III secretion systems. *Nat Rev Microbiol.* 2017;15(6):323–37.
38. Nelson MS, Sadowsky MJ. Secretion systems and signal exchange between nitrogen-fixing rhizobia and legumes. *Front Plant Sci.* 2015;6:491.
39. Alvarez-Martinez CE, Christie PJ. Biological diversity of prokaryotic type IV secretion systems. *Microbiol Mol Biol Rev.* 2009;73(4):775–808.
40. Ma LS, Hachani A, Lin JS, Filloux A, Lai EM. *Agrobacterium tumefaciens* deploys a superfamily of type VI secretion DNase effectors as weapons for interbacterial competition in planta. *Cell Host Microbe.* 2014;16(1):94–104.
41. Abby SS, Cury J, Guglielmini J, Neron B, Touchon M, Rocha EP. Identification of protein secretion systems in bacterial genomes. *Sci Rep.* 2016;6:23080.
42. Fischer HM. Genetic regulation of nitrogen-fixation in rhizobia. *Microbiol Rev.* 1994;58(3):352–86.
43. Gutiérrez D, Hernando Y, Palacios JM, Imperial J, Ruiz-Argüeso T. FnrN controls symbiotic nitrogen fixation and hydrogenase activities in *Rhizobium leguminosarum* bv. *viciae* UPM791. *J Bacteriol.* 1997;179(17):5264–70.
44. Colombo MV, Gutiérrez D, Palacios JM, Imperial J, Ruiz-Argüeso T. A novel autoregulation mechanism of fnrN expression in *Rhizobium leguminosarum* bv. *viciae*. *Mol Microbiol.* 2000;36(2):477–86.
45. Baginsky C, Brito B, Imperial J, Palacios JM, Ruiz-Argüeso T. Diversity and evolution of hydrogenase systems in rhizobia. *Appl Environ Microbiol.* 2002;68(10):4915–24.
46. Field D, Garrity G, Gray T, Morrison N, Selengut J, Sterk P, Tatusova T, Thomson N, Allen MJ, Angiuoli SV, et al. The minimum information about a genome sequence (MIGS) specification. *Nat Biotechnol.* 2008;26(5):541–7.
47. Field D, Amaral-Zettler L, Cochrane G, Cole JR, Dawyndt P, Garrity GM, Gilbert J, Glockner FO, Hirschman L, Karsch-Mizrachi I, et al. The genomic standards consortium. *PLoS Biol.* 2011;9(6):e1001088.
48. Woese CR, Kandler O, Wheelis ML. Towards a natural system of organisms: proposal for the domains archaea, bacteria, and eucarya. *PNAS.* 1990;87(12):4576–9.
49. Garrity GM, Bell JA, Lilburn T, Phylum XIV. *Proteobacteria* phyl. nov., vol. 2, Part B, 2 edn. New York: Springer; 2005.
50. Euzéby J. Validation list no. 107. List of new names and new combinations previously effectively, but not validly, published. *Int J Syst Evol Microbiol.* 2006;56:1–6.
51. Garrity GM, Bell JA, Lilburn T, Class I. *Alphaproteobacteria* class. nov., vol. 2, Part C, 2nd ed. New York: Springer; 2005.
52. Kuykendall LD. Order VI. *Rhizobiales* ord. nov. In: *Bergey's Manual of Systematic Bacteriology*. Edited by Garrity GM, Brenner DJ, Kreig NR, Staley JT, vol. 2, Part C, 2 edn. New York: Springer; 2005: 324.
53. Kuykendall LD. *Rhizobiaceae*. In: Garrity GM, Brenner DJ, Kreig NR, Staley JT, editors. *Bergey's Manual of Systematic Bacteriology*. New York: Springer; 2005.
54. Conn HJ. Taxonomic relationships of certain non-sporeforming rods in soil. *J Bacteriol.* 1938;36:320–1.
55. Skerman VDB, McGowan V, Sneath PHA. Approved lists of bacterial names. *Int J Syst Bacteriol.* 1980;30(1):225–420.
56. Kuykendall LD, J.M. Y, Martínez-Romero E, Kerr A, Sawada H. *Rhizobium*. In: *Bergey's manual of systematic bacteriology*. Edited by Garrity GM, Brenner DJ, Kreig NR, Staley JT. New York: Springer; 2005.
57. Frank B. Über die Pilzsymbiose der Leguminosen. *Ber Dtsch Bot Ges.* 1889;7: 332–46.
58. Young JM, Kuykendall LD, Martínez-Romero E, Kerr A, Sawada H. A revision of *Rhizobium* frank 1889, with an emended description of the genus, and the inclusion of all species of *Agrobacterium* conn 1942 and *Allorhizobium undicola* de Lajudie et al. 1998 as new combinations: *Rhizobium radiobacter*, *R. rhizogenes*, *R. rubi*, *R. undicola* and *R. vitis*. *Int J Syst Evol Microbiol* 2001, 51(Pt 1):89–103.

59. Ramírez-Bahena MH, García-Fraile P, Peix A, Valverde A, Rivas R, Igual JM, Mateos PF, Martínez-Molina E, Velázquez E. Revision of the taxonomic status of the species *Rhizobium leguminosarum* (Frank 1879) Frank 1889AL, *Rhizobium phaseoli* Dangeard 1926AL and *Rhizobium trifolii* Dangeard 1926AL. *R. trifolii* is a later synonym of *R. leguminosarum*. Reclassification of the strain *R. leguminosarum* DSM 30132 (=NCIMB 11478) as *Rhizobium pisi* sp. nov. *Int J Syst Evol Microbiol*. 2008;58(Pt 11):2484–90.
60. Ashburner M, Ball CA, Blake JA, Botstein D, Butler H, Cherry JM, Davis AP, Dolinski K, Dwight SS, Eppig JT, et al. Gene ontology: tool for the unification of biology. the Gene Ontology Consortium. *Nat Genet*. 2000;25(1):25–9.
61. Stothard P, Wishart DS. Circular genome visualization and exploration using CGView. *Bioinformatics*. 2005;21(4):537–9.
62. Sullivan MJ, Petty NK, Beatson SA. Easyfig: a genome comparison visualizer. *Bioinformatics*. 2011;27(7):1009–10.
63. Alikhan NF, Petty NK, Ben Zakour NL, Beatson SA. BLAST ring image generator (BRIG): simple prokaryote genome comparisons. *BMC Genomics*. 2011;12(1):1.

**Ready to submit your research? Choose BMC and benefit from:**

- fast, convenient online submission
- thorough peer review by experienced researchers in your field
- rapid publication on acceptance
- support for research data, including large and complex data types
- gold Open Access which fosters wider collaboration and increased citations
- maximum visibility for your research: over 100M website views per year

**At BMC, research is always in progress.**

Learn more [biomedcentral.com/submissions](https://biomedcentral.com/submissions)



## Supplementary materials

A1 Water	A2 $\alpha$ -Cyclodextrin	A3 Dextrin	A4 Glycogen	A5 Tween 40	A6 Tween 80	A7 N-Acetyl-D-galactosamine	A8 N-Acetyl-D-glucosamine	A9 Adonitol	A10 L-Arabinose	A11 D-Arabitol	A12 D-Cellulose
B1 l-Erythritol	B2 D-Fructose	B3 L-Fucose	B4 D-Galactose	B5 Gentiobiose	B6 $\alpha$ -D-Glucose	B7 m-Inositol	B8 $\alpha$ -D-Lactose	B9 Lactulose	B10 Maltose	B11 D-Mannitol	B12 D-Mannose
C1 D-Melibiose	C2 $\beta$ -Methyl-D-Glucoside	C3 D-Palcose	C4 D-Raffinose	C5 L-Rhamnose	C6 D-Sorbitol	C7 Sucrose	C8 D-Trehalose	C9 Turannose	C10 Xylitol	C11 Methyl Pyruvate	C12 Mono-Methyl-Succinate
D1 Acetic Acid	D2 Cis-Aconitic Acid	D3 Citric Acid	D4 Formic Acid	D5 D-Galactonic Acid Lactone	D6 D-Galacturonic Acid	D7 D-Gluconic Acid	D8 D-Glucosaminic Acid	D9 D-Glucuronic Acid	D10 $\alpha$ -Hydroxy Butyric Acid	D11 $\beta$ -Hydroxy Butyric Acid	D12 $\gamma$ -Hydroxy Butyric Acid
E1 p-Hydroxy Phenylacetic Acid	E2 Itaconic Acid	E3 $\alpha$ -Keto Butyric Acid	E4 $\alpha$ -Keto Glutaric Acid	E5 $\alpha$ -Keto Valeric Acid	E6 D,L-Lactic Acid	E7 Malonic Acid	E8 Propionic Acid	E9 Quinic Acid	E10 D-Saccharic Acid	E11 Sebacic Acid	E12 Succinic Acid
F1 Bromo Succinic Acid	F2 Succinamic Acid	F3 Glucuronamide	F4 L-Alaninamide	F5 D-Alanine	F6 L-Alanine	F7 L-Alanyl-glycine	F8 L-Asparagine	F9 L-Aspartic Acid	F10 L-Glutamic Acid	F11 Glycyl-L-Aspartic Acid	F12 Glycyl-L-Glutamic Acid
G1 L-Histidine	G2 Hydroxy-L-Proline	G3 L-Leucine	G4 L-Ornithine	G5 L-Phenylalanine	G6 L-Proline	G7 L-Pyrogutamic Acid	G8 D-Serine	G9 L-Serine	G10 L-Threonine	G11 D,L-Carnitine	G12 $\gamma$ -Amino Butyric Acid
H1 Urocanic Acid	H2 Inosine	H3 Uridine	H4 Thymidine	H5 Phenyethylamine	H6 Putrescine	H7 2-Aminoethanol	H8 2,3-Butanediol	H9 Glycerol	H10 D,L- $\alpha$ -Glycerol Phosphate	H11 Glucose-1-Phosphate	H12 Glucose-6-Phosphate

**Figure S1. *R/* Norway substrate utilization pattern determined by Biolog.** In blue and yellow are indicated substrates only utilized by *R/* Norway and *R/v* 3841, respectively. Green indicates substrates used by both strains, whereas white depicts condition in which both strains did not grow. *R/v* 3841 utilization pattern was extracted from [1].

1. Kumar N, Lad G, Giuntini E, Kaye ME, Udomwong P, Shamsani NJ, Young JPW, Bailly X. Bacterial genospecies that are not ecologically coherent: population genomics of *Rhizobium leguminosarum*. Open Biol 2015, 5(1).

**Table S1.** Nodulation phenotypes of *R/* Norway on selected hosts.

Species Name	Phenotype	Reference
<i>L. japonicus</i> Gifu	Nod-	(Gossmann et al. 2012)
<i>L. japonicus</i> MG20	Bump/Nod+Fix-	(Gossmann et al. 2012)
<i>L. japonicus</i> Nepal	Bump+Fix-	(Gossmann et al. 2012)
<i>L. filicaulis</i>	Nod-	(Gossmann et al. 2012)
<i>L. burtii</i>	Bump/Nod+Fix-	(Gossmann et al. 2012)
<i>L. pedunculatus</i>	Bump+Fix-	(Gossmann et al. 2012)
<i>L. glaber</i>	Tumor+/Fix-	(Gossmann et al. 2012)
<i>P. sativum</i> Sparkle	Nod-	(Gossmann et al. 2012)
<i>P. sativum</i> Little Marvel	Nod+Fix-	This work
<i>Latyrus sativus</i>	Nod+Fix-	This work

1. Gossmann JA, Markmann K, Brachmann A, Rose LE, Parniske M. Polymorphic infection and organogenesis patterns induced by a *Rhizobium leguminosarum* isolate from *Lotus* root nodules are determined by the host genotype. *New Phytol* 2012, **196**(2):561-573.

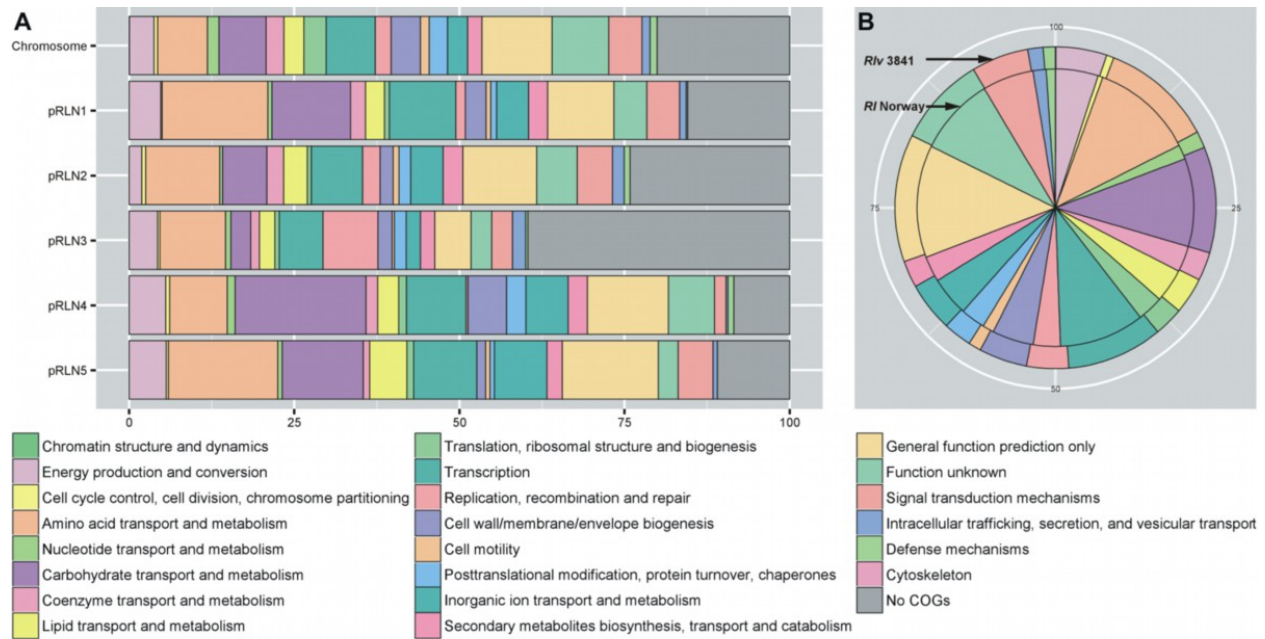


**Figure S2. Distribution of functional classes of protein encoding genes within the *R/* Norway genome.** (A) Functional class distribution across the six *R/* Norway replicons. (B) Comparison of the relative occurrence of functionally classified protein encoding genes between the *R/* Norway and *R/v* 3841 genomes. Functional annotation (COG) was performed on WebMGA server [1].

1. Wu ST, Zhu ZW, Fu LM, Niu BF, Li WZ. WebMGA: a customizable web server for fast metagenomic sequence analysis. BMC Genomics 2011, 12.



Table S2. Genome statistics for *R/* Norway.

Replicon	Size [base pairs]	GC content	Protein- encoding genes	Proportion coding sequences	Mean protein length [amino acids]	rRNA operons	tRNA genes
Chromosome	4,906,123	61.0%	5045	87.6%	284	3	54
pRLN1	1,098,158	60.5%	1079	90.8%	308		
pRLN2	592,529	60.9%	595	88.9%	295		
pRLN3	557,386	57.4%	570	83.5%	272		
pRLN4	354,350	60.7%	312	89.0%	337		
pRLN5	279,539	61.3%	265	90.2%	317		
Total	7,788,085	60.3%	7866	88.3%	302	3	54

## **Publication II:**

**A subcompatible *Rhizobium* strain reveals infection duality in *Lotus***



## RESEARCH PAPER

# A subcompatible rhizobium strain reveals infection duality in *Lotus*

Juan Liang<sup>1</sup>, Andreas Klingl<sup>2</sup>, Yen-Yu Lin<sup>1</sup>, Emily Boul<sup>3</sup>, Jane Thomas-Oates<sup>3</sup> and Macarena Marín<sup>1,\*</sup>

<sup>1</sup> Genetics, Faculty of Biology, Ludwig Maximilians University Munich, Germany

<sup>2</sup> Botany, Faculty of Biology, Ludwig Maximilians University Munich, Germany

<sup>3</sup> Department of Chemistry, University of York, UK

\* Correspondence: [m.marin@biologie.uni-muenchen.de](mailto:m.marin@biologie.uni-muenchen.de)

Received 12 September 2018; Editorial decision 25 January 2019; Accepted 31 January 2019

Editor: Miriam Gifford, University of Warwick, UK

## Abstract

***Lotus* species develop infection threads to guide rhizobia into nodule cells. However, there is evidence that some species have a genetic repertoire to allow other modes of infection. By conducting confocal and electron microscopy, quantification of marker gene expression, and phenotypic analysis of transgenic roots infected with mutant rhizobia, we elucidated the infection mechanism used by *Rhizobium leguminosarum* Norway to colonize *Lotus burtii*. *Rhizobium leguminosarum* Norway induces a distinct host transcriptional response compared with *Mesorhizobium loti*. It infects *L. burtii* utilizing an epidermal and transcellular infection thread-independent mechanism at high frequency. The entry into plant cells occurs directly from the apoplast and is primarily mediated by ‘peg’-like structures, the formation of which is dependent on the production of Nod factor by the rhizobia. These results demonstrate that *Lotus* species can exhibit duality in their infection mechanisms depending on the rhizobial strain that they encounter. This is especially relevant in the context of interactions in the rhizosphere where legumes do not encounter single strains, but complex rhizobial communities. Additionally, our findings support a perception mechanism at the nodule cell entry interface, reinforcing the idea that there are successive checkpoints during rhizobial infection.**

**Keywords:** Infection thread, intercellular infection, *Lotus burtii*, Nod factor, nodulation, ‘peg’-like structure, *Rhizobium leguminosarum*, root nodule symbiosis.

## Introduction

Legumes engage in a mutualistic interaction with a group of diazotrophic bacteria collectively known as rhizobia. In this interaction, the host plant provides photosynthetic products in exchange for ammonia converted from atmospheric nitrogen by the rhizobia (Oldroyd *et al.*, 2011). This intimate bidirectional nutrient exchange takes place within cells of root organs called nodules. One of the fundamental questions in the field of root nodule symbiosis is how rhizobia enter these plant cells during nodule organogenesis.

The programmes leading to nodule organogenesis and cell infection are distinct, but interconnected (Madsen *et al.*, 2010). Furthermore, the host controls both processes. The infection programme ensures that the rhizobia are guided from the root surface into cells of a dividing nodule primordium in three conceptual steps: (i) crossing of the epidermis; (ii) cortical spreading; and (iii) uptake of rhizobia into plant cells. However, this is attained differently depending on the host legume (Ibáñez *et al.*, 2017). For example, in model organisms such as

*Medicago truncatula* and *Lotus japonicus*, and crops such as *Pisum sativum*, infection is initiated in epidermal root hairs by the inward growth of plant-made tubular structures called infection threads. Progression of a transcellular infection thread network in developing nodule primordia ultimately leads to the internalization of rhizobia by cells in this tissue (Gage, 2002, 2004; Murray, 2011). The semi-aquatic legume *Sesbania rostrata* is infected under flooding conditions through physical cracks in the root epidermis, for example at lateral root emergence sites (Ndoye *et al.*, 1994). Here, proliferating bacteria accumulate in intercellular infection pockets that give rise to trans- and intercellular infection threads (Ndoye *et al.*, 1994). Some subtropical legumes, such as *Neptunia natans* and *Aeschynomene afraaspera*, also become infected through cracks, but the uptake into plant cells occurs directly from intercellular accumulations of bacteria, in the absence of infection threads (James *et al.*, 1992; Subbarao *et al.*, 1995; Bonaldi *et al.*, 2011). As a final example, there are plants such as *Lupinus albus*, in which bacteria cross the epidermis intercellularly, but are also directly internalized from intercellular accumulations (Gonzalez-Sama *et al.*, 2004). Thus, conceptually, there are infection thread-dependent and -independent infection mechanisms controlled by epidermal and nodule primordium programmes (Madsen *et al.*, 2010).

Genetic studies using gain-of-nodulation mutants have elegantly illustrated these different infection programmes in *L. japonicus* (Madsen *et al.*, 2010). *Mesorhizobium loti* infects *L. japonicus* wild-type plants via infection threads (van Spronsen *et al.*, 2001). However, it invades *nfr1-1 nfr5-2 snf1* triple mutant plants in a process resembling the epidermal thread-independent crack-entry infection observed in *S. rostrata* (Ndoye *et al.*, 1994; Madsen *et al.*, 2010). Another major discovery of this work was that a *M. loti nodC* mutant strain infects *nfr1-1 nfr5-2 snf1* triple mutants at low frequency in the absence of epidermal and transcellular infection threads (Madsen *et al.*, 2010). These results demonstrate that *Lotus* possesses a genetic repertoire allowing multiple types of infection. However, whether this also occurs in wild-type plants and natural *Lotus* strains has not yet been conclusively demonstrated.

The existence of an infection mechanism mediating the direct entry into plant cells from the intercellular space (independent of epidermal and transcellular infection threads) at high frequency would constitute an invaluable tool to study this key step in the evolution of root nodule symbiosis. In this work, we investigated whether wild-type *Lotus* can be infected by an infection thread-independent mechanism, using molecular approaches and detailed microscopy. We discovered that a natural *Lotus* isolate infects different wild-type *Lotus* plants utilizing an epidermal and transcellular infection thread-independent mechanism at high frequency. Moreover, the penetration into plant cells is primarily mediated by 'peg'-like structures, the formation of which is dependent on the production of Nod factors by the rhizobia.

## Materials and methods

### Bacterial strains and growth conditions

The bacterial strains used in this study are listed in Supplementary Table S1 at JXB online. Rhizobia cultures were grown for 2 d at 28 °C

in different media depending on the experiment. For nodulation and infection assays, rhizobia were grown in tryptone yeast extract (TY) broth (Beringer, 1974). For gene expression analyses, strains were grown in yeast mannitol broth (YMB) (Vincent, 1970). Finally, for Nod factor production, *Rhizobium leguminosarum* (Rl) Norway was grown in TY broth and then subcultured in modified B<sup>-</sup> medium (modified from Spaink *et al.*, 1992). As the carbon source, 5 g l<sup>-1</sup> mannitol and 5 g l<sup>-1</sup> sodium gluconate were used. For *nod* gene induction, the medium was supplemented with 1 μM naringenin for 2 d. *Agrobacterium* strains used in the hairy root transformation experiment were grown for 1 d at 28 °C in yeast extract broth (YEB) (Vervliet *et al.*, 1975). The *Escherichia coli* strains used in the conjugation assay were grown for 1 d at 37 °C in Luria Bertani (LB) broth. The following antibiotic concentrations were used: tetracycline (Tc, 2–10 μg ml<sup>-1</sup>); gentamicin (Gm, 25 μg ml<sup>-1</sup>); kanamycin (Km, 50 μg ml<sup>-1</sup>); streptomycin (Sm, 500 μg ml<sup>-1</sup>); rifampicin (Rf, 50 μg ml<sup>-1</sup>); and carbenicillin (Cb, 50 μg ml<sup>-1</sup>).

### Plant growth and inoculation conditions

*Lotus burttii* B-303 (seed bag numbers: 91091, 91101, and 91103) and *Lotus japonicus* MG-20 (seed bag number: 92147) seeds were surface sterilized with a 1.2% NaClO solution, rinsed, and soaked in water at room temperature for 2 h. Seeds were then transferred to 1/2 B5 medium agar plates and kept at 24 °C for 3 d in the dark and 3 d under a long-day photoperiod (16 h:8 h, light:dark). For shoot growth, nodulation, and infection quantification, three independent time-course experiments were conducted with 20 plants per condition and per time point. Six-day-old seedlings were transferred to sterile jars containing 300 ml of a sand:vermiculite mixture supplemented with 40 ml of FAB medium. After 2 d, each plant was inoculated with 1 ml of bacterial suspension ( $A_{600}=0.005$ ). For root hair phenotypic analysis and infection thread quantification, four independent experiments were conducted with 20 plants per condition. Six-day-old seedlings were gently placed over sterile filter paper (Whatman) on square Petri plates containing FAB medium. After 2 d, vertically grown plants were inoculated with bacterial suspensions ( $A_{600}=0.05$ ), covered with a second sheet of sterile filter paper, and incubated under a long-day photoperiod. Plants were inspected 1, 2, and 3 weeks post-inoculation (wpi).

### Hairy root transformation

To overexpress SYMRK in the roots of *L. burttii* plants, the roots of 6-day-old seedlings were cut and the remaining hypocotyl regions were dipped into *Agrobacterium rhizogenes* AR1193 (Stougaard *et al.*, 1987) suspensions carrying the relevant plasmids (Supplementary Table S1). Transformed plants were grown on B5 medium in the dark at room temperature for 3 d and then moved to a long-day photoperiod at 24 °C. After 2 d, plants were transferred to B5 medium supplemented with cefotaxime (300 μg ml<sup>-1</sup>) to clear the *Agrobacterium*. After 23 d, seedlings were screened for transformation, using a green fluorescent protein (GFP)-based transformation marker. Transformed plants were transferred to closed sterile jars containing 300 ml of a sand:vermiculite mixture supplemented with 40 ml of FAB medium. After 2 d, each plant was inoculated with a 1 ml bacterial suspension ( $A_{600}=0.01$ ) and grown under a long-day photoperiod. Plants were harvested 9 wpi and phenotypically analysed. Three independent experiments were conducted with at least 20 plants per condition.

### Histological staining and microscopy

To inspect nodule colonization, samples were fixed with a 2.5% glutaraldehyde solution in 0.5 M potassium phosphate buffer and progressively dehydrated in 30, 50, 70, and 100% ethanol solutions for 1 h each. Nodules were then embedded in a Technovit 7100 resin (Heraeus Kulzer) according to the manufacturer's instructions, and 2 μm thin sections were cut with an RM2125 RT rotary microtome (Leica Biosystems). Sections were placed on glass slides and dried at 60 °C for 30 min. Dried sections were stained with a 1% toluidine blue and 0.2% methylene blue mixed solution for 30–60 s and rinsed with water until the background cleared. Stained sections were inspected on a DM6 B upright microscope (Leica

Microsystems) equipped with  $\times 5$ ,  $\times 10$ , and  $\times 40$  dry objectives and a  $\times 20$  oil/water immersion lens.

For fluorescence microscopy analyses of nodule colonization, samples were fixed with a 4% formaldehyde solution in 50 mM PIPES buffer by 30 min vacuum infiltration and then kept at room temperature for 45 min. The fixed samples were embedded in 6% low melting agarose (Carl Roth), and semi-thin sections (40–50  $\mu\text{m}$ ) were cut with a VT1000S vibratome (Leica Biosystems) at speed five and frequency five. Nodule sections were counterstained with a fresh 0.01% calcofluor white solution for 10 min. To visualize the colonization of *Rl* Norway  $\Delta\text{nodC}$  in spontaneously induced nodules, sections were additionally stained with a 20  $\mu\text{M}$  propidium iodide (PI) solution for 10 min. For the rhizobia viability assay, fresh nodules were sectioned and stained with a Live/Dead BacLight Bacterial Viability kit (3.34  $\mu\text{M}$  SYTO9 and 20  $\mu\text{M}$  PI; Invitrogen) for 10 min at room temperature. Agarose semi-thin sections were observed using a TCS SP5 confocal microscope (Leica Microsystems) equipped with a  $\times 20$  HCX PL APO water immersion lens. Calcofluor white was excited with UV and the emission was detected at 405–450 nm. GFP, SYTO9, and PI were excited with an argon laser line at 488 nm and the emissions were detected at 500–550, 500–550, and 600–650 nm, respectively. DsRed was excited with a diode pumped solid-state laser at 561 nm and detected at 600–650 nm.

#### Quantitative analysis of images

To quantify the percentage of nodule colonization, an area comprising the total inner tissue of the nodule was manually defined using Fiji v.2.0.0-rc-59/1.51j (Schindelin *et al.*, 2012). The colonized area was calculated for each section by defining a signal threshold and masking the regions below it. The average percentage of 1–3 sections per nodule and at least 5–6 nodules per condition were used for the calculations.

#### Electron microscopy

Root nodules were pre-fixed in 50 mM PIPES buffer (fixation buffer 1) containing 2.5% glutaraldehyde. The nodules were cut into smaller pieces in this fixation buffer and afterwards transferred to 50 mM cacodylate buffer containing 2 mM  $\text{MgCl}_2$  (fixation buffer 2) and 2.5% glutaraldehyde for complete fixation overnight at 4 °C. After washing the samples four times (10, 30, 30, and 50 min) with fixation buffer 2 without glutaraldehyde, post-fixation with 1% osmium tetroxide was carried out for 1.5 h. Afterwards, they were washed again twice with fixation buffer 2 (without glutaraldehyde) and four times with double-distilled water (45, 35, 30, and 30 min). The dehydration of the samples was achieved in a graded acetone series before infiltration and embedding in Spurr's resin. The thin sections of embedded samples were post-stained with lead citrate for 2 min and investigated on a Zeiss EM 912 transmission electron microscope with an integrated OMEGA filter. The acceleration voltage was set to 80 kV and the images were recorded with a Tröndle 2k $\times$ 2k slow-scan CCD camera.

#### Quantitative RT-PCR

For the quantification of gene expression, materials were collected from whole root systems, nodules, and rhizobia pellets, and then snap-frozen in liquid nitrogen. All samples were lysed with an MM40 tissue lyser (Retsch). Total RNA was extracted with the Spectrump<sup>TM</sup> Plant Total RNA kit (Sigma-Aldrich) according to the manufacturer's instructions. To eliminate DNA contamination, DNase I (Ambion) treatment was conducted, and then plant and bacterial samples were analysed by PCR using *ATP-synthase* (*ATP*) and *ubiquitin* primers, and *initiation factor 1* (*IF-1*) primers, respectively (Supplementary Table S2). RNA integrity was verified on an agarose gel. Superscript III reverse transcriptase (Thermo Fisher) was used to synthesize first-strand cDNA using 270 ng of total RNA. Quantitative reverse transcription-PCR (qRT-PCR) was performed on a 384-well plate with the Quantstudio5 system (Thermo Fisher) and using the Evagreen Master mix (Metabion) according to the manufacturer's instructions. The reaction was performed with a 1:10 (v/v) dilution of the cDNA, with 0.3  $\mu\text{M}$  of each primer in a total reaction volume of 7  $\mu\text{l}$ . The thermal cycler conditions were: 95 °C 2 min, 40

cycles of 95 °C 30 s, 58 °C 30 s, and 72 °C 20 s, followed by dissociation curve analysis. At least five biological replicates and 2–3 technical replicates were included for the quantification of each gene. Normalization of plant and rhizobia genes was performed using the *ATP* and *IF-1* house-keeping genes, respectively. All qRT-PCR primers used in this work are listed in Supplementary Table S3.

#### Nod factor isolation

The Nod factors were extracted from the supernatant of a 3 litre *Rl* Norway culture with 1-butanol (300 ml l<sup>-1</sup> culture). The Nod factors were collected by evaporating the butanol phase in a Hei-VAP Value Rotary Evaporator (Heidolph Instruments). The dried extract was redissolved in 3.5 ml of 60% aqueous acetonitrile (ACN) (v:v) by shaking for 18 h. A 1.5 ml aliquot of the resulting solution was diluted by addition of ACN to a final concentration of 20% (v/v) aqueous ACN and loaded onto a primed C18 solid phase extraction cartridge (Supelclean ENVI-18, 1 g bed weight; Sigma-Aldrich). The cartridge was washed with 5 ml of 20% (v:v) aqueous ACN and the Nod factors were eluted with 5 ml of 45% ACN, followed by 5 ml of 60% ACN. The two eluted fractions were collected separately and dried under vacuum, prior to reconstitution in 0.7 ml of 60% ACN for HPLC fractionation.

#### HPLC fractionation of Nod factors

The 45% and 60% SPE fractions were each diluted to a final concentration of 20% ACN. A 1.5 ml aliquot of the resulting solution was injected onto an Agilent Technologies 1200 series HPLC instrument fitted with a reversed phase column (Waters SymmetryShield RP18, 5  $\mu\text{m}$  particles, 4.6 $\times$ 250 mm, with guard column) eluted at 1 ml min<sup>-1</sup>, using UV detection at 205 nm. The column was eluted using the following gradient: 20 min isocratic at 20% ACN, linear elution from 20% to 60% ACN over 20 min, linear gradient 60% to 90% over 0.5 min, isocratic at 90% ACN for 4.5 min, and then re-equilibrated at 20% ACN for 5 min. Fractions of 1 min were collected and dried under vacuum.

#### Nod factor structure determination

Mass determination of the Nod factors in the HPLC fractions was carried out using a Bruker 9.4 T solarix HR Fourier-transform ion cyclotron resonance instrument in the York Centre of Excellence in Mass Spectrometry (CoEMS). The instrument was operated in the positive ion mode using a matrix-assisted laser desorption/ionization (MALDI) source. HPLC fractions were redissolved in 50  $\mu\text{l}$  of 80% ACN, and 2  $\mu\text{l}$  of this sample solution was mixed with 2  $\mu\text{l}$  of MALDI matrix solution (2,5-dihydroxybenzoic acid; 7 mg in 500  $\mu\text{l}$  of 80% ACN); 0.8  $\mu\text{l}$  of this mixture was spotted onto a ground steel MALDI target plate and allowed to air dry. Spectra were acquired by irradiating the dried sample spots with the laser (Smartbeam: Nd:YAG 355 nm) set at 35% laser power and a frequency of 500 Hz. Fragmentation was generated using collision-induced dissociation (CID) with collision voltage settings varied between 25V and 35V, and product ion spectra were recorded. Alternatively, CID product ion spectra were recorded using static nano-electrospray ionization in the positive ion mode with a Thermo Scientific Orbitrap Fusion in CoEMS. Samples were dissolved in 50  $\mu\text{l}$  of 50% ACN, and 2  $\mu\text{l}$  was transferred to the electrospray tip (made in-house). Higher energy collisional dissociation spectra were recorded using collision 'energy' settings between 20V and 30V. Nod factor structures were determined from interpretation of the product ion spectra obtained on the two instruments.

#### Conjugation

The GFP-expressing plasmid pFAJ-GFP and the suicide replacement plasmid pK19MOBSACB (Supplementary Table S1) were introduced into rhizobia by conjugation using *E. coli* ST18 (Thoma and Schobert, 2009) as donor strain. The donor and acceptor strains ( $A_{600}=1$ ) were mixed in a 10:1 ratio. The mixtures were placed on TY plates and incubated at 28 °C. After 24 h, bacteria were suspended and grown on selective TY plates.

### Generation of the *Rl* Norway $\Delta$ nodC deletion mutant

The two-step homologous recombination method described previously (Sant'anna et al., 2011) was used to generate deletion mutants in *Rl* Norway. Two 500 bp fragments flanking the *nodC* gene were amplified by PCR and cloned into the suicide vector pK19MOBSACB (Supplementary Table S1). The plasmid was delivered into *Rl* Norway by conjugation. The first recombination event was selected on TY medium supplemented with Km. Positive colonies were verified by PCR using plasmid- and genome-specific primers (Supplementary Table S2). The second recombination event was counter-selected on TY medium containing 10% sucrose. Mutants were verified by PCR and sequencing using primers annealing upstream and downstream of the flanking fragments (Supplementary Table S2).

### Statistical analyses

All statistical analyses were performed in R-studio by using ANOVA and Tukey honest significant difference (TukeyHSD) methods.

## Results

### *Rhizobium leguminosarum* Norway induces ineffective nodules in wild-type *Lotus burttii*

*Lotus burttii* is a *Lotus* species originally identified in West Pakistan (Borsos et al., 1972) and is nodulated by a wide range of rhizobia including *Mesorhizobium loti* MAFF303099 (*Ml*

MAFF) (Gossmann et al., 2012), *Sinorhizobium fredii* HH103 (Acosta-Jurado et al., 2016), and *Rhizobium leguminosarum* (*Rl*) Norway, a natural *Lotus* isolate (Gossmann et al., 2012). Interestingly, *Rl* Norway infects *L. burttii* nodules apparently in the absence of epidermal infection threads (Gossmann et al., 2012). We characterized the symbiotic interaction between this strain and *L. burttii*, and compared it with the interaction with *Ml* MAFF. We inoculated *L. burttii* plants under axenic conditions and analysed growth and nodule organogenesis in time-course experiments. *Ml* MAFF promoted shoot growth and induced pink nodules on the roots of *L. burttii* (Fig. 1a). In comparison, *Rl* Norway induced a larger number of nodules (Fig. 1b; Supplementary Fig. S1a). However, these nodules were ineffective, as the inoculated seedlings had stunted shoots and their leaves were pale yellow, a sign of nitrogen starvation (Fig. 1a; Supplementary Fig. S1b).

To validate further the lack of nitrogen fixation in *Rl* Norway-induced nodules, we determined by qRT-PCR the relative expression of the rhizobial *nifH* gene. This gene encodes a nitrogenase subunit that is essential for nitrogen fixation and is markedly induced in nitrogen-fixing nodules (Uchiumi et al., 2004). The *nifH* gene of *Ml* MAFF was induced in nodules in comparison with free-living conditions. In contrast, *Rl* Norway exhibited no induction of *nifH* under the same conditions (Fig. 1c). This shows that *Rl* Norway induces ineffective nodules in *L. burttii*.

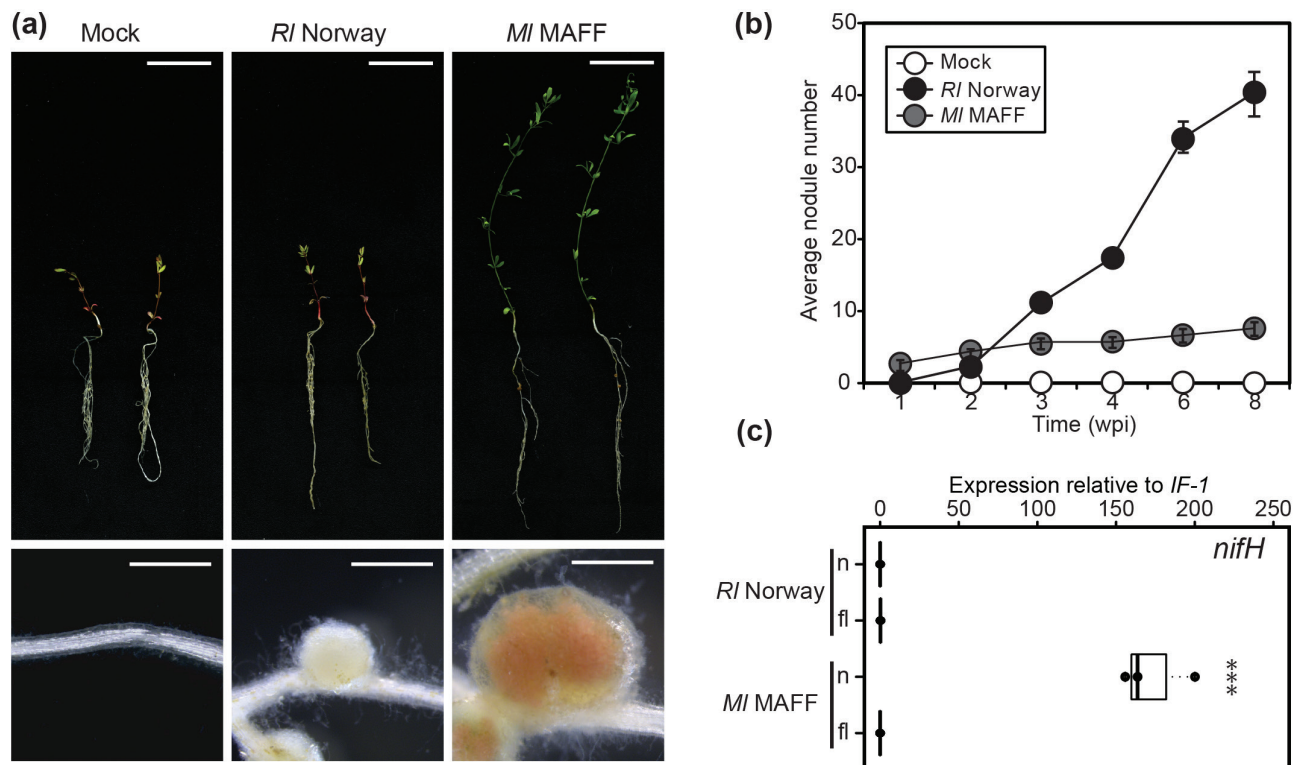


**Fig. 1.** *Rhizobium leguminosarum* Norway induces ineffective nodules in *Lotus burttii*. (a) Images of shoot (upper panel) and nodule (lower panel) phenotypes exhibited by representative *L. burttii* plants 6 weeks after mock treatment, or inoculation with *Rl* Norway and *Mesorhizobium loti* MAFF303099. Scale bars: (upper panel) 1 cm; (lower panel) 1 mm. (b) Time-course quantification of the average nodule number per plant. Three independent experiments were conducted with 20 plants per condition and per time point. Error bars indicate the SDs. (c) Quantification of *nifH* transcript abundance by qRT-PCR. Total RNA was extracted from *L. burttii* nodules (n) induced by *Rl* Norway and *Ml* MAFF at 4 wpi, and from free-living (fl) rhizobia grown in liquid culture. Relative transcript expression was normalized against the housekeeping gene *Initiation factor-1*. Each dot represents one independent biological replicate. The bold black line and the box represent the median and the interquartile range, respectively. The statistical analysis was performed by ANOVA; \*\*\* $P < 0.001$ . (This figure is available in colour at JXB online.)

*Rhizobium leguminosarum* Norway induces a distinct early symbiotic response

To investigate the mechanism by which *Rhizobium leguminosarum* Norway infects *Lotus*, we visually inspected the root hairs of *L. burtii* plants grown on plates. The roots inoculated with *Rhizobium leguminosarum* Norway showed extensive root hair swelling, and branching, but only rarely curling (Fig. 2a–d). In contrast to the responses to *Mesorhizobium loti* MAFF, the root hair deformations were not confined to the susceptible zone, but extended throughout the majority of the root. Such an unrestricted response has been observed in roots of *L. japonicus* and *Glycine max* after Nod factor application (Niwa *et al.*, 2001; Duzan *et al.*, 2004) or in the *L. japonicus symrk-3* mutant upon inoculation with *M. loti* R7A (Stracke *et al.*, 2002).

In accordance with previous reports (Gossmann *et al.*, 2012), no epidermal infection threads were observed upon inoculation with *Rhizobium leguminosarum* Norway under the experimental conditions tested. We analysed >100 plants grown on plates for a period of 1–3 weeks.

Infection threads were also absent upon inoculation of *L. japonicus* MG-20. In contrast, *L. burtii* and *L. japonicus* MG-20 plants exhibited only minor root hair deformations 1 week after inoculation with *M. loti* MAFF, but developed an average of  $7 \pm 3$  and  $17 \pm 6$  infection threads per plant, respectively (Fig. 2e).

To determine molecular responses induced by *Rhizobium leguminosarum* Norway, we quantified by qRT-PCR the expression of symbiotic marker genes involved in infection, such as *Nodule INception* (*NIN*), *Nodulation Pectate Lyase* (*NPL*), *Exopolysaccharide receptor 3* (*EPR3*), *ERF Required for Nodulation 1* (*ERN1*), and *SYMBiotic REMorin 1* (*SYMREM1*) at 3, 7, and 14 days post-inoculation (dpi). *Rhizobium leguminosarum* Norway induced distinct gene expression compared with *M. loti* MAFF (Fig. 3). At 3 dpi, a time point at which nodules had not developed in any of the conditions, only roots inoculated with *M. loti* MAFF significantly induced the expression of *NIN*, *ERN1*, and *EPR3*. *NIN* induction was slightly delayed in *Rhizobium leguminosarum* Norway-inoculated roots. This coincided

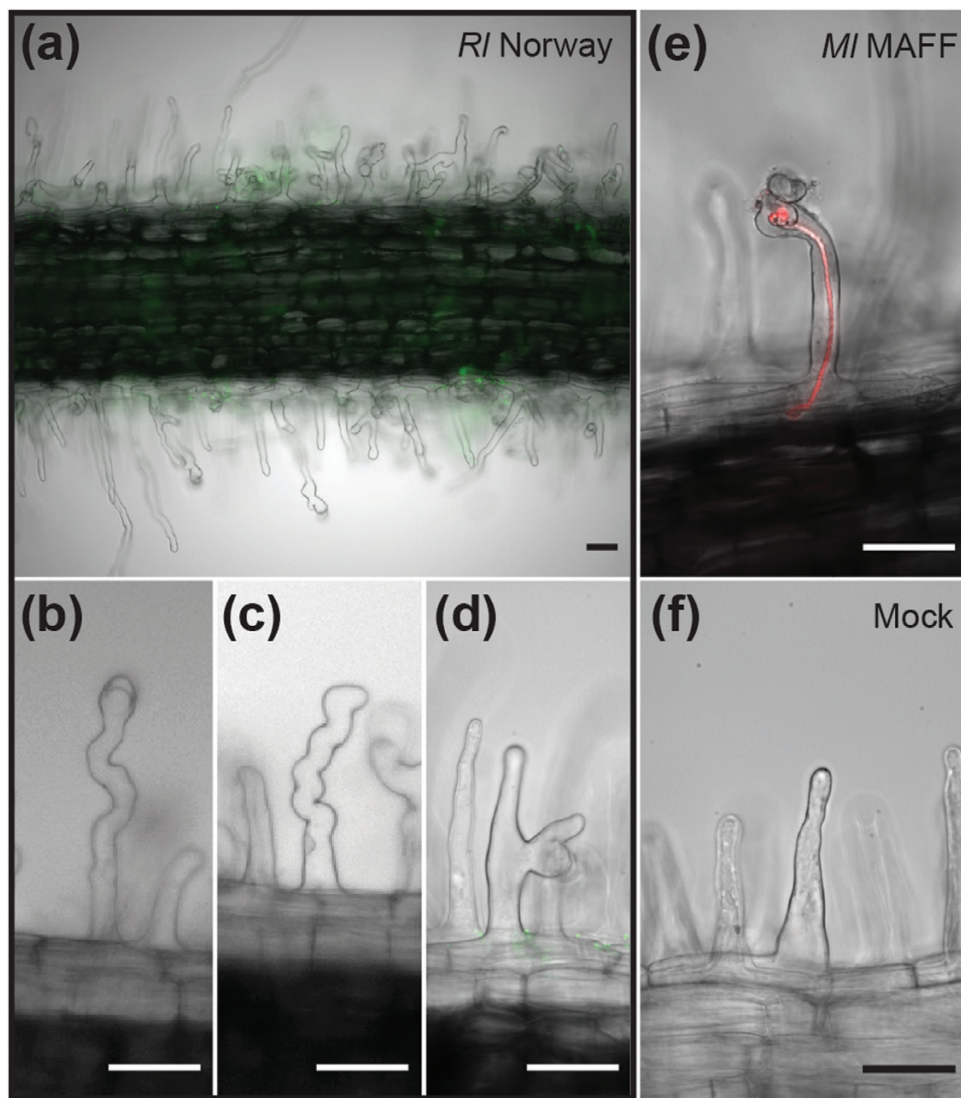


**Fig. 2.** *Rhizobium leguminosarum* Norway induces root hair deformations in *Lotus burtii*. (a) Overview of a root segment colonized by *Rhizobium leguminosarum* Norway-GFP that displays no epidermal infection threads, but massive root hair deformation, including different degrees of swelling (b, c), and branching (d). Representative micrographs of an infection thread induced by *Mesorhizobium loti* MAFF303099-DsRed (e) and of root hairs upon mock treatment (f). Four independent experiments were conducted with 20 plants per condition on the square Petri plates. Scale bars=50  $\mu\text{m}$ . (This figure is available in colour at *JXB* online.)

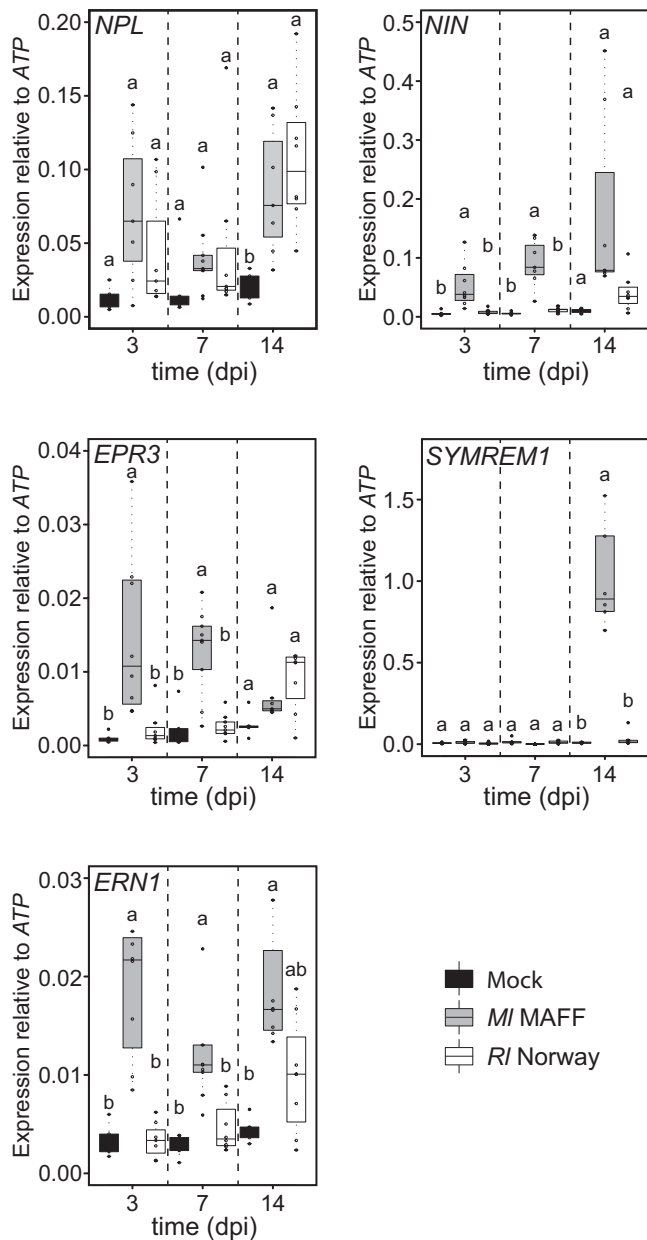


**Fig. 3.** Gene expression analysis of *Lotus burtii* roots upon rhizobial inoculation. Quantification of *NPL*, *NIN*, *ERN1*, *EPR3*, and *SYMREM1* transcript abundance by qRT-PCR. Total RNA was extracted from *L. burtii* whole root systems after mock treatment and after 3 d, 1 week, and 2 weeks post-inoculation with *Rhizobium leguminosarum* Norway and *Mesorhizobium loti* MAFF303099. Relative transcript expression levels were normalized against the housekeeping gene *ATP-synthase*. Each dot represents one independent biological replicate. The bold black line and the box represent the median and the interquartile range, respectively. The statistical analysis was performed for each time point using ANOVA and TukeyHSD methods. Lower case letters indicate significance groups within each time point.

with a delayed nodulation phenotype exhibited in these roots (Fig. 1b). A similar pattern was observed for *ERN1* and *EPR3* (Fig. 3). Most strikingly, at 14 dpi, *SYMREM1* expression was almost 30-fold higher in *MI MAFF*-inoculated roots compared with *RI Norway*-inoculated roots (Fig. 3). These quantitative differences in the expression of infection marker genes at 3 dpi could explain the absence of epidermal infection threads. These results indicate that *RI Norway* induces a distinct response in *L. burtii* compared with *MI MAFF*.

### *RI Norway* induces intercellular ‘peg-like’ structures

The differential expression of infection marker genes and the absence of infection threads suggested that *RI Norway* utilizes an infection mechanism distinct from that of *MI MAFF* to colonize *Lotus*. To investigate this, we sectioned nodules in different developmental stages and visualized their colonization by confocal microscopy using fluorescently tagged strains and TEM. Upon *MI MAFF* inoculation, infection threads were visible on top of the growing primordia, and underlying cells were infected (Fig. 4a, b). In contrast, *RI Norway* accumulated on top of empty nodule primordia at sites in which the epidermis had been disrupted due to the nodule emergence (Fig. 4c, d). Structures reminiscent of infection pockets formed at these sites (Supplementary Fig. S2a). This suggests that *RI Norway* crosses the epidermis through cracks induced by the emergence of nodule primordia and not necessarily at lateral root emergence sites. Accordingly, nodules formed along the complete root system and not preferentially at lateral root bases (Supplementary Fig. S1a).

At 3 wpi, *MI MAFF* induced fully developed nodules that were largely colonized (nodule colonization =  $67.1 \pm 13.5\%$ ) and contained transcellular infection threads (Fig. 4e, f). In contrast, *RI Norway* infected cells intracellularly (nodule colonization =  $1.4 \pm 0.7\%$ ), but induced no transcellular infection threads in >35 sectioned nodules (Fig. 4g, h; Supplementary Fig. S2b, c). We observed in 100% of the nodules analysed intercellular *RI Norway* accumulations (Fig. 4h; Supplementary Fig. S2d). For a more detailed view, we conducted TEM, which also showed intercellular accumulations (Fig. 5a, b). In 40% of the agarose sections, cells contained structures with densely packed bacteria (Supplementary Fig. S2e). These structures were reminiscent of ‘peg-like’ structures, which have been described previously in *Aeschynomere afiaspera* (Bonaldi et al., 2011) and *Lupinus albus* (Gonzalez-Sama et al., 2004). To describe these structures unequivocally, we conducted TEM of ultra-thin nodule sections. A dense material surrounded invading intercellular bacteria (Fig. 5c). These results suggest that cell invasion is mediated via ‘peg’-entry.

*RI Norway* invaded intact plant cells and formed symbiosomes surrounded by a peri-bacteroid membrane (Fig. 5a). However, infected cells exhibited signs of early senescence, such as disorganized nuclei (Fig. 5a). Furthermore, the symbiosomes had an enlarged peri-bacteroid space, and a polymeric material surrounded the bacteroids (Fig. 5d). At 4 wpi, symbiosome integrity was disrupted and bacteroids were partially degraded (Fig. 5e). To investigate the viability of bacteria, we conducted live/dead staining using PI and SYTO9, which label dead and living bacteria, respectively. *MI MAFF* bacteria were viable at least up to 6 wpi (Supplementary Fig. S3a, b), in contrast to a fraction of *RI Norway* bacteria that died as early as 4 wpi (Supplementary Fig. S3c, d).

### The ‘peg’-like infection of *SYMREK*-induced spontaneous nodules is Nod factor dependent

The Nod factors produced by *M. loti* induce root hair deformations and cortical cell divisions in *Lotus* (Niwa et al., 2001) and are essential for epidermal infection thread formation (Madsen et al., 2010). However, their role in cell entry has not been thoroughly studied. To investigate the role of the Nod



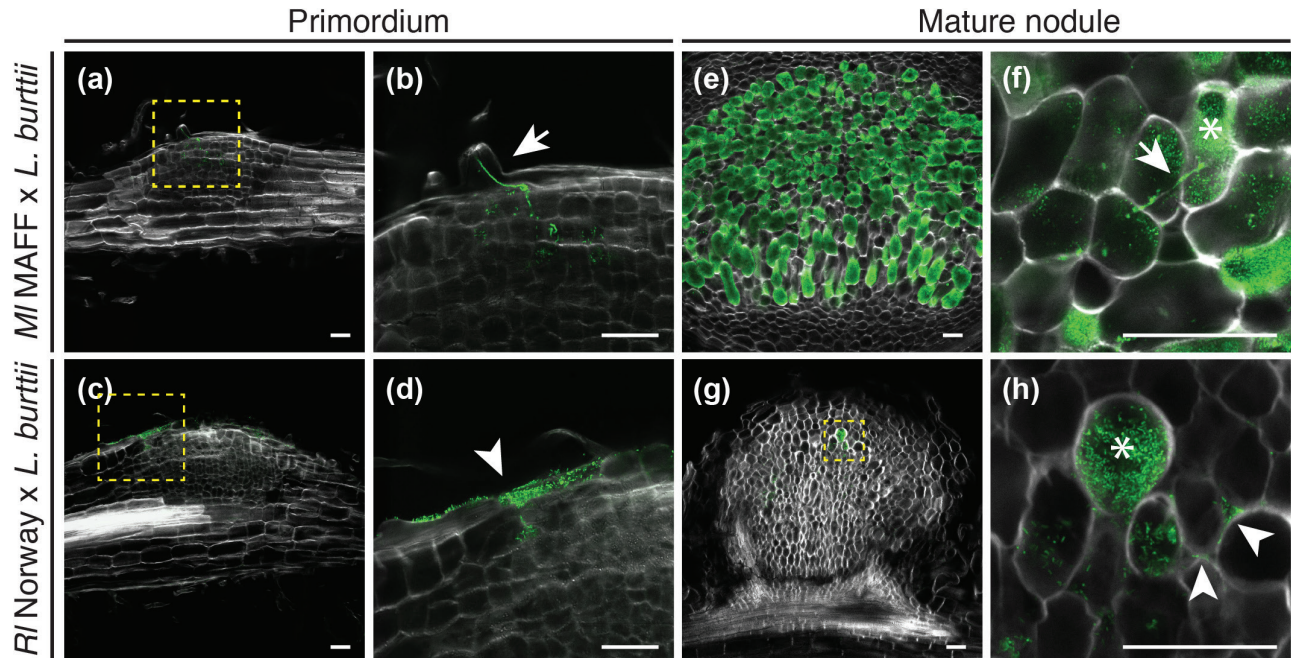


**Fig. 4.** *Rhizobium leguminosarum* Norway colonizes *Lotus burttii* nodules in the absence of transcellular infection threads. Representative confocal laser scanning micrographs of nodule semi-thin sections (50  $\mu\text{m}$ ) counterstained with calcofluor white (white) show that (a, b) *Mesorhizobium loti* MAFF303099-GFP bacteria invade the nodule primordium at 5 dpi through epidermal infection threads (b, arrow), while *R/* Norway-GFP bacteria (c, d) invade the nodule primordium at 11 dpi in the absence of epidermal infection threads (d, arrowhead). (e, f) *M/* MAFF-GFP bacteria fully colonize the nodule (e) and induce transcellular infection threads (f, arrow) at 3 wpi. In contrast, (g, h) *R/* Norway-GFP bacteria partially colonize the nodule inter- (h, arrowhead) and intra- (h, asterisk) cellularly at 4 wpi in the absence of transcellular infection threads. The images shown here are representative of 20 primordia and 20 nodules infected by *R/* Norway, and 5 primordia and 7 nodules infected by *M/* MAFF. Scale bars=50  $\mu\text{m}$ . (This figure is available in colour at *JXB* online.)

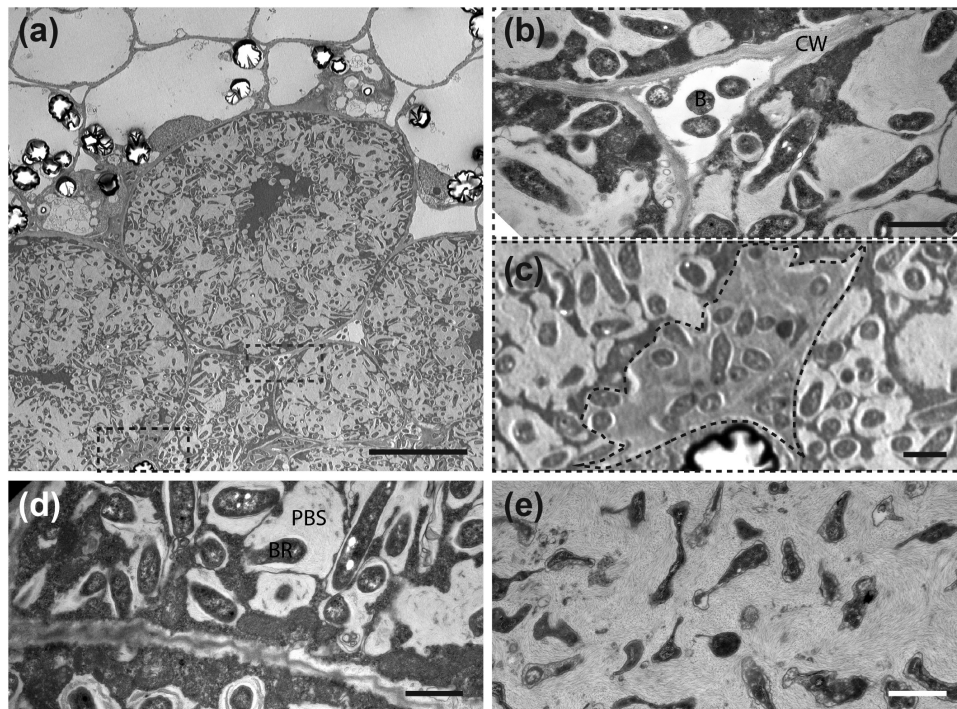


**Fig. 5.** *Rhizobium leguminosarum* Norway enters *Lotus burttii* root nodule cells through 'peg'-like structures and forms symbiosomes. TEM micrographs of nodule sections infected by *R/* Norway at 4 wpi. (a) Overview displays intact plant cells infected with rhizobia. Magnifications show: (b) bacteria (B) colonizing the intercellular space, and (c) bacteria surrounded by a dense matrix entering a cell from the intercellular space ('peg'-like structure surrounded by a dashed line). (d) A nodule cell contains symbiosomes with enlarged peribacteroid spaces (PBS) and elongated bacteroids (BR). (e) Bacteria undergoing degradation. CW, cell wall. Scale bars: (a), 10  $\mu\text{m}$ ; (b-e), 1  $\mu\text{m}$ .

factors in the formation of the ‘peg-like’ structures induced by *RI* Norway, we generated in this strain an in-frame deletion of the *nodC* gene, which encodes the *N*-acetylglucosaminyl transferase responsible for the synthesis of the Nod factor backbone. The *RI* Norway *nodC* gene is located in a cluster resembling the *nod* operon of *R. leguminosarum* biovar *viciae* 3841 (Liang *et al.*, 2018) (Supplementary Fig. S4a). Consequently, the Nod factors produced by *RI* Norway resemble the factors produced by other *R. leguminosarum* strains (D’Haeze and Holsters, 2002) (Supplementary Table S4).

The deletion in *nodC* abolished the capacity of *RI* Norway to induce root hair deformations and nodule organogenesis in *L. burtii* (Supplementary Fig. S4b–d). To study the infection of nodule cells, we induced spontaneous nodules by overexpressing the SYMBiotic Receptor-like Kinase SYMRK in transgenic roots (as described in Ried *et al.*, 2014), and inoculated them with *RI* Norway wild type or *nodC* mutant. Spontaneous nodules only developed in SYMRK transgenic roots, and not in roots transformed with the empty vector. These nodules were excised, fixed, and sectioned. Nodule sections were stained with calcofluor white and PI to visualize the cell wall and bacteria, respectively. Wild-type *RI* Norway colonized 28.3% of the sectioned nodules. This contrasts with the 100% colonization rate of *RI* Norway-induced nodules. Approximately 20–50% of the infected cells exhibited ‘peg’-like structures (Fig. 6). In contrast, the *nodC* mutant colonized only 2% of the nodules analysed. The colonization of these nodules was mostly restricted to regions with active cell division, as indicated by smaller plant cell size and multiple nuclei (Fig. 6). In all sections analysed, although infected cells were present, no ‘peg’-like structure was observed with the *nodC* mutant strain. This result suggests that these structures are induced upon Nod factor production and supports a perception mechanism at the interface of nodule cell entry.

## Discussion

Bacterial entry into nodule cells is one of the key steps in the evolution of the root nodule symbiosis. Independent of the infection mechanism, a common feature is the formation of structures that mediate internalization. These are either transcellular (infection threads) (Gage, 2002, 2004) or intercellular (‘peg’-like structures) (Gonzalez-Sama *et al.*, 2004; Bonaldi *et al.*, 2011). The presence of a matrix material in these structures has been proposed as one of the unifying features allowing the intracellular uptake of bacteria into plant cells (Parniske, 2018). Here we describe that *Lotus* allows cell colonization through either transcellular infection threads or ‘peg’-like structures depending on the rhizobial strain encountered.

### Duality in symbiotic infection

Most legumes studied so far are predominantly infected by one infection mechanism. However, duality in infection has been documented. *Sesbania rostrata*, a robinoid plant like *Lotus*, exhibits dual infection behaviour depending on the growth

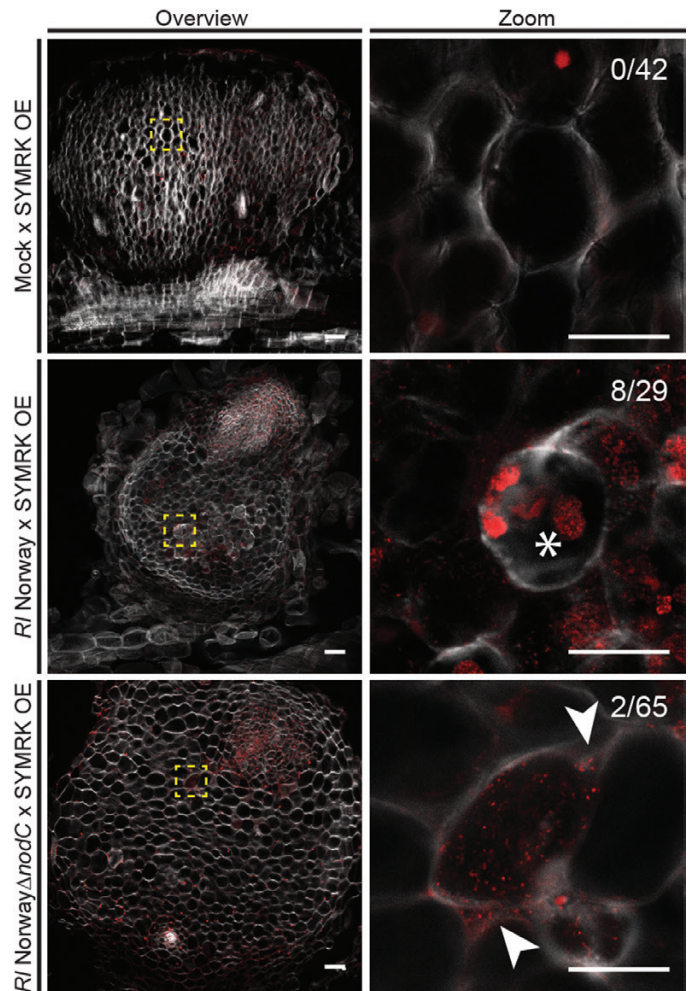


**Fig. 6.** Infection of spontaneously induced nodules in the absence of Nod factors. Hairy roots of *Lotus burtii* transformed with *pUBi:SYMRK-mOrange* were analysed 9 weeks after mock treatment, and inoculation with *Rhizobium leguminosarum* Norway and *RI* Norway $\Delta$ *nodC*. Semi-thin sections (50  $\mu$ m) of nodules were incubated with calcofluor white and propidium iodine that stain the plant cell wall and bacteria (and plant nuclei), respectively. Confocal laser scanning micrographs show that spontaneously generated nodules are induced even in the absence of rhizobia. *RI* Norway colonizes nodule cells, and dense bacterial accumulations reminiscent of ‘peg’-like structures (asterisk) are formed. In contrast, nodule cells infected by *RI* Norway $\Delta$ *nodC* do not exhibit these structures. Arrowheads indicate intercellular accumulations. Three independent experiments were conducted with at least 20 plants per condition. Representative micrographs are shown for each condition. Fractions indicate the number of nodules with detectable rhizobial infection per total nodule number for one of the experiments. Scale bars=50  $\mu$ m. (This figure is available in colour at JXB online.)

conditions (Goormachtig *et al.*, 2004). Upon flooding, *Sesbania* represses the growth of root hairs, and thus infection threads are not formed. Rhizobia then exploit lateral root bases as entry points (Ndoye *et al.*, 1994). Similar behaviour was described for *Lotus pedunculatus*. Bacteria infect enlarged epidermal cells and accumulate intercellularly in nodules formed on adventitious roots of flooded plants (James and Sprent, 1999). Another example is the ineffective strain NZP2213 that induces pseudonodules on *L. pedunculatus* roots. These organs are colonized intercellularly, but no cell infection is observed (Pankhurst *et al.*, 1979). Genetic manipulation of *L. japonicus* leads to

differential colonization modes. *Mesorhizobium loti* normally infects *L. japonicus* through infection threads. However, Nod factor perception mutants in an *snf1* genetic background (*nfr1-1 nfr5-2 snf1*) can be infected with or without infection threads if inoculated with wild-type or nod mutant strains, respectively (Madsen *et al.*, 2010). This can be re-created using wild-type strains. In *L. burttii* roots inoculated with *S. fredii* HH103, micro-colonies form, but infection threads abort shortly after initiation of progression. Nodules nevertheless emerge and are infected probably in the absence of epidermal infection threads. However, the absence of transcellular infection threads was not demonstrated (Acosta-Jurado *et al.*, 2016). On the other hand, *R1 Norway*, an ineffective strain, infects *L. burttii* via an infection thread-independent mechanism. Our work gives independent proof of this infection duality under natural conditions. These results provide evidence that robinoid plants have an inherent ability to support different types of infection. To our knowledge, this has not been described in other legume clades.

### Epidermal infection

Crack-entry penetration of the epidermis in natural systems is often restricted to lateral or adventitious root emergence sites (Ndoye *et al.*, 1994; Subbarao *et al.*, 1995; Bonaldi *et al.*, 2011). However, in a series of *Lotus* mutants that are impaired in epidermal infection thread formation, such as *nena-1* (Groth *et al.*, 2010), *ern1-2* (Cerri *et al.*, 2017; Kawaharada *et al.*, 2017), and *rhl1* (Karas *et al.*, 2005), nodules are infected via epidermal cracks throughout the whole root. In a similar fashion, *R1 Norway* infection sites are not located at lateral root emergence sites or between intact epidermal cells (Supplementary Fig. S1a). Very often bacteria accumulated on top of empty nodule primordia, the formation of which most probably creates natural openings on the epidermis.

*R1 Norway* induces widespread root hair deformation, but no infection threads (Fig. 2). The absence of epidermal infection threads in *R1 Norway*-inoculated roots is supported by the reduced induction of *NIN*, *ERN1*, and *EPR3* at 3 dpi (Fig. 3). Moreover, the absence of cortical infection threads correlates with the reduced induction of *SYMREM1* at 14 dpi (Fig. 3), which is essential for efficient infection thread progression (Lefebvre *et al.*, 2010; P. Liang *et al.*, 2018). Recently, *SYMREM1* has been shown to mediate the formation of a specific symbiotic perception hub and regulate the stability of the NFP receptor (P. Liang *et al.*, 2018). Induction of *NIN* in *R1 Norway*-treated roots was also reduced at 7 dpi. However, at 14 wpi, it reached slightly higher levels. This correlates with the appearance of the first nodule primordia. In conclusion, the microscopy and molecular evidence support an infection thread-independent crossing of the epidermis.

### Perception at the cell entry interface

'Peg'-like structures have been described in *Lupinus albus* (Gonzalez-Sama *et al.*, 2004), *Aeschynomene afraspera* (Bonaldi *et al.*, 2011), and *Lotus* mutants (Madsen *et al.*, 2010). They resemble enlarged and deformed infection threads that arise from intercellular bacterial accumulations. By inducing spontaneous nodulation in *L. burttii*, we could assess the role of

Nod factor in their formation. Nod factor synthesis is essential for the formation of these structures, as no 'peg'-like structure was observed upon inoculation with *R1 Norway*  $\Delta$ *nodC*. Bacteria nevertheless colonized nodule cells at a very low frequency. This remaining colonization is unlikely to be caused by residual Nod factor synthesis, as the *nodC* mutant induced no root hair deformation, a sensitive Nod factor response (Supplementary Fig. S4d). It is tempting to speculate that there is a Nod factor-independent entry mechanism, as has been previously postulated (Madsen *et al.*, 2010). However, we cannot discard the possibility that by activating symbiotic signalling through SYMRK overexpression, we bypassed Nod factor signalling. Differences in the dependency of Nod factor for the formation of 'peg'-like structures in *L. japonicus* Gifu *nfr1-1 nfr5-2 snf1* and in *L. burttii* overexpressing SYMRK could be caused by induction of an alternative signalling pathway in the latter. However, we cannot exclude that the observed effect is due to host plant differences.

The Nod factor-dependent formation of 'peg'-like structures supports the existence of a perception checkpoint prior to cell entry. In *Medicago truncatula*, the NFP and LYK3 receptors accumulate in a narrow zone at the border between the meristematic and the infection zones (Moling *et al.*, 2014). Down-regulation of NFP impairs release of bacteria (Moling *et al.*, 2014). Moreover, Nod factors accumulate strongly in the pre-fixation zone, specially in infection threads (Timmers *et al.*, 1998). Our results are independent support for this hypothesis.

In summary, *R1 Norway* infects *Lotus* spp. through an infection thread-independent mechanism. It penetrates nodule cells via 'peg'-like structures, the formation of which depends on Nod factor production. This reveals that *Lotus* exhibits a dual infection pattern depending on the rhizobia that it encounters. This dual infection of *Lotus* by *M. loti* MAFF and *R1 Norway* represents an exiting opportunity to perform comparative studies of infection.

## Supplementary data

Supplementary data are available at *JXB* online.

Fig. S1. Nodule distribution on root and shoot phenotype of *Lotus burttii* upon *Rhizobium leguminosarum* Norway inoculation.

Fig. S2. Intra- and intercellular colonization of *Rhizobium leguminosarum* Norway in *Lotus burttii* root nodules.

Fig. S3. *Mesorhizobium loti* MAFF303099 and *Rhizobium leguminosarum* Norway viability in *Lotus burttii* nodules.

Fig. S4. Nod operon and phenotypes of *Lotus burttii* upon *Rhizobium leguminosarum* Norway  $\Delta$ *nodC* inoculation.

Table S1. Strains and plasmids.

Table S2. PCR primer list.

Table S3. qRT-PCR primer list.

Table S4. Nod factor structures assigned from product ion mass spectra.

## Acknowledgements

We thank Martin Parniske and Marion R. Cerri for insightful discussions and critical reading of the manuscript, and Thomas Ott for sharing

the sequences of the *LjSYMREM1* qRT-PCR primers. We kindly thank Elina Makarenko for technical support. This work was funded by the German Research Foundation (DFG-grant: MA7269-1). The York Centre of Excellence in Mass Spectrometry was created thanks to a major capital investment through Science City York, supported by Yorkshire Forward with funds from the Northern Way Initiative, and subsequent support from EPSRC (EP/K039660/1; EP/M028127/1).

## Author contributions

JL phenotypically analysed the plants, conducted confocal microscopy, generated rhizobial strains, and performed the gene expression quantification; AK performed the TEM; MM extracted the Nod factor; EB and JT-O purified and solved the Nod factor structure; YYL phenotypically analysed plants, and performed the gene expression quantification; MM conceived and designed the experiments; JL and MM analysed the data, prepared figures, and wrote the manuscript.

## References

- Acosta-Jurado S, Rodriguez-Navarro DN, Kawaharada Y, et al.** 2016. *Sinorhizobium fredii* HH103 invades *Lotus burttii* by crack entry in a Nod factor- and surface polysaccharide-dependent manner. *Molecular Plant-Microbe Interactions* **29**, 925–937.
- Beringer JE.** 1974. R factor transfer in *Rhizobium leguminosarum*. *Journal of General Microbiology* **84**, 188–198.
- Bonaldi K, Gargani D, Prin Y, Fardoux J, Gully D, Nouwen N, Goormachtig S, Giraud E.** 2011. Nodulation of *Aeschynomene afraspera* and *A. indica* by photosynthetic *Bradyrhizobium* Sp. strain ORS285: the nod-dependent versus the nod-independent symbiotic interaction. *Molecular Plant-Microbe Interactions* **24**, 1359–1371.
- Borsos OS, Somaroo BH, Grant WF.** 1972. New diploid species of *Lotus* (Leguminosae) in Pakistan. *Canadian Journal of Botany* **50**, 1865–1870.
- Cerri MR, Wang Q, Stolz P, et al.** 2017. The ERN1 transcription factor gene is a target of the CcMK/CYCLOPS complex and controls rhizobial infection in *Lotus japonicus*. *New Phytologist* **215**, 323–337.
- D’Haeze W, Holsters M.** 2002. Nod factor structures, responses, and perception during initiation of nodule development. *Glycobiology* **12**, 79R–105R.
- Duzan HM, Zhou X, Souleimanov A, Smith DL.** 2004. Perception of *Bradyrhizobium japonicum* Nod factor by soybean [*Glycine max* (L.) Merr.] root hairs under abiotic stress conditions. *Journal of Experimental Botany* **55**, 2641–2646.
- Gage DJ.** 2002. Analysis of infection thread development using Gfp- and DsRed-expressing *Sinorhizobium meliloti*. *Journal of Bacteriology* **184**, 7042–7046.
- Gage DJ.** 2004. Infection and invasion of roots by symbiotic, nitrogen-fixing rhizobia during nodulation of temperate legumes. *Microbiology and Molecular Biology Reviews* **68**, 280–300.
- Gonzalez-Sama A, Lucas MM, de Felipe MR, Pueyo JJ.** 2004. An unusual infection mechanism and nodule morphogenesis in white lupin (*Lupinus albus*). *New Phytologist* **163**, 371–380.
- Goormachtig S, Capoen W, James EK, Holsters M.** 2004. Switch from intracellular to intercellular invasion during water stress-tolerant legume nodulation. *Proceedings of the National Academy of Sciences, USA* **101**, 6303–6308.
- Gossmann JA, Markmann K, Brachmann A, Rose LE, Parniske M.** 2012. Polymorphic infection and organogenesis patterns induced by a *Rhizobium leguminosarum* isolate from *Lotus* root nodules are determined by the host genotype. *New Phytologist* **196**, 561–573.
- Groth M, Takeda N, Perry J, et al.** 2010. NENA, a *Lotus japonicus* homolog of Sec13, is required for rhizodermal infection by arbuscular mycorrhizal fungi and rhizobia but dispensable for cortical endosymbiotic development. *The Plant Cell* **22**, 2509–2526.
- Ibáñez F, Wall L, Fabra A.** 2017. Starting points in plant–bacteria nitrogen-fixing symbioses: intercellular invasion of the roots. *Journal of Experimental Botany* **68**, 1905–1918.
- James EK, Sprent JI.** 1999. Development of N<sub>2</sub>-fixing nodules on the wetland legume *Lotus uliginosus* exposed to conditions of flooding. *New Phytologist* **142**, 219–231.
- James EK, Sprent JI, Sutherland JM, Mcinroy SG, Minchin FR.** 1992. The structure of nitrogen-fixing root-nodules on the aquatic mimosoid legume *Neptunia plena*. *Annals of Botany* **69**, 173–180.
- Karas B, Murray J, Gorzelak M, Smith A, Sato S, Tabata S, Szczyglowski K.** 2005. Invasion of *Lotus japonicus* root hairless 1 by *Mesorhizobium loti* involves the nodulation factor-dependent induction of root hairs. *Plant Physiology* **137**, 1331–1344.
- Kawaharada Y, James EK, Kelly S, Sandal N, Stougaard J.** 2017. The ethylene responsive factor required for nodulation 1 (ERN1) transcription factor is required for infection-thread formation in *Lotus japonicus*. *Molecular Plant-Microbe Interactions* **30**, 194–204.
- Lefebvre B, Timmers T, Mbengue M, et al.** 2010. A remorin protein interacts with symbiotic receptors and regulates bacterial infection. *Proceedings of the National Academy of Sciences, USA* **107**, 2343–2348.
- Liang J, Hoffrichter A, Brachmann A, Marin M.** 2018. Complete genome of *Rhizobium leguminosarum* Norway, an ineffective *Lotus* micro-symbiont. *Standards in Genomic Sciences* **13**, 36.
- Liang P, Stratil TF, Popp C, Marin M, Folgmann J, Mysore KS, Wen J, Ott T.** 2018. Symbiotic root infections in *Medicago truncatula* require remorin-mediated receptor stabilization in membrane nanodomains. *Proceedings of the National Academy of Sciences, USA* **115**, 5289–5294.
- Madsen LH, Tirichine L, Jurkiewicz A, Sullivan JT, Heckmann AB, Bek AS, Ronson CW, James EK, Stougaard J.** 2010. The molecular network governing nodule organogenesis and infection in the model legume *Lotus japonicus*. *Nature Communications* **1**, 10.
- Moling S, Pietraszewska-Bogiel A, Postma M, Fedorova E, Hink MA, Limpens E, Gadella TW, Bisseling T.** 2014. Nod factor receptors form heteromeric complexes and are essential for intracellular infection in *Medicago* nodules. *The Plant Cell* **26**, 4188–4199.
- Murray JD.** 2011. Invasion by invitation: rhizobial infection in legumes. *Molecular Plant-Microbe Interactions* **24**, 631–639.
- Ndoye I, de Billy F, Vasse J, Dreyfus B, Truchet G.** 1994. Root nodulation of *Sesbania rostrata*. *Journal of Bacteriology* **176**, 1060–1068.
- Niwa S, Kawaguchi M, Imazumi-Anraku H, Chechetka SA, Ishizaka M, Ikuta A, Kouchi H.** 2001. Responses of a model legume *Lotus japonicus* to lipochitin oligosaccharide nodulation factors purified from *Mesorhizobium loti* JRL501. *Molecular Plant-Microbe Interactions* **14**, 848–856.
- Oldroyd GE, Murray JD, Poole PS, Downie JA.** 2011. The rules of engagement in the legume–rhizobial symbiosis. *Annual Review of Genetics* **45**, 119–144.
- Pankhurst CE, Craig AS, Jones WT.** 1979. Effectiveness of *Lotus* root-nodules. 1. morphology and flavolan content of nodules formed on *Lotus pedunculatus* by fast-growing *Lotus* rhizobia. *Journal of Experimental Botany* **30**, 1085–1093.
- Parniske M.** 2018. Uptake of bacteria into living plant cells, the unifying and distinct feature of the nitrogen-fixing root nodule symbiosis. *Current Opinion in Plant Biology* **44**, 164–174.
- Ried MK, Antolin-Llovera M, Parniske M.** 2014. Spontaneous symbiotic reprogramming of plant roots triggered by receptor-like kinases. *eLife* **3**, e03891.
- Sant’anna FH, Andrade DS, Trentini DB, Weber SS, Schrank IS.** 2011. Tools for genetic manipulation of the plant growth-promoting bacterium *Azospirillum amazonense*. *BMC Microbiology* **11**, 107.
- Schindelin J, Arganda-Carreras I, Frise E, et al.** 2012. Fiji: an open-source platform for biological-image analysis. *Nature Methods* **9**, 676–682.
- Spaink HP, Aarts A, Stacey G, Bloemberg GV, Lugtenberg BJ, Kennedy EP.** 1992. Detection and separation of *Rhizobium* and *Bradyrhizobium* Nod metabolites using thin-layer chromatography. *Molecular Plant-Microbe Interactions* **5**, 72–80.
- Stougaard J, Abildsten D, Marcker KA.** 1987. The *Agrobacterium rhizogenes* Pri TI-DNA segment as a gene vector system for transformation of plants. *Molecular and General Genetics* **207**, 251–255.
- Stracke S, Kistner C, Yoshida S, et al.** 2002. A plant receptor-like kinase required for both bacterial and fungal symbiosis. *Nature* **417**, 959–962.
- Subbarao NS, Mateos PF, Baker D, Pankratz HS, Palma J, Dazzo FB, Sprent JI.** 1995. The unique root-nodule symbiosis between *Rhizobium* and the aquatic legume, *Neptunia natans* (L-F) Druce. *Planta* **196**, 311–320.

- Thoma S, Schobert M.** 2009. An improved *Escherichia coli* donor strain for diparental mating. *FEMS Microbiology Letters* **294**, 127–132.
- Timmers AC, Auriac MC, de Billy F, Truchet G.** 1998. Nod factor internalization and microtubular cytoskeleton changes occur concomitantly during nodule differentiation in alfalfa. *Development* **125**, 339–349.
- Uchiumi T, Ohwada T, Itakura M, et al.** 2004. Expression islands clustered on the symbiosis island of the *Mesorhizobium loti* genome. *Journal of Bacteriology* **186**, 2439–2448.
- van Spronsen PC, Grønlund M, Pacios Bras C, Spaik HP, Kijne JW.** 2001. Cell biological changes of outer cortical root cells in early determinate nodulation. *Molecular Plant-Microbe Interactions* **14**, 839–847.
- Vervliet G, Holsters M, Teuchy H, Van Montagu M, Schell J.** 1975. Characterization of different plaque-forming and defective temperate phages in *Agrobacterium*. *Journal of General Virology* **26**, 33–48.
- Vincent JM.** 1970. The cultivation, isolation and maintenance of rhizobia. In: Vincent JM, ed. *A manual for the practical study of root-nodule*. Oxford: Blackwell Scientific Publications, 1–13.

## Supplementary materials

## SUPPLEMENTARY DATA

Article title: A sub-compatible rhizobium strain reveals infection duality in *Lotus*.

Authors: Juan Liang, Andreas Klingl, Yen-Yu Lin, Emily Boul, Jane Thomas-Oates, and Macarena Marín.

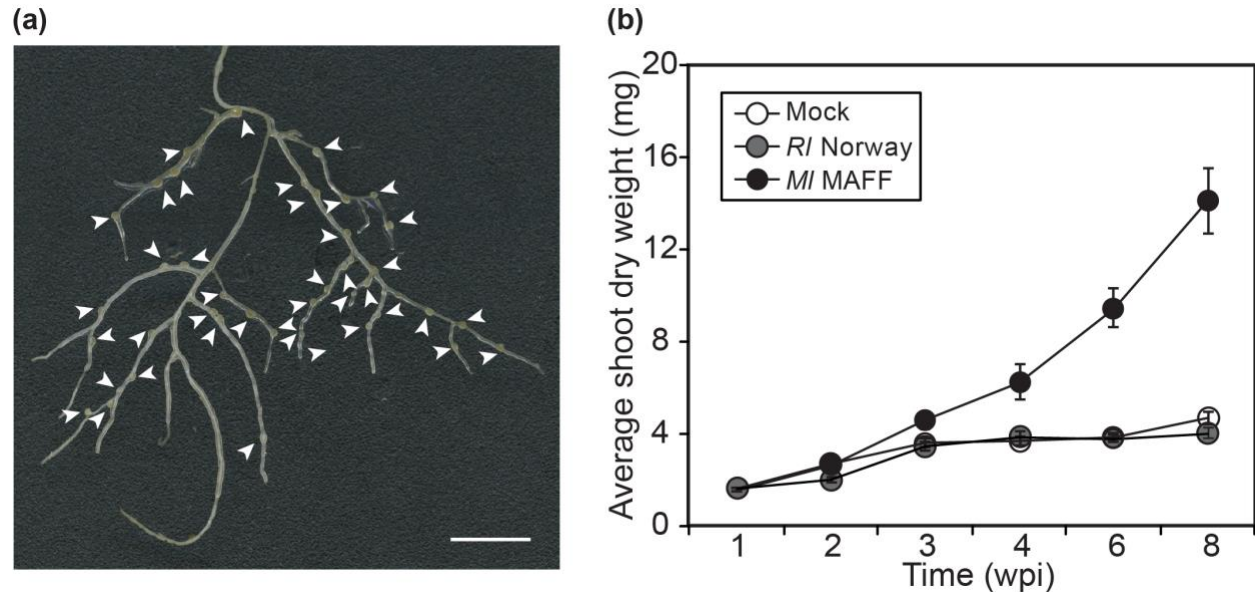


**Fig. S1** Nodule distribution on root and shoot phenotype of *Lotus burtii* upon *Rhizobium leguminosarum* Norway inoculation. (a) Distribution of ineffective nodules along a representative *L. burtii* root 6 weeks after inoculation with *Rhizobium leguminosarum* Norway (*R/* Norway). Arrowheads indicate the nodule position on the root. Bar: 1 cm. (b) Quantification of *L. burtii* average shoot dry weight upon mock treatment, and inoculation with *R/* Norway and *Mesorhizobium loti* MAFF 303099 (*M/* MAFF). The graph represents one of three independent experiments that were conducted with 20 plants per condition and per time point. Error bars indicate standard deviations.

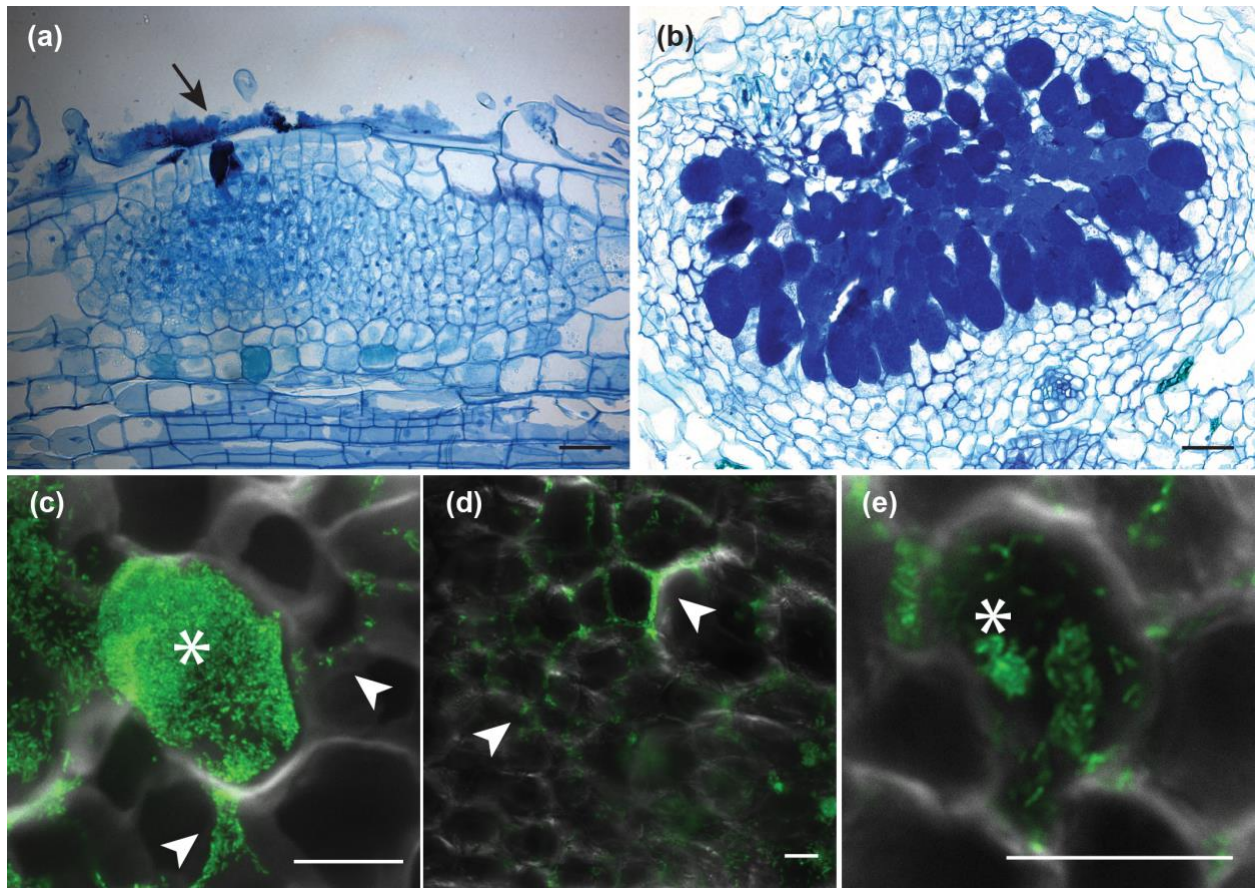


**Fig. S2** Intra- and inter- cellular colonisation of *Rhizobium leguminosarum* Norway in *Lotus burttii* root nodules. Light micrographs of thin sections (5 µm) stained with toluidine blue and methylene blue show that *Rl* Norway induces the formation of infection pockets (a; arrow) and colonises in the cortex in the absence of both epidermal and trans-cellular infection threads (a, b). Enlarged cells are stained dark blue. This intense coloration is often associated with senescing cells (Van de Velde *et al.*, 2006; Regus *et al.*, 2017). Representative CLSM micrographs of nodule sections (50 µm) stained with calcofluor white (white) show that *Rl* Norway-GFP bacteria colonise nodules intra- (c, e; asterisk) and inter- cellularly (c, d; arrowheads). Abundant intercellular colonization could arise from bacteria release from plant cells (Regus *et al.*, 2017). Dense bacterial accumulations reminiscent of “pegs” often form close to the cell border (e; asterisk). Bars: (a, b) 50 µm, (c-e) 10 µm.



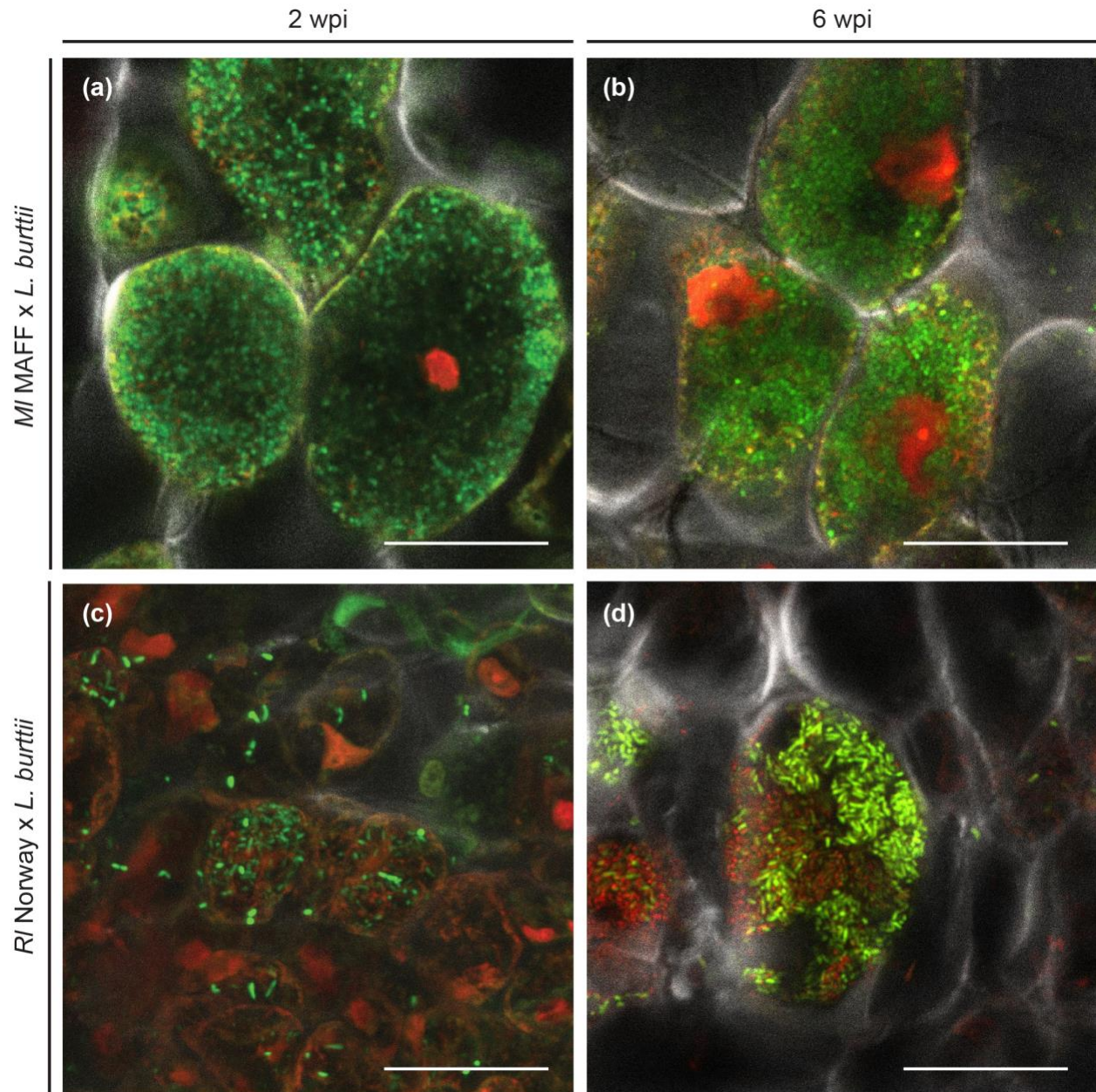


**Fig. S3** *Mesorhizobium loti* MAFF303099 and *Rhizobium leguminosarum* Norway viability in *Lotus burttii* nodules. Viability was determined by live/dead staining using SYTO9 (green) and propidium iodide (red), which stain living and dead bacteria, respectively. The nodule semi-thin sections (50  $\mu$ m) were counterstained with calcofluor white (white). Representative CLSM micrographs show that *MI MAFF* bacteria are alive in nodules 2 and 4 weeks after inoculation (a, b). *RI Norway* bacteria are alive in nodule 2 weeks post inoculation (c). However, some dead bacteria appear after 4 weeks (d). Micrographs show representative phenotypes of more than 12 nodules collected in three independent experiments. Bars: 25  $\mu$ m.

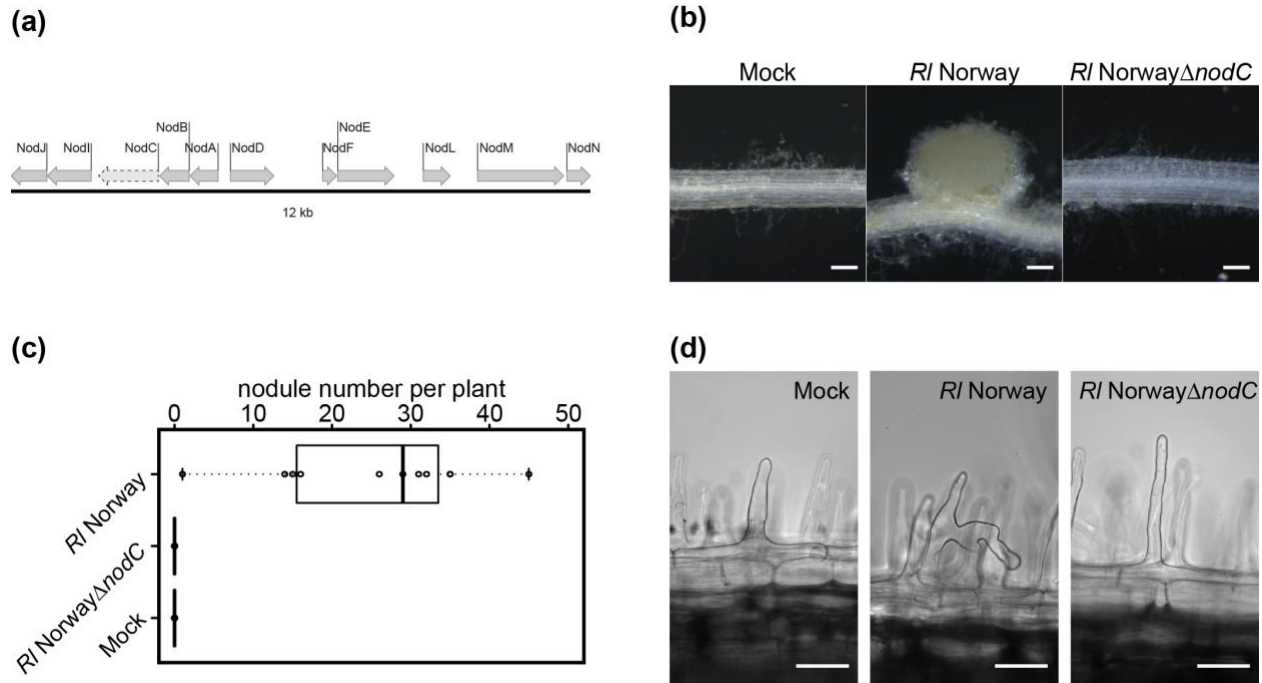


**Fig. S4** Nod operon and phenotypes of *Lotus burttii* upon *Rhizobium leguminosarum* Norway $\Delta$ nodC inoculation. (a) The dashed box indicates the region deleted in frame by homologous recombination in the *nod* operon. Micrographs of representative root nodule phenotypes (b) and boxplot of nodule number quantification (c) 4 weeks post inoculation. Representative root hair responses to mock treatment, and inoculation with *RI* Norway and the *RI* Norway $\Delta$ nodC mutant at 2 wpi (d). Bars: (b) 100  $\mu$ m; (d) 50  $\mu$ m.

**Table S1 Strains and plasmids**

<b>Strain or plasmid</b>	<b>Derivation and relevant genotype</b>	<b>Reference</b>
<i>Rhizobium leguminosarum</i>		
Norway	Wild type	(Gossmann <i>et al.</i> , 2012)
Norway GFP	<i>R. leguminosarum</i> Norway containing the pHC60 plasmid, IncP, Tc <sup>R</sup>	(Gossmann <i>et al.</i> , 2012)
Norway Sm <sup>R</sup>	Spontaneous Sm <sup>R</sup> mutant of <i>R. leguminosarum</i> Norway, Sm <sup>R</sup>	This work
Norway $\Delta$ <i>nodC</i> DsRed	<i>NodC</i> deletion of <i>R. leguminosarum</i> Norway containing pFAJ- <i>DsRed</i> plasmid, Tc <sup>R</sup>	This work
<i>Mesorhizobium loti</i>		
MAFF303099 DsRed	MAFF3030999 strain expressing <i>DsRed</i> , Gm <sup>R</sup>	(Maekawa-Yoshikawa <i>et al.</i> , 2009)
MAFF303099 GFP	MAFF 303099 containing the pFAJ-GFP plasmid, Tc <sup>R</sup>	This work
<i>Agrobacterium rhizogenes</i>		
AR1193	pRi1193 carrying pBR322 in the TL segment, Rf <sup>R</sup> , Cm <sup>R</sup>	(Stougaard <i>et al.</i> , 1987)
<i>Escherichia coli</i>		
TOP10	F- <i>mcrA</i> $\Delta$ ( <i>mrr-hsdRMS-mcrBC</i> ) $\Phi$ 80 <i>lacZ</i> $\Delta$ M15 $\Delta$ <i>lacX74 recA1 araD139</i> $\Delta$ ( <i>araleu</i> )7697 <i>galU galK rpsL endA1 nupG</i> , Sm <sup>R</sup>	Invitrogen
ST18	S17 $\lambda$ pir $\Delta$ <i>hemA</i> , Tp <sup>R</sup> , Sm <sup>R</sup>	(Thoma & Schobert, 2009)

---

Plasmids		
pFAJ-GFP	pFAJ1708 carries the GFP encoding gene, Tc <sup>R</sup>	(Kelly <i>et al.</i> , 2013)
pK19MOBSACB	Integration vector with the ColE1 replication origin, <i>mob</i> , <i>sacB</i> , <i>lacZα</i> , Km <sup>R</sup>	(Schäfer <i>et al.</i> , 1994)
pK19MOBSACB- <i>nodC</i> -AB	pK19MOBSACB derivative carrying upstream 637bp and downstream 631bp flanking fragments of <i>nodC</i> (downstream of <i>nodJ</i> and <i>nodL</i> ) regions, Km <sup>R</sup>	This work
<i>pUBi:SYMRK-mOrange</i>	Assembled by BpiI cut ligation from: LII dy 1-2 + LII F 2-3 <i>pUBi:SYMRK:mOrange</i> + LII dy 3-4 + LII F 5-6 <i>p35S:GFP</i> + LIII β F A-B, Km <sup>R</sup>	(Ried <i>et al.</i> , 2014)

---

Tp, trimethoprim; Sm, streptomycin; Tc, tetracycline; Km, kanamycin; Gm, gentamicin; Cb, carbenicillin; Rf, rifampicin.

**Table S2 PCR primer list**

Primers	Sequence (5'-3')
M13_Fwd	TGTAAAACGACCCCCCAGT
M13_Rev	GGAAACAGCTATGACCAT
nodC_FrA_F	GGGAAGCTTCAGAATGAGTAGCTGCGG
nodC_FrA_R	ATGCTCTCCACCGTTTACGCATATAGTGGCGAGTGATGATCGC
nodC_FrB_F	GTAAACGGTGGAGAGCAT
nodC_FrB_R	CCCTCTAGACTAATCCATTCTGCACGCC
nodC_outer_F	TGGGTCGTTAGAAGAATTGT
nodC_outer_R	ATGTCCTCGTATTGGTAGT

**Table S3 qRT-PCR primer list**

Primers	Sequence (5'-3')	Reference
Rl_nifH_qF	TCCAAACTCATCCATTTTCGT	This work
Rl_nifH_qR	AGTCCGGCGCATATTGGATCA	This work
IF-1_F	CGAAAACGAACACGAGATCA	(Garcia Angulo <i>et al.</i> , 2013)
IF-1_R	GTAGGGCGTCATTTCCACAA	(Garcia Angulo <i>et al.</i> , 2013)
<i>nifH</i> (Forward)	TCCAAGCTCATCCACTTCGTG	(Ott <i>et al.</i> , 2005)
<i>nifH</i> (Reverse)	AGTCCGGCGCATACTGGATTA	(Ott <i>et al.</i> , 2005)
Ml_IF_qF	GAAGTCCTCGAGTTTCCGGG	This work
Ml_IF_qR	TTGAAGCGGTAGGTGATGCG	This work
<i>ERN1</i> -314-Fw	TGTCTCCTTGGATTCCCCTC	(Cerri <i>et al.</i> , 2012)
<i>ERN1</i> -391-Rev	TTGGGGCAGGAACATCAACA	(Cerri <i>et al.</i> , 2012)
<i>nin</i> (Fw)	AACTCACTGGAAACAGGTGCTTTC	(Kumagai <i>et al.</i> , 2006)
<i>nin</i> (Rev)	CTATTGCGGAATGTATTAGCTAGA	(Kumagai <i>et al.</i> , 2006)
Ljnpl qF	CCACATTGCTGGAGGGCCTTG	(Xie <i>et al.</i> , 2012)
Ljnpl qR	GCTCACGTACCCACTGCCAC	(Xie <i>et al.</i> , 2012)
<i>epr3</i> (Fw)	TGGCAGCAGTTTTGAACAAG	(Kawaharada <i>et al.</i> , 2015)
<i>epr3</i> (Rev)	GTCTTCAGCGGGGTATTTGA	(Kawaharada <i>et al.</i> , 2015)
<i>ATP</i> (Fw)	CAATGTCCCAAGGCCCATGGTG	(Kawaharada <i>et al.</i> , 2015)
<i>ATP</i> (Rev)	AACACCACTCTCGATCATTTCTCTG	(Kawaharada <i>et al.</i> , 2015)

**Table S4 Nod Factor structures assigned from product ion mass spectra**

<b>Strain</b>	<b>Structures</b>
<i>R. leguminosarum</i> Norway	IV(16:1-OH) IV(16:1, Ac)/(C18:2-OH) IV(C18:4, Ac) IV(C18:3, Ac) IV(18:1, Ac) IV(18:0, Ac) IV(C18:1-OH, Ac) IV(C20:4, Ac) IV(C20:1, Ac) IV(C20:4-OH, Ac) V(C16:1-OH) V(18:1) V(C16:1, Ac)/(C18:2-OH) V(C16:1-OH, Ac)/(C20:0) V(C18:4, Ac) V(18:1, Ac)/(C20:2-OH) V(C18:0, Ac)(C20:1-OH) V(C20:3,Ac) V(C20:1, Ac)

## References

- Cerri MR, Frances L, Laloum T, Auriac MC, Niebel A, Oldroyd GE, Barker DG, Fournier J, de Carvalho-Niebel F. 2012.** *Medicago truncatula* ERN transcription factors: regulatory interplay with NSP1/NSP2 GRAS factors and expression dynamics throughout rhizobial infection. *Plant Physiology* **160**(4): 2155-2172.
- Garcia Angulo VA, Bonomi HR, Posadas DM, Serer MI, Torres AG, Zorreguieta A, Goldbaum FA. 2013.** Identification and characterization of RibN, a novel family of riboflavin transporters from *Rhizobium leguminosarum* and other proteobacteria. *Journal of Bacteriology* **195**(20): 4611-4619.
- Gossmann JA, Markmann K, Brachmann A, Rose LE, Parniske M. 2012.** Polymorphic infection and organogenesis patterns induced by a *Rhizobium leguminosarum* isolate from *Lotus* root nodules are determined by the host genotype. *New Phytologist* **196**(2): 561-573.
- Kawaharada Y, Kelly S, Nielsen MW, Hjuler CT, Gysel K, Muszynski A, Carlson RW, Thygesen MB, Sandal N, Asmussen MH, et al. 2015.** Receptor-mediated exopolysaccharide perception controls bacterial infection. *Nature* **523**(7560): 308-312.
- Kelly SJ, Muszynski A, Kawaharada Y, Hubber AM, Sullivan JT, Sandal N, Carlson RW, Stougaard J, Ronson CW. 2013.** Conditional requirement for exopolysaccharide in the *Mesorhizobium-Lotus* symbiosis. *Molecular Plant Microbe Interactions* **26**(3): 319-329.

- Kumagai H, Kinoshita E, Ridge RW, Kouchi H. 2006.** RNAi knock-down of *ENOD40s* leads to significant suppression of nodule formation in *Lotus japonicus*. *Plant and Cell Physiology* **47**(8).
- Maekawa-Yoshikawa M, Müller J, Takeda N, Maekawa T, Sato S, Tabata S, Perry J, Wang TL, Groth M, Brachmann A, et al. 2009.** The temperature-sensitive brush mutant of the legume *Lotus japonicus* reveals a link between root development and nodule infection by rhizobia. *Plant Physiology* **149**(4): 1785-1796.
- Ott T, van Dongen JT, Gunther C, Krusell L, Desbrosses G, Vigeolas H, Bock V, Czechowski T, Geigenberger P, Udvardi MK. 2005.** Symbiotic leghemoglobins are crucial for nitrogen fixation in legume root nodules but not for general plant growth and development. *Current Biology* **15**(6): 531-535.
- Regus JU, Quides KW, O'Neill MR, Suzuki R, Savory EA, Chang JH, Sachs JL. 2017.** Cell autonomous sanctions in legumes target ineffective rhizobia in nodules with mixed infections. *American Journal of Botany* **104**(9): 1-14.
- Ried MK, Antolin-Llovera M, Parniske M. 2014.** Spontaneous symbiotic reprogramming of plant roots triggered by receptor-like kinases. *Elife* **3**.
- Schäfer A, Tauch A, Jäger W, Kalinowski J, Thierbach G, Pühler A. 1994.** Small mobilizable multi-purpose cloning vectors derived from the *Escherichia coli* plasmids pK18 and pK19: selection of defined deletions in the chromosome of *Corynebacterium glutamicum*. *Gene* **145**(1): 69-73.
- Stougaard J, Abildsten D, Marcker KA. 1987.** The *Agrobacterium rhizogenes* pRi TL-DNA segment as a gene vector system for transformation of plants. *Molecular and General Genetics* **207**(2-3): 251.
- Thoma S, Schobert M. 2009.** An improved *Escherichia coli* donor strain for diparental mating. *FEMS Microbiology Letters* **294**: 127-132.
- Van de Velde W, Guerra JC, De Keyser A, De Rycke R, Rombauts S, Maunoury N, Mergaert P, Kondorosi E, Holsters M, Goormachtig S. 2006.** Aging in legume symbiosis. A molecular view on nodule senescence in *Medicago truncatula*. *Plant Physiology* **141**(2): 711-720.
- Xie F, Murray JD, Kim J, Heckmann AB, Edwards A, Oldroyd GE, Downie JA. 2012.** Legume pectate lyase required for root infection by rhizobia. *Proceedings of the National Academy of Sciences* **109**(2): 633-638.



# General discussion

The sub-compatible strain *Rl* Norway induces nodules in different *Lotus* species (Gossmann et al. 2012), including *L. burtii* (Liang et al. 2019) and more than 90 *L. japonicus* ecotypes (Fig. 3). Diverse nodule morphologies, including nodules, arrested nodule primordia, and tumours, are induced by *Rl* Norway on *Lotus* roots (Fig. 3) (Gossmann et al. 2012). Strikingly, the epidermal inspection showed that *Rl* Norway does not induce epidermal infection threads on *Lotus* (Gossmann et al. 2012). To investigate the underlying mechanism of the nodule organogenesis and infection phenotypes, we sequenced and characterised the genome of *Rl* Norway and investigated the infection mechanism on *L. burtii* in detail. Furthermore, the co-isolated *Mn* 10.2.2 strain and *Rl* Norway were used to investigate the rhizobia behaviours associated with their root colonisation.

## 1. Infection thread-independent mechanisms

The unifying feature of the infection process includes at least three steps: i) crossing of the epidermis, ii) cortical spreading and iii) intracellular uptake of rhizobia (Venado et al. 2020). Model legumes from *Lotus* and *Medicago* genus are infected by their compatible microsymbionts in an infection thread-dependent manner (Gage 2004). The study of the root nodule symbiosis using model legumes has discovered many genes, the majority of which are involved in nodule organogenesis and early stages of infection (Roy et al. 2020). However, the genes involved in the later stages of infection are poorly studied. This is because the later infection process is interlinked with the complex infection thread formation in model systems, which is not amenable to address the infection mechanism underlying this process. Alternatively, legumes can be invaded by rhizobia via infection thread independent strategies, which can uncouple the infection threads formation with the infection process. Numerous mutants in *L. japonicus* Gifu are invaded in the absence of epidermal infection threads. In the *nen-1* mutant, which is impaired in the generation of  $Ca^{2+}$  oscillation, *M. loti* MAFF 303099 invades the nodule via “crack-entry” (Groth et al. 2010). Epidermal infection threads on the *ern1-2* mutant are dramatically reduced and only infection thread-like structures are observed (Cerri et al. 2017). The *epr3-10* and *epr3-11* mutants display impaired infection thread formation in both the epidermis and cortex (Kawaharada et al. 2015, Kawaharada et al. 2017). Strikingly, *M. loti* R7A $\Delta$ *nodC* can be internalised from the intercellular space into host cells of the *L. japonicus* Gifu triple mutant in Nod factor receptors in the gain of function allele in

CCaMK background, *nfr1-1 nfr5-2 snf1*, via “peg”-like structures (Madsen et al. 2010). These studies on *Lotus* encouraged us to further investigate the infection mode of *R/ Norway* on *L. burtii* in detail. We have characterised that *R/ Norway* colonised nodules in the absence of both epidermal and cortical infection threads (Liang et al. 2019). Strikingly, the TEM inspection showed that *R/ Norway* was probably internalised into the host cell directly from the apoplast via a “peg”-like structure. The *M. loti* R7A *nodC* mutant presents a 10-20-fold lower infection frequency than in the wild-type infecting *L. japonicus* Gifu (Madsen et al. 2010). In contrast, the infection frequency of *R/ Norway* on *L. burtii* was 100% (Liang et al. 2019). Although the direct internalisation of rhizobia from the apoplast has been widely identified in the leguminous plant from the Genistoid and Dalbergioid clades, such as in *Lupinus* (Gonzalez-Sama et al. 2004), *Arachis* (Chandler 1978), *Stylosanthes* (Chandler et al. 1982), and *Aeschynomene* (Loureiro et al. 1995, Arrighi et al. 2012). Besides, the infection thread-independent mechanism has also been identified in *M. scabrella*, which does not belong to the Genistoid and Dalbergioid clades (de Faria et al. 1988). However, these hosts are less amenable to study the mechanism behind. Therefore, the interaction of *R/ Norway* and *Lotus* can be used as a model to study the infection mechanisms in later stages.

The alternative infection in other non-model legume hosts has been applied to uncover the mechanism in different infection stages. *S. rostrata* grown under flooding conditions can be invaded via “cracks” in the epidermis (Ndoye et al. 1994, Goormachtig et al. 2004). The pattern of calcium oscillations in *S. rostrata* upon treatment by Nod factors of *A. caulinodans* ORS571 varies compared with that of *M. truncatula* treated with Nod factors of *S. meliloti* (Capoen et al. 2009). In addition, *A. caulinodans* ORS571 can still infect the primordium of a *CCaMK* RNAi knockdown line (Capoen et al. 2009). Therefore, the studies of *S. rostrata* indicate that Nod factor-mediated  $Ca^{2+}$  oscillation is not required for epidermal infection via “crack-entry”. To investigate the host gene expression induced in *L. burtii*, we compared the expression of several crucial symbiotic markers upon the infection with *R/ Norway* or with *M. loti* MAFF 303099. In general, symbiotic marker genes induced by *R/ Norway* displayed a distinct expression pattern in comparison with *M. loti* MAFF 303099. *NIN* is a hub transcriptional factor regulating both the nodule organogenesis and rhizobial infection network (Liu et al. 2019a). There are hundreds of downstream genes that are controlled by *NIN* (Liu et al. 2019a). Expression of *NIN* in *L. burtii* was induced only at 14 dpi by *R/ Norway*, while *M. loti* MAFF 303099 induced *NIN* expression already at 3 dpi. Intriguingly, the expression of *nodulation pectate lyase (NPL)*, which is a direct target of *NIN*, was not significantly reduced, although *NPL* is involved in both epidermal and cortical infection thread formation (Xie et al. 2012).

Nevertheless, The NIN expression of *R/ Norway* probably mirrors the delayed nodulation and infection phenotypes that *R/ Norway* induced. ERN1 is another crucial transcriptional factor targets downstream genes, which are limited and distinct from the targets of NIN (Liu et al. 2019a). *R/ Norway* induced lower expression of *ERN1* in comparison with *M. loti* MAFF 303099. Overall, the distinct expression of *NIN* and *ERN1* upon *R/ Norway* inoculation compared with *M. loti* MAFF 303099 may induce the change of the downstream gene expression pattern. Strikingly, *Symbiotic remorin 1 (SYMREM1)* was not induced by *R/ Norway* up to 14 dpi in *L. burttii*. SYMREM1 is proposed to act as a scaffold to stabilise the symbiotic membrane nanodomain formed by the flotillin protein FLOT4 (Liang et al. 2018b). In this membrane nanodomain, SYMREM1 recruits the ligand-activated Lysin Motif Receptor-LIKE Kinase3 (LYK3) (Liang et al. 2018b, Lefebvre et al. 2010). It has been hypothesised that the symbiotic nanodomain is involved in the elongation of infection threads (Ott 2017). This suggests that the lack of SYMREM1 in this nanodomain might contribute to the absence of infection threads upon *R/ Norway* infection.

## 2. The internalisation process of *R/ Norway*

Rhizobia are commonly surrounded by an electron-dense matrix during internalisation (Parniske 2018). The cytoskeleton rearrangement and the vacuole degeneration are largely engaged in the internalisation process (Timmers et al. 1998, Kitaeva et al. 2016). The internalisation of rhizobia is crucial for the nitrogen fixation, because the intracellular environment in the nodule provides the necessary conditions for the rhizobial nitrogen fixation (Burén and Rubio 2018). However, the mechanism of the rhizobial internalisation is not well elucidated. It has been proposed that there is a unique perception mechanism before rhizobia entry (Moling et al. 2014). Evidence showed that there is a perception of Nod factors in the cortex of the indeterminate *Medicago* type of nodule. The indeterminate nodule contains distinct zones from the distal to the proximal of the root, including meristem zone, infection zone, fixation zone, and senescence zone (Patriarca et al. 2004). In the infection and fixation zone, the internalisation of rhizobia via the infection threads actively occur (Patriarca et al. 2004). Nod factor biosynthesis genes have been found to be expressed in the infection and fixation zone in *M. truncatula* (Roux et al. 2014, Sharma and Signer 1990). In addition, Nod factor receptors Nod Factor Perception (NFP) and LYK3 in *Medicago* accumulate in about two layers close to the fixation zone of the nodule (Moling et al. 2014). These studies suggest that there is a Nod factor-perception in the cortex to regulate the formation of the symbiotic interface.

This thesis further addresses whether Nod factors are involved in the formation of “peg”-like structures. A strain containing a *nodC* mutation in *R/ Norway* which impairs the gene involved in the biosynthesis of the core of Nod factors, was generated. However, *R/ Norway* $\Delta$ *nodC* was not able to induce nodule formation on *L. burttii*. To assess this, we inoculated *R/ Norway* $\Delta$ *nodC* on *L. burttii* transgenic roots overexpressing SYMRK, which can induce spontaneous nodules in the absence of rhizobial inoculation, as described in a previous report in *L. japonicus* Gifu (Ried et al. 2014). We observed that *R/ Norway* $\Delta$ *nodC* was able to inter- and intra-cellularly colonise the cortex of the spontaneous nodules (Liang et al. 2019). Interestingly, *R/ Norway* $\Delta$ *nodC* was internalised into the host cells in the absence of “peg”-like structures. However, this observation is in contrast to the previous study of a triple mutation of *L. japonicus* Gifu, which the *M. loti* R7A $\Delta$ *nodC* can be internalised via “peg”-like structures (Madsen et al. 2010). There is the possibility that *R/ Norway* $\Delta$ *nodC* colonised the dead host cells so that *R/ Norway* was not actively internalised by the host. Another explanation could be that the overexpression of SYMRK in the root activated an alternative symbiotic signalling. This alternative signalling would instead mediate the internalisation of *R/ Norway* $\Delta$ *nodC* in the absence of “peg”-like structures. In the study of Madsen et al., the gain-of-function mutation of CCaMK (*snf1*) background can also possibly induce downstream signalling involved in the infection so that gives rise to “peg”-like structures formation. Nevertheless, we concluded that the formation of “peg”-like structures depends on the Nod factors of *R/ Norway*. Together, our results reinforce the hypothesis that there is a perception of Nod factors before the internalisation of rhizobia.

In addition to *L. burttii*, *R/ Norway* induced diverse infection patterns in more than 90 *L. japonicus* ecotypes in the absence of infection threads (Fig. 3). Strikingly, the internalisation phenotypes of *R/ Norway* on *L. japonicus* ecotypes were contrastive (unpublished data, R. Venado). This contrastive internalisation capacity in *L. japonicus* ecotypes in combination with genome-wide transcriptional analysis can be further explored to identify genes involved in the internalisation process. In addition, a genome-wide association study (GWAS) can also be applied to associate the internalisation trait to the related genes. Overall, infection-thread independent mode on *Lotus* induced by *R/ Norway* can be used as a system to identify genes involved in the internalisation process.

### 3. Approaches to identify rhizobial genes involved in the internalisation process

In the infection thread-dependent infection process, Nod factors are the best-known rhizobial signal involved in the infection processes. In addition, EPS is known involved in the infection thread formation, but the downstream signalling induced by the EPS perception is not well elucidated (Kawaharada et al. 2015). In the Nod factor-independent infection process, effectors have been found to play an important role in the infection process (Teulet et al. 2019). However, the downstream signalling that effectors induced is not well elucidated. Therefore, the signalling induced by other symbiotic molecules instead of Nod factors needs to be further examined. As discussed in the above section, *R/* Norway can be internalised into the host cell in the absence of cortical infection threads. This phenotype provides the possibility to study symbiotic signals involved in the internalisation. However, uncovering the role of symbiotic molecules still remains a challenge. Although laser capture microdissection has been used to analyse gene expression of both rhizobia and host cells in different zones of the *Medicago* nodule (Roux et al. 2014, Roux et al. 2018, Limpens et al. 2013), this is not applicable on *R/* Norway infected nodules. This is because *R/* Norway infected nodules are mosaic and contain infected cells next to non-infected cells as well as a large number of intercellular bacteria. The resolution of the laser capture microdissection is not enough to separate these different types of cells. During my doctoral studies, protoplast isolation was attempted to separate the infected host cells (intracellular colonised rhizobia) from the rhizobia colonised between host cells (intercellular colonised rhizobia). However, the low colonisation rate of *R/* Norway in the nodule cells resulted in a very limited number of infected host cells successfully isolated (unpublished data). The infected cells also very easily lysed after isolation. The cell membrane in the nodule cells was probably disrupted during the rhizobia internalisation process, which could contribute to the cell lysis. Therefore, alternative methods need to be carried out in future studies.

Several T3Es of *Bradyrhizobium* spp. have been shown to mediate infection in the absence of infection threads. The *nopT* mutation in *Bradyrhizobium* ORS3257 colonises only between the cortex cells but not in the host cells in the nodules of *A. indica* (Teulet et al. 2019). NopT is known to function as a cysteine protease located in the cytoplasmic membrane of the host cell (Fotiadis et al. 2012). Besides, *nopAB* mutant in *Bradyrhizobium* ORS3257 shows no colonisation (Teulet et al. 2019). Different infection phenotypes induced by the T3Es mutants suggest that T3Es are involved in the infection of *Bradyrhizobium* spp. at different steps (Teulet et al. 2019). One hypothesis is that effectors released from *R/* Norway could mediate the

infection on *L. burtii*. A targeted approach can be used to identify possible candidate rhizobial genes involved in the internalisation process. To further study the function of secreted proteins of *RI* Norway in the infection process, we analysed the secretion systems of *RI* Norway. *RI* Norway has several protein secretion systems, including T1SS, T4SS, T5SS, and T6SS, but does not have the best-studied T3SS (Liang et al. 2018a). The T1SS of rhizobia secrete Raps and glycanases, which are involved in the biofilm formation in *RI* species but are not essential for the root nodule symbiosis (Russo et al. 2006). T5SSs are categorised as auto-transporters (reviewed in (Meuskens et al. 2019, Henderson et al. 2004)) and two-partner systems (Jacob-Dubuisson et al. 2013) to translocate proteins across the plasma membrane. Proteins secreted via T5SSs are often toxins, adhesins or proteinases (reviewed in (Meuskens et al. 2019, Henderson et al. 2004)). However, the function of T5SS in root nodule symbiosis is unknown. The T5SS of *RI* bv. *viciae* 3841 does not play a role in the root nodule symbiosis with *Pisum sativum* cv. Frisson and other hosts (Krehenbrink and Downie 2008). Interestingly, *RI* Norway contains a two-partner system that is absent in *RI* bv. *viciae* 3841 (Liang et al. 2018a). The cargo protein of the two-partner system of *RI* Norway is a putative filamentous hemagglutinin. Members of this family are involved in the biofilm formation of virulent *Bordetella* spp. (Locht et al. 1993). The functions of T1SSs and T5SSs of *RI* Norway are less likely involved in the infection, but the actual functions of them are worth to be further examined. T4SS and T6SS can directly translocate proteins into the host cytoplasm (Fauvart and Michiels 2008). Interestingly, the expression of the T4SS in *M. loti* R7A depends on NodD (Hubber, Sullivan and Ronson 2007). T6SS is the least studied secretion system and proteins secreted by the T6SS have not been identified in rhizobia. The role of T4SS and T6SS in mediating the nodulation compatibility has been reported in other strains of *RI* species (Hubber et al. 2004, Bladergroen, Badelt and Spaink 2003, Salinero-Lanzarote et al. 2019), but the functionality of them in infection process has not been investigated. A targeted approach to delete the essential genes involved in the secretion systems can be further used to inspect the infection of *RI* Norway in *L. burtii*.

#### **4. Nodulation incompatibility on *L. japonicus* Gifu**

In addition to the striking infection process that *RI* Norway induced on *Lotus*, *RI* Norway can nodulate a broad range of plants from *Lotus* genus (Gossmann et al. 2012). Interestingly, *RI* Norway failed to induce nodule organogenesis on *L. japonicus* Gifu and MG-86 growing in the Seramis substrate (Fig. 3) (Gossmann et al. 2012). The stringent nodulation phenotype of *L. japonicus* Gifu and MG-86 indicates that rhizobial signals are tightly recognised by the hosts.

The different nodulation phenotypes induced on the hosts by *Rl* Norway can be applied to further study the perception mechanism. This reinforces the advantage of using natural diversity to uncover this phenomenon.

Some substituents of Nod factors are known to play a role in the specific nodulation compatibility in different hosts (López-Lara et al. 1996, Stacey et al. 1994, Rodpothong et al. 2009). We have compared the *nod* genes of *Rl* Norway with *M. loti* MAFF 303099. The *nod* gene analysis showed that *M. loti* MAFF 303099 harbours the *nodZ* gene (Kaneko et al. 2000), which is not present in the *nod* cluster of *Rl* Norway (Liang et al. 2018a). *nodZ* encodes the enzyme responsible for adding fucosyl residues at the reducing end of the Nod factors (Mergaert et al. 1996, Quesada-Vincens et al. 1997, Lerouge et al. 1990). Mass spectrometry analysis showed that *Rl* Norway produces Nod factors with unsaturated lipid chains and without the fucosyl decorations (Liang et al. 2019), which is also consistent with the *nod* gene analysis (Liang et al. 2018a). The fucosyl substituents, added by the *nodZ* gene, is involved in the nodulation compatibility with *Lotus*. For example, *M. loti* R7A $\Delta$ *nodZ* induces severely decreased nodule numbers in several *Lotus* species (Rodpothong et al. 2009). Interestingly, the delayed nodulation in *L. japonicus* Gifu is more pronounced compared to *L. burtii* (Rodpothong et al. 2009). This suggests that the structure of Nod factors required for inducing nodule organogenesis are more stringent for *L. japonicus* Gifu than for *L. burtii*. This is consistent with the nodule organogenesis phenotype induced by *Rl* Norway on the two hosts. The *nodZ* gene affects the specificity of nodulation of other legumes as well. The *nodZ* mutant in *B. japonicum* USDA110 is defective in nodulating *Macroptilium atropurpureum* (Stacey et al. 1994). Introduction of the *nodZ* gene from *B. japonicum* USDA110 into *Rl* bv. *viciae* RBL5560 (*Rl* bv. *viciae* - DZ) enables *Rl* bv. *viciae* RBL5560 to gain the nodulation capacity on *M. atropurpureum* (López-Lara et al. 1996). Similar results obtained in the study in *Lotus*. *Rl* bv. *viciae* - D, which is a genetically engineered derivative of *Rl* bv. *viciae* RBL5560, produces an unfucosylated reducing-terminal Nod factors. This strain cannot nodulate *Lotus* species, including *L. burtii*, *L. filicaulis*, *L. japonicus* MG-20, Gifu and Nepal (Gossmann et al. 2012). Interestingly, *Rl* bv. *viciae* - DZ can nodulate the *Lotus* species above, but not *L. filicaulis* (Gossmann et al. 2012). These results suggest that the fucosyl substituents in the Nod factor may play a role in the specificity of nodulation. Ectopic expression in *Rl* Norway of the *nodZ* gene from a compatible *M. loti* strain could be further applied to determine the role of it in the nodulation compatibility of *L. japonicus* Gifu.

The effector-triggered immunity (ETI) of hosts has been shown involved in the nodulation incompatibility in soybean. For example, *Rj2* & *Rfg1* genes of soybean, encoding a plant

resistance (R) protein, restrict nodulation compatibility of *B. japonicum* USDA257 (Yang et al. 2010). The restriction of nodulation is elicited by triggering defence response of the *Rj2*-soybean by the NopP effector of *Bradyrhizobium* USDA122 (Sugawara et al. 2018). As *R/* Norway harbours several secretion systems, there is another hypothesis that *R/* Norway could release molecules to block the nodulation on *L. japonicus* Gifu. Based on this hypothesis, the genes involved in the specificity of nodulation could be determined by a forward genetic screen. When the gene involved in the blocking effect is mutated, it can induce nodule organogenesis on *L. japonicus* Gifu. During my doctoral studies, I generated a transposon insertion mutant pool of *R/* Norway by using a Transposon insertion sequencing (Tnseq) approach that has been successfully applied in *R/* bv. *viciae* 3841 (Perry and Yost 2014). The genome analysis showed that this mutant pool potentially contains more than 100,000 different mutants. To reduce the laborious work, the collection of mutants needs to be mixed as an inoculum to identify the candidate genes. However, *R/* Norway contains more than 7,000 genes in the genome (Liang et al. 2018a). As the *R/* bv. *viciae* 3841 strain contains 89.5% neutral genes in the genome (Perry and Yost 2014), we speculated that the number of neutral genes of *R/* Norway is also considerable. In the mixed inoculum, the wild-type-like rhizobia mutants are likely to be dominant in the population. The wild-type-like rhizobia can still release proteins or other compounds to block the nodulation. One strategy to overcome this challenge is to reduce the number of mutants in the mixed inoculum for each plant to decrease this blocking effect from the rhizobia on the host. By using this approach, unknown factors involved in the nodulation compatibility maybe can be determined.

## **5. Synergistic effect of dual species root colonisation**

Root colonisation is the prerequisite for establishing the root nodule symbiosis. The root colonisation of rhizobia has not been shown to directly influence the root nodule symbiosis in previous studies (Smit et al. 1987, Mongiardini et al. 2008). Although, it is probably more relevant for the root nodule symbiosis in the environment where microbial communities are more complex (Williams et al. 2008, Ormeño-Orrillo et al. 2008). Rhizosphere is a nutrient rich niche for microbes, where up to 20% of the photosynthetic compounds are released from the roots (Walker et al. 2003). There are up to  $10^{12}$  bacteria present in one gram of soil in the rhizosphere (Kennedy and de Luna 2005). In order to colonise the nutrient rich root, there are competition and cooperation among rhizobia. However, the impact of bacteria interaction on the root colonisation has not been well addressed under laboratory conditions. One reason is that current studies on the root colonisation mainly focus on single strain inoculums. Another



reason is that the root colonisation involves complex bacterial behaviours, including chemotaxis, motility, biofilm formation, etc. (Wheatley and Poole 2018). *Rl* Norway was co-isolated with *Mn* 10.2.2 from the same nodule (Gossmann et al. 2012), which indicates that they originated from a close spatial niche instead of an arbitrary system. The level of root colonisation between the two rhizobia was very different. *Rl* Norway colonised massively on the root, while the colonisation of *Mn* 10.2.2 was not very pronounced (Fig. 8). Interestingly, the root colonisation by both rhizobia was enhanced in the 24-well plate (Fig. 8) and the distal inoculation assays (Fig. 10). Strikingly, in the distal inoculation assay, the nodule number induced by the co-inoculation was significantly higher than the single inoculation condition (Fig. 10). This suggests that *Rl* Norway and *Mn* 10.2.2 could influence the behaviour of each other in the root colonisation process. To reduce the complexity of studying the rhizobia interaction *in planta*, the motility and the biofilms formation *in vitro* were inspected as a first step to investigate the reason underlying the enhanced root colonisation.

The motility is crucial for rhizobia to colonise the root in the early stage (Zheng et al. 2015, Ormeño-Orrillo et al. 2008). The swarming motility of *Rl* Norway was higher than *Mn* 10.2.2 (Fig. 11), which mirrors the higher root colonisation of *Rl* Norway from the distal inoculation assay (Fig. 10). Interestingly, the motility of *Mn* 10.2.2 was increased in the presence of *Rl* Norway (Fig. 11), which possibly contributes to the increased nodule number and root colonisation of *Mn* 10.2.2 in the co-inoculation condition of the distal inoculation assay (Fig. 10). The motility alteration of *Mn* 10.2.2 on the soft agar plate may include not only swarming but also other types of motility, for example, the growth-induced sliding motility (Kearns 2010, Hölscher and Kovács 2017, Janczarek 2011). Thus, the increased motility of *Mn* 10.2.2 in the presence of *Rl* Norway was probably not completely result from the swarming motility of *Rl* Norway. The movement of bacteria driven by the flagella and pili contribute greatly to different types of motility depend on the environment (Mitchell and Kogure 2006, Gordon and Wang 2019, Merz, So and Sheetz 2000). To address how motility influences root colonisation, it would be interesting to use the flagella and pili impaired mutants to colonise the root in a short growth period. The short growth period aims to eliminate other motilities, which could occur later, for example, the sliding motility.

In the later stage, biofilms are crucial for the root colonisation of rhizobia (reviewed in (Fujishige et al. 2006, Wheatley and Poole 2018). Biofilms are normally constructed by cohesive polymers to enhance the surface attachment of bacteria (Rinaudi and Giordano 2010, Flemming and Wingender 2010). In a microbe community, the formation of the mixed biofilms is normally a consequence of a synergistic effect of bacteria (Burmølle et al. 2006, Lopes et

al. 2012, Lee et al. 2014). It is hypothesised that mixed biofilms can provide higher adhesion (Burmølle et al. 2014). However, the formation of mixed biofilms of rhizobia has not been addressed. *Rl* Norway was observed forming biofilms alone, while *Mn* 10.2.2 only attached on the glass slides with few cells (Fig. 13). Interestingly, *Mn* 10.2.2 was embedded in the dense area of biofilms together with *Rl* Norway (Fig. 13). This suggests that mixed biofilms were successfully formed, which is hypothesised to provide higher adhesion for the root colonisation.

Surface polysaccharides are key components of the biofilm matrix, because they act as the scaffold to adhere to bacteria. For example, the reduced production of surface polysaccharides impairs the biofilms formation of *Rl* and *S. meliloti* strains (Fujishige et al. 2006, Russo et al. 2006, Vanderlinde et al. 2009). The role of the surface polysaccharides of *Rl* Norway in the biofilm formation was investigated in this thesis. The quantity of biofilms detected of *Rl* Norway $\Delta$ exo5 in the 24-well plate assay was not reduced in comparison with the wild type *Rl* Norway, but slightly higher (Fig. 12). However, the pattern of *Rl* Norway $\Delta$ exo5 attached on the glass slide was significantly changed. Water channels were obviously visible in the presence of the wild type *Rl* Norway, while a more homogeneous structure of biofilms formed in the culture of *Rl* Norway $\Delta$ exo5 (Fig. 13). Under the co-culture condition, although the lower quantity of biofilms was detected in the 24-well plate assay, the structure of biofilms was not different from the single culture condition (Fig. 13). This indicates that the structure formation of the mixed biofilms largely depends on the surface polysaccharides of *Rl* Norway. In addition to rhizobia, numerous studies illustrate that surface polysaccharides affect the biofilms formation in different bacteria. For example, a similar structural change of biofilms has been observed in the acetylation-defective exopolysaccharides (alginate) of *P. aeruginosa* FDR1 (Tielen et al. 2005). The authors observed that the alginate contributes to the microcolony formation in the biofilms initiation stage (Tielen et al. 2005), which possibly influences the structure formation of biofilms. The structure of the surface polysaccharides of *Rl* Norway could be determined in future studies to identify the role of specific surface polysaccharides during biofilms formation.

In addition to root colonisation, mixed biofilms formation aid bacteria to be more resilient to harsh environmental conditions compared to single-species biofilms (Crespi 2001, Elias and Banin 2012). This is evidenced by studies in which mixed biofilms of *Pseudomonas* and other species endure more antimicrobial compounds than single-species biofilms (Lee et al. 2014, Lopes et al. 2012). A similar phenomenon occurs in the mixed biofilms of four marine isolates belonging to *Microbacterium phyllosphaerae*, *Shewanella japonica*, *Dokdonia donghaensis*,

and *Acinetobacter lwoffii* species (Burmølle et al. 2006). Although the mixed biofilms formation is a cooperative behaviour of many bacteria, the function of them in rhizobia is yet unknown. It can be hypothesised that mixed rhizobial biofilms are more tolerant to antimicrobial compounds released by roots or other microbes. Therefore, *Mn* 10.2.2 and *R/* Norway may have a synergistic effect with each other in terms of the mixed biofilms formation. However, the exact role of the mixed biofilms needs to be further investigated.

Overall, the enhanced root colonisation in the presence of both strains suggests there is a synergistic effect on the root colonisation. The motility promotion and the mixed biofilms formation in the presence of the two strains may contribute to the enhanced root colonisation. However, direct evidence needs to be shown in future studies in order to fully explain the enhanced root colonisation.

## 6. General Conclusion

In summary, a previous study that identified a *R/* Norway strain, which can infect and nodulate a broad range of *Lotus* (Gossmann et al. 2012). We later discovered that *R/* Norway induces an infection thread-independent infection on *Lotus*. Strikingly, *R/* Norway is directly internalised from the apoplast into the nodule cells via “peg”-like structures. This thesis also showed that the formation of “peg”-like structures depends on the biosynthesis of Nod factors from *R/* Norway. Together, these results support the previous hypothesis that there is a perception mechanism before the rhizobial internalisation. This opens the possibility of identifying the fundamental genetic basis of the internalisation in combination with powerful next generation sequencing (NGS) and GWAS approaches.

Furthermore, co-inoculation of *R/* Norway and *Mn* 10.2.2 enhanced the root colonisation of both strains on the *L. japonicus* Gifu in both the 24-well plate and the distal inoculation assays. The co-culture of *R/* Norway and *Mn* 10.2.2 induced mixed biofilms formation. This opens the possibility to study the function of the mixed biofilms in root colonisation, which is not elucidated so far. In addition, these phenotypes can be provided as a preliminary model to establish the system to further study the interaction of bacteria within the soil microbe communities in the rhizosphere.

# Appendix

## Supplementary figures

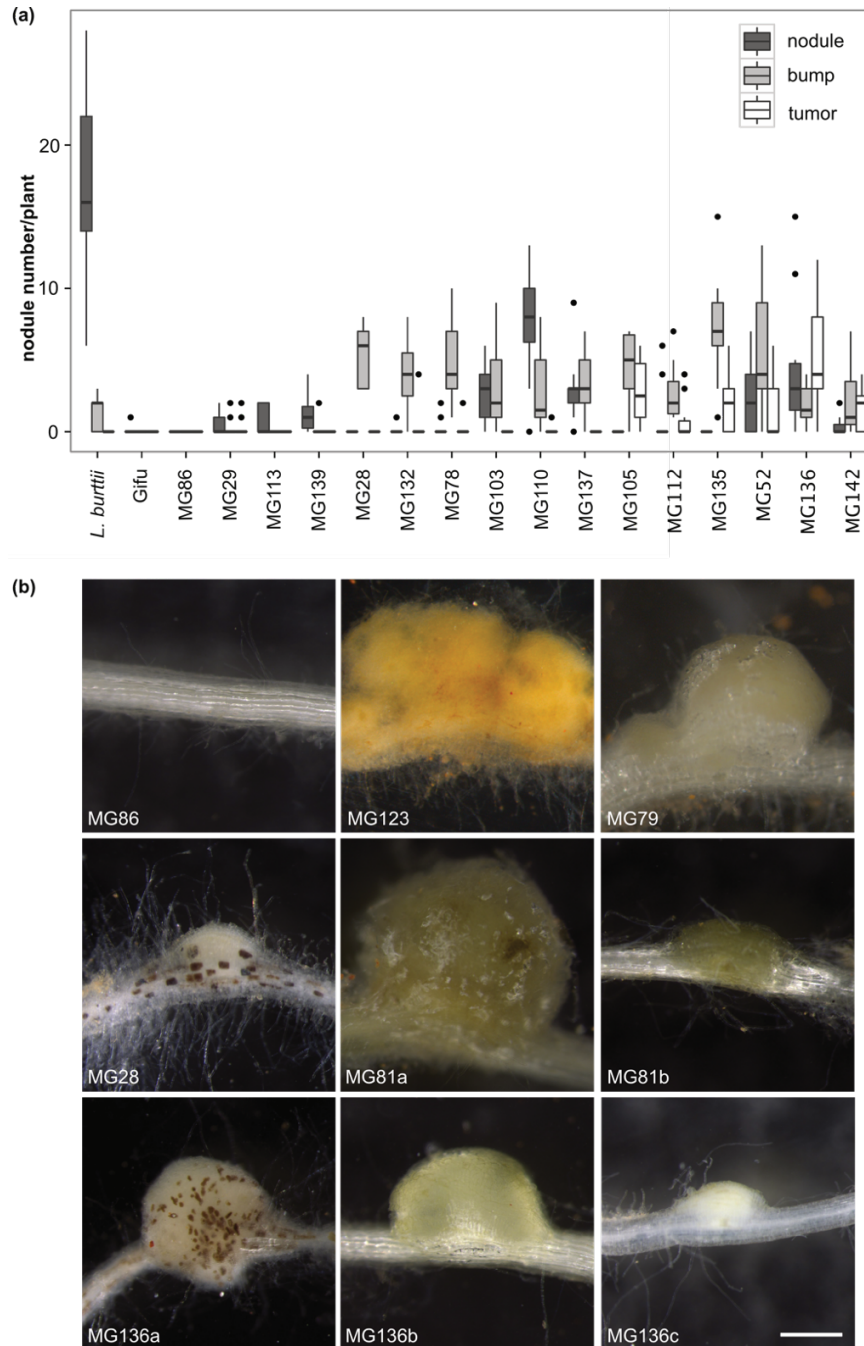


**Figure 3: Nodule phenotypes of *Lotus* upon *RI* Norway inoculation at 6 wpi.**

(a) Boxplot of the nodule number per plant of *L. burttii* and a subset of *L. japonicus* ecotypes. Dark grey, light grey and white boxes indicate nodules, bumps, and tumours, respectively. (b) Representative morphologies of nodules (MG81a, MG136a), bumps (MG28, MG81b, MG136c), and tumours (MG123, MG79, MG136b). Scale bar: 500  $\mu$ m.

## Supplementary results

### 1. *Rl* Norway co-colonised *L. japonicus* Gifu nodules in the presence of *Mn* 10.2.2

*Rl* Norway and *Mn* 10.2.2 were originally co-isolated from a single root nodule of *L. corniculatus* (Gossmann et al. 2012). However, a previous study showed that *Rl* Norway cannot induce nodules on the root of *L. corniculatus* by itself, but *Mn* 10.2.2 can induce (Gossmann et al. 2012). Thus, the co-isolation of *Rl* Norway and *Mn* 10.2.2 suggests that *Rl* Norway can co-colonise nodules with *Mn* 10.2.2. Nodules hosting multiple rhizobia have been observed in many studies (Checcucci et al. 2016, Friesen and Mathias 2010) and have been proposed to be a reservoir for inefficient symbionts under natural conditions (Westhoek et al. 2017, Mendoza-Suárez et al. 2020). To further investigate how *Rl* Norway co-infects nodules, we first aimed to reconstruct this observation under laboratory conditions. *L. corniculatus* is not a well characterised *Lotus* species, lacking defined germplasms, inbred lines, mutant collections and a completely published genome sequence. Therefore, we compared the growth and nodule organogenesis of the well-established model species *L. japonicus* Gifu upon rhizobia inoculation. As shown in Figure 4, even three weeks post-inoculation (wpi), *Rl* Norway did not induce nodulation in *L. japonicus* Gifu (Fig. 4, *Rl* Norway, lower panel). Shoots displayed a stunted phenotype, pale green leaves and purple stems, which indicate nutrient deficiency (Fig. 4, *Rl* Norway, upper panel). In contrast, *Mn* 10.2.2 induced pink nodules on the roots (Fig. 4, *Mn* 10.2.2, lower panel) and promoted shoot growth of *L. japonicus* Gifu (Fig. 4, *Mn* 10.2.2, upper panel). Upon *Rl* Norway and *Mn* 10.2.2 co-inoculation, *L. japonicus* Gifu developed pink nodules on their roots and shoot growth was promoted as well (Fig. 4). To assess whether nodules were co-infected by *Rl* Norway and *Mn* 10.2.2 *DsRed*, the nodule colonisation was quantified by isolating rhizobia from around 100 *L. japonicus* Gifu nodules. Surface sterilised nodules were crushed, and the suspensions were grown on rhizobium selective media. Different strains were distinguished by supplementing the medium with different antibiotics. All of the nodules were infected with *Mn* 10.2.2. Five percent of nodules in *L. japonicus* Gifu were co-infected by both *Rl* Norway and *Mn* 10.2.2. Therefore, we conclude that *Rl* Norway is capable of colonising *L. japonicus* Gifu nodules in the presence of *Mn* 10.2.2.

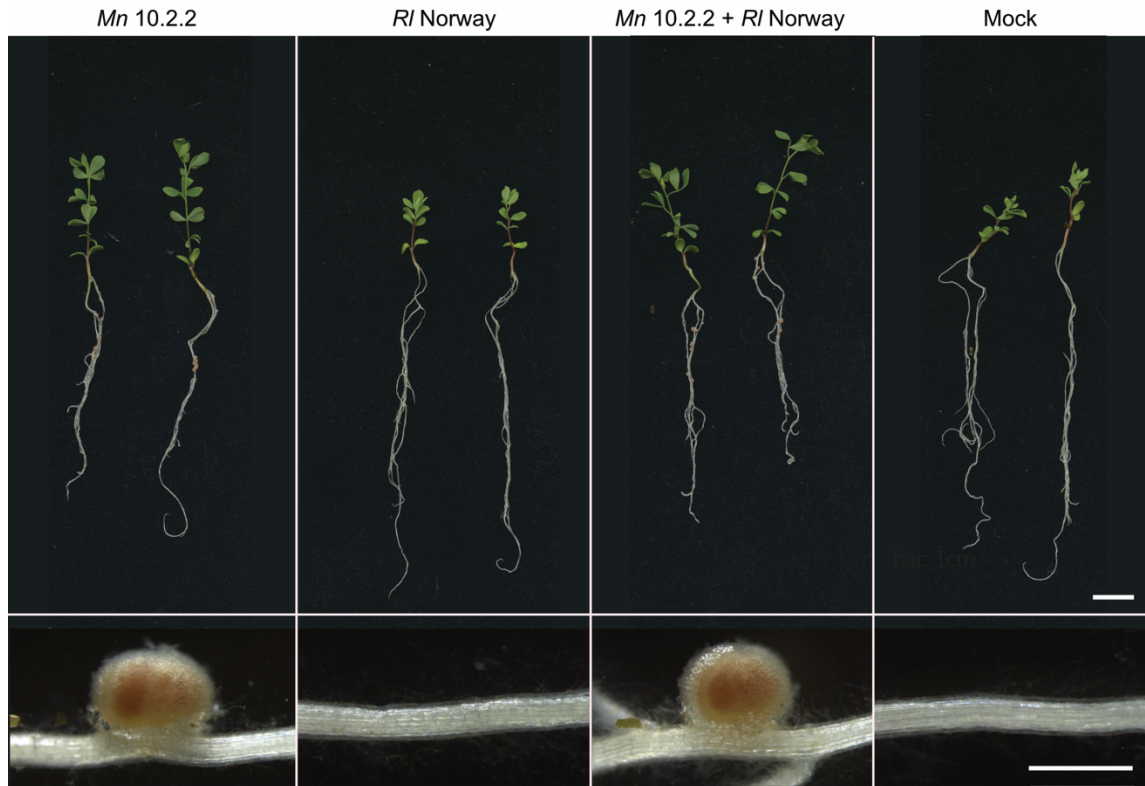


**Figure 4: Plant growth phenotypes upon rhizobia inoculation.**

Representative images of *L. japonicus* Gifu plantlets upon *Mn* 10.2.2, *RI* Norway, or *Mn* 10.2.2 + *RI* Norway inoculation at 3 weeks post-inoculation (3 wpi). Upper panel: plantlets inoculated with FAB medium without bacteria were used as mock control. Lower panel: a close up of the root morphology, showing the presence or absence of nodule formation. Scale bars: upper panel: 1 cm, lower panel: 1 mm. The experiment was conducted with 20 plants per condition.

## **2. Co-colonisation by *RI* Norway and *Mn* 10.2.2 does not impair the growth of the host**

Although *RI* Norway cannot nodulate *L. japonicus* Gifu alone, it can co-infect to the nodules induced by *Mn* 10.2.2. To address whether the co-colonisation by *RI* Norway and *Mn* 10.2.2 causes an impairment in host growth, we inoculated *L. japonicus* Gifu plants and quantified nodule organogenesis and plant growth in time course experiments (Fig. 5). *RI* Norway single inoculation does not promote the growth of *L. japonicus* Gifu (Fig. 5a). Moreover, at 6 wpi, shoot length was significantly reduced in comparison to the mock condition (Fig. 5a). The dry weight of the shoot of the mock condition was on average  $4.63 \pm 0.67$  mg and upon *RI* Norway inoculation was  $4.16 \pm 0.48$  mg. This result indicates *RI* Norway alone slightly impaired the

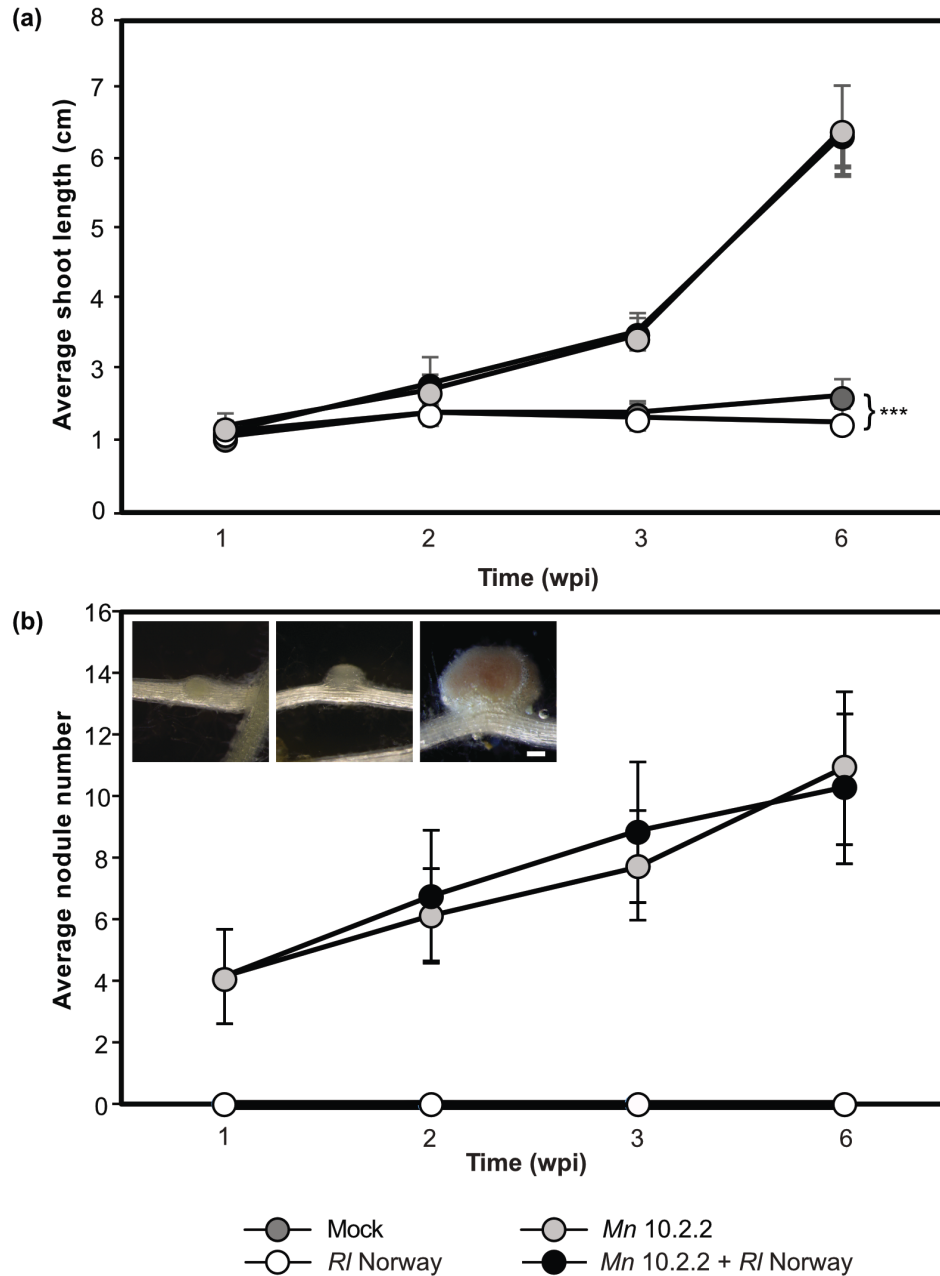


**Figure 5: Co-inoculation with *RI* Norway and *Mn* 10.2.2 induced no growth defects on the host.**

*L. japonicus* Gifu seedlings were treated with a mock solution or inoculated with *RI* Norway, *Mn* 10.2.2, and *Mn* 10.2.2 + *RI* Norway. Average shoot length (a) and nodule number (b) per plant were quantified after 1 wpi, 2 wpi, 3 wpi, and 6 wpi. Nodule morphologies developed in three stages showed in (b) were quantified as nodules. Scale bar: 200 μm. The experiment was conducted with 20 plants per condition. Error bars indicate standard deviations (SDs). The statistical analysis was performed by t-test method, \*\*\* indicates  $p < 0.005$ .

host growth. In contrast, *Mn* 10.2.2 and *RI* Norway co-inoculation promoted the plant growth from 2 wpi to 6 wpi, which is comparable to the single inoculation with *Mn* 10.2.2 (Fig. 5a). The number of nodules in three developmental stages was quantified, as shown in Fig. 5b. The proportions between the different morphologies did not significantly vary among the different treatments. The average nodule number upon *Mn* 10.2.2 single- and co-inoculation were not significantly different over the time period (Fig. 5b). These results demonstrate that in the presence of *Mn* 10.2.2, *RI* Norway does not impair host growth under the tested conditions.

### **3. *RI* Norway hitchhikes in the nodule independent of the infection thread**

*RI* Norway did not nodulate *L. japonicus* Gifu alone, but it entered nodules of *L. japonicus* Gifu together with *Mn* 10.2.2. This observation motivated us to further study how *RI* Norway invades the root nodule of *L. japonicus* Gifu together with *Mn* 10.2.2. To that aim, we inspected roots of over 40 *L. japonicus* Gifu plants co-inoculated with fluorescently tagged *Mn* 10.2.2 and *RI* Norway in comparison with single inoculations. *Mn* 10.2.2 *DsRed* induced the formation of infection threads on root hairs, both alone and in the presence of *RI* Norway (Fig. 6, infection thread indicated by an arrow). Infection threads penetrating the epidermis and spreading in primordia were also widely detected (Fig. 6b, d). In contrast, no infection threads were detected by *RI* Norway GFP alone or in the co-inoculation condition (Fig. 6a). Instead, *RI* Norway GFP colonises the surface of the root or the nodule primordium under both conditions (Fig. 6a, c, d). No infection threads containing both bacteria were observed under the co-inoculation condition (Fig. 6). Nevertheless, a fraction of the mature nodules was colonised by both *RI* Norway GFP and *Mn* 10.2.2 *DsRed* (Fig. 6f). Altogether, these results suggest that *RI* Norway infects the nodule independent of the infection threads induced by *Mn* 10.2.2. This is consistent with the infection route that *RI* Norway uses to invade the nodules of *L. burttii* (Liang et al. 2019).

To further study the colonisation pattern of co-infected nodules, we pre-screened them under the light microscope and selected three-mixed nodules that were sectioned and later visualised by confocal laser scanning microscopy (CLSM). To compare the infection pattern in different hosts, we used *L. burttii* plants, as they can be nodulated and infected by *RI* Norway alone (Gossmann et al. 2012, Liang et al. 2019). *Mn* 10.2.2 *DsRed* alone fully colonised the inner tissue of nodules induced on both species (Fig. 7a, e). The cells in this tissue were enlarged and fully filled with *Mn* 10.2.2 *DsRed* (Fig. 7a, b, e, f). Transcellular infection threads were



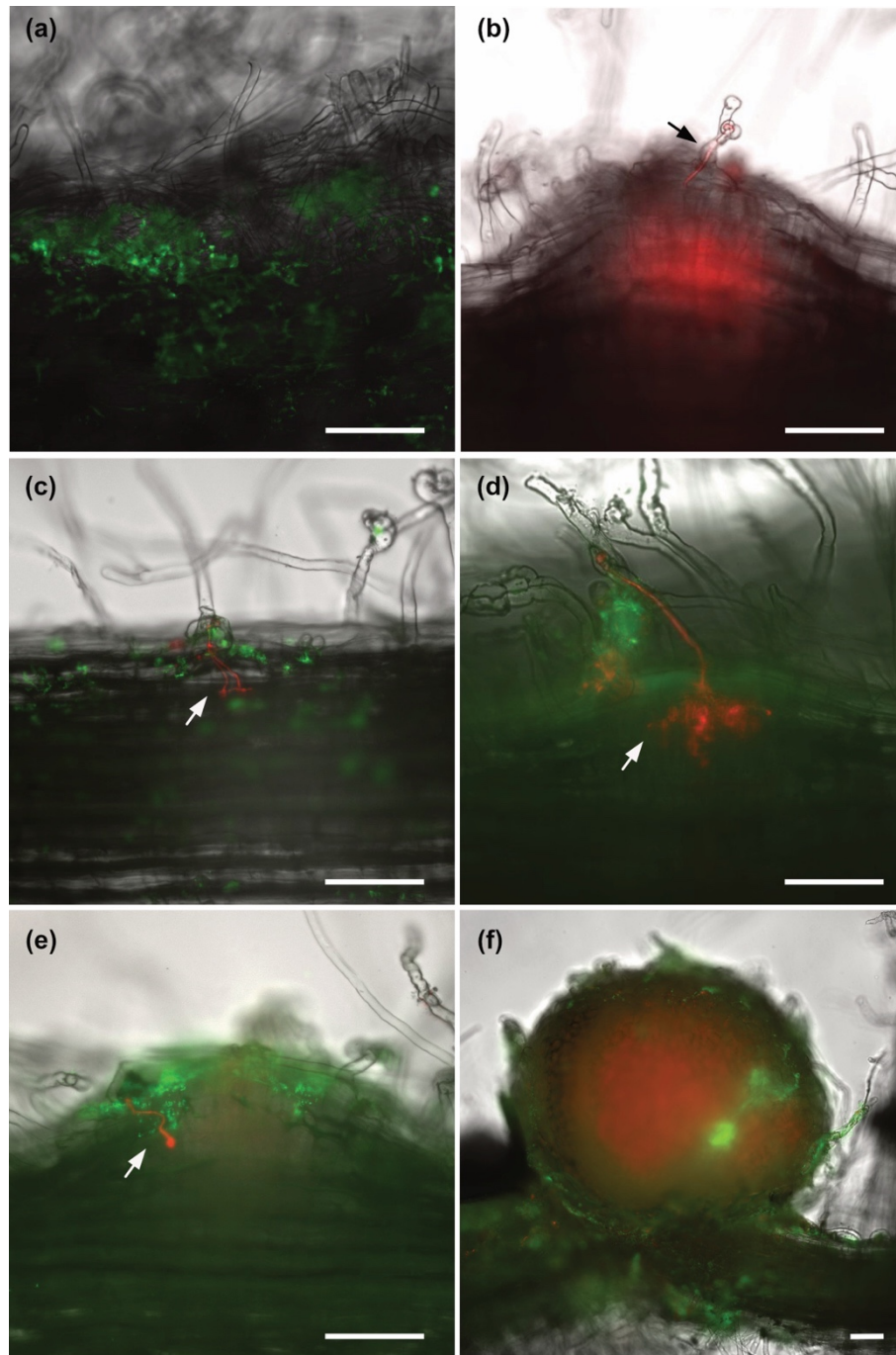


**Figure 6: *L. japonicus* Gifu colonisation by rhizobia.**

Representative micrographs of root nodule colonisation by *RI* Norway GFP, *Mn* 10.2.2 *DsRed*, and *Mn* 10.2.2 *DsRed* + *RI* Norway GFP. 40 roots were inspected under a fluorescence microscope. *RI* Norway GFP colonises a wider root area (a), *Mn* 10.2.2 *DsRed* is restricted mainly to infection threads (b, arrows) on the root surface. *Mn* 10.2.2 *DsRed* + *RI* Norway GFP colonise on the root (c), primordium in early stage (d), primordium in later stage (e), and mature nodule (f). Scale bars: 100  $\mu$ m.

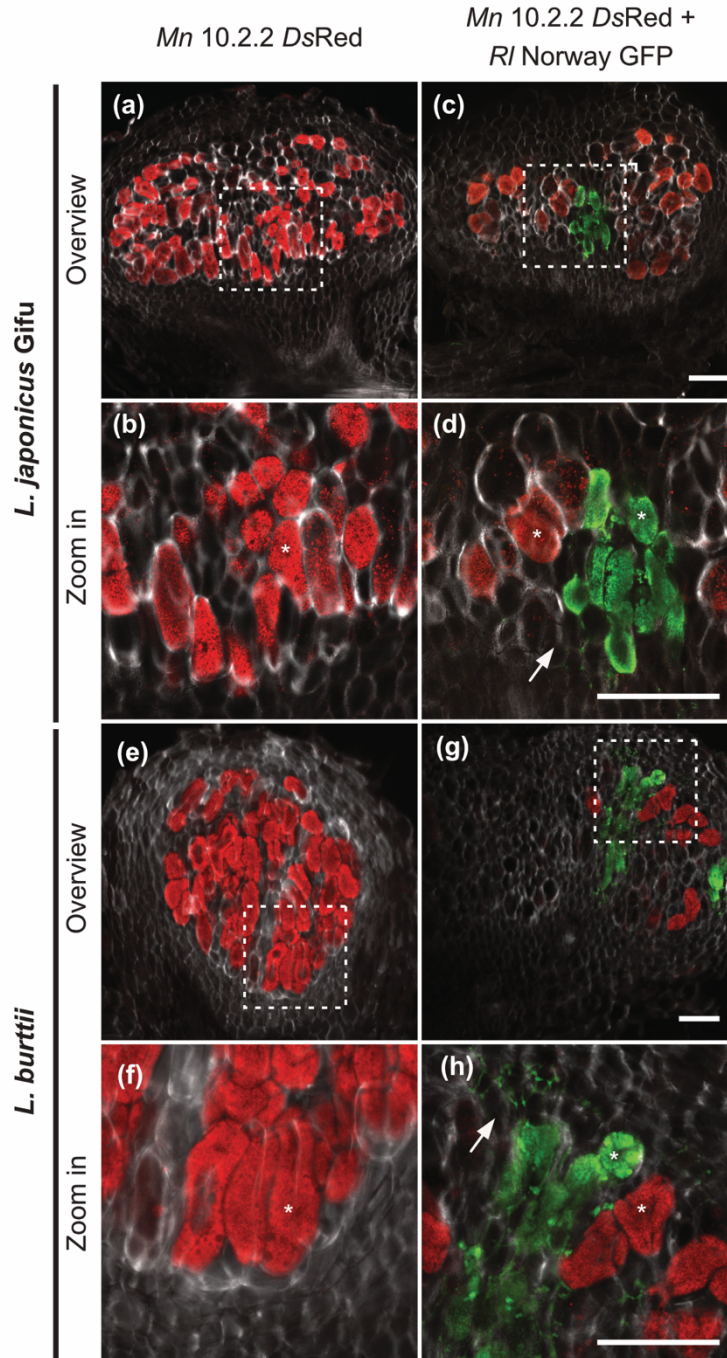


**Figure 7: *RI* Norway GFP colonises mixed nodules inter- and intra- cellularly.**

Representative confocal laser scanning micrographs of nodule sections (50  $\mu$ m) of *L. japonicus* Gifu and *L. burttii* infected by rhizobia at 3 wpi. *Mn* 10.2.2 *DsRed* colonised nodules alone (a, b, e, f) or together with *RI* Norway GFP (c, d, g, h). Cell walls were counterstained with calcofluor white (white). Square-dashed boxes indicate the area shown on the zoom-in panels. Asterisks and arrows indicate the intra- and inter- cellular colonisation, respectively. At least three nodules and six sections were inspected for each condition. Scale bars: 100  $\mu$ m.

detected; however, they are not clearly visible in the displayed images. In nodules co-infected by both strains, *L. japonicus* Gifu and *L. burtii* displayed a similar nodule colonisation pattern (Fig. 7c, d, g, h). *Mn* 10.2.2 *DsRed* colonised only the interior of plant cells (Fig. 7b, f). By contrast, *R/* Norway GFP colonised both intra- and inter-cellularly (Fig. 7d, h asterisks and arrows, respectively). No trans-cellular infection threads induced by *R/* Norway were observed. *R/* Norway GFP and *Mn* 10.2.2 *DsRed* never co-infected the same cell. They always colonised distinct areas of a nodule section. The absence of *R/* Norway GFP on epidermal infection threads and the distinct separation in the colonisation area in the nodule, suggests that *R/* Norway did not enter the nodule through *Mn* 10.2.2-made infection threads.

#### **4. Co-inoculation of *Mn* 10.2.2 and *R/* Norway promotes root colonisation by both strains**

During the inspection of the infection on the root, we observed that *R/* Norway colonised a broad area of the root, whereas the colonisation by *Mn* 10.2.2 was mainly restricted to the epidermal infection threads. Interestingly, we also observed that *R/* Norway GFP colonised massively around primordia and nodules in the co-inoculation condition (Fig. 6). From this observation, we hypothesised that *R/* Norway and *Mn* 10.2.2 exhibit synergism during root colonisation. To address this question, we used a simplified root attachment assay based on a 24-well plate system, as under these growth conditions rhizobia can directly contact the roots. *L. japonicus* Gifu germinated seedlings were grown in 24-well plates supplemented with liquid FAB medium and inoculated with fluorescently tagged bacteria. *Mn* 10.2.2 *DsRed* colonised at a lower density on the root surface compared to *R/* Norway GFP (Fig. 8a). The three-dimensional (3D) views of the root surface reconstructed from CLSM z-stack graphs showed that *R/* Norway, under both single and co-inoculation conditions, formed a thick bacterial layer on the root surface in the co-inoculation condition (Fig. 8a). *R/* Norway GFP and *Mn* 10.2.2 *DsRed* colonised together on the root surface (Fig. 8a). The colonisation of two strains did not segregate into different sections. Further, semi-quantification by visualising the fluorescence intensity of rhizobia on the root showed that root colonisation by both *R/* Norway and *Mn* 10.2.2 was increased under co-inoculation conditions (Fig. 8b).

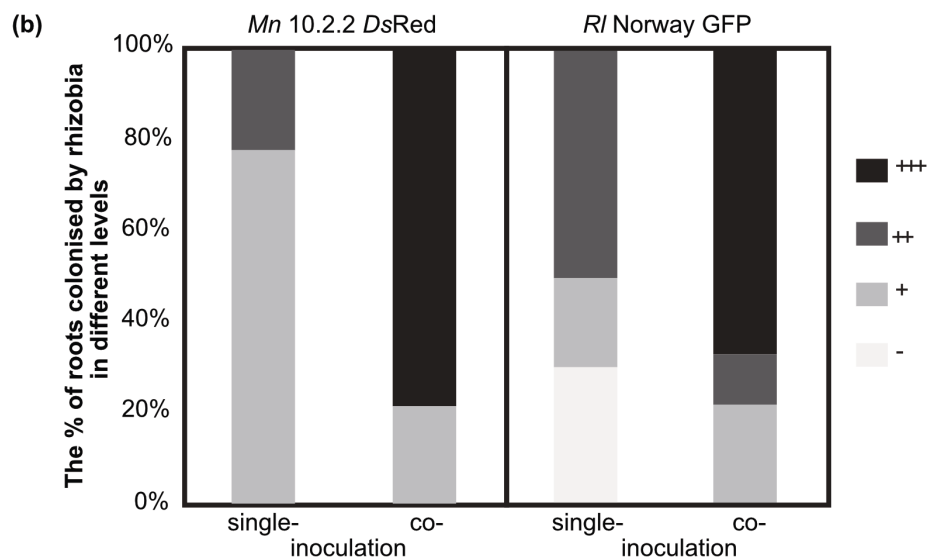
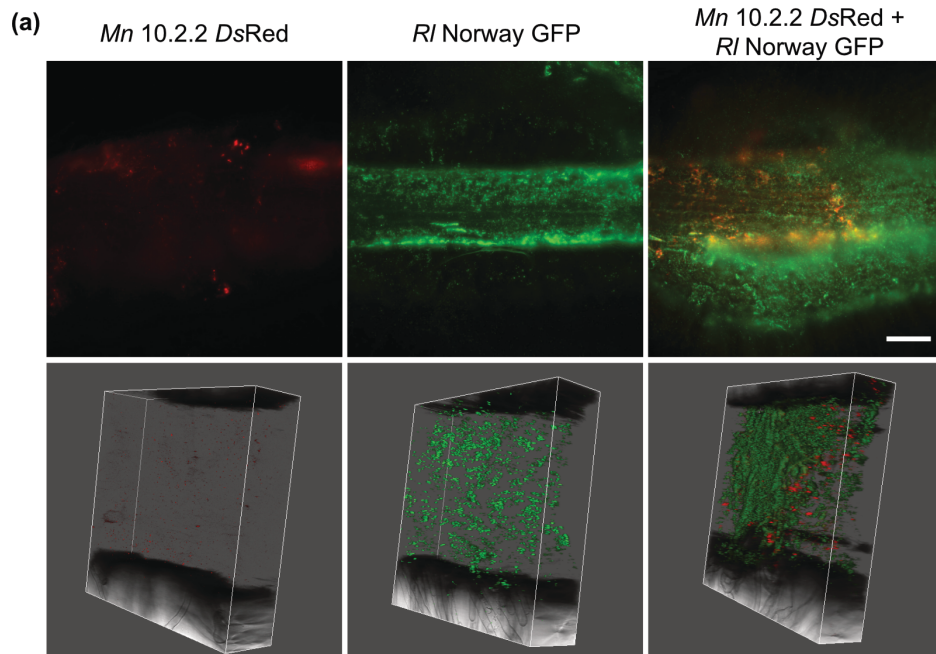


**Figure 8: Co-inoculation with *Mn* 10.2.2 and *RI* Norway increases root colonisation.**

Root colonisation of *L. japonicus* Gifu upon rhizobia inoculation in 24-well plates at 11 dpi. (a) Upper panel: representative z-stack view of a segment of root close to root tip colonised by *Mn* 10.2.2 *DsRed*, *RI* Norway GFP, or *Mn* 10.2.2 *DsRed* + *RI* Norway GFP. Scale bar: 200  $\mu$ m. Lower panel: representative three-dimensional (3D) view of rhizobia on the root surface generated from z-stacks. (b) Semi-quantification of the percentage of roots colonised by rhizobia using epifluorescence microscopy. Colonisation is classified as: ++++ corresponds to the strongest colonisation; + corresponds to the weakest colonisation; +++, ++ correspond to intermediate levels. 10 roots were quantified per condition.

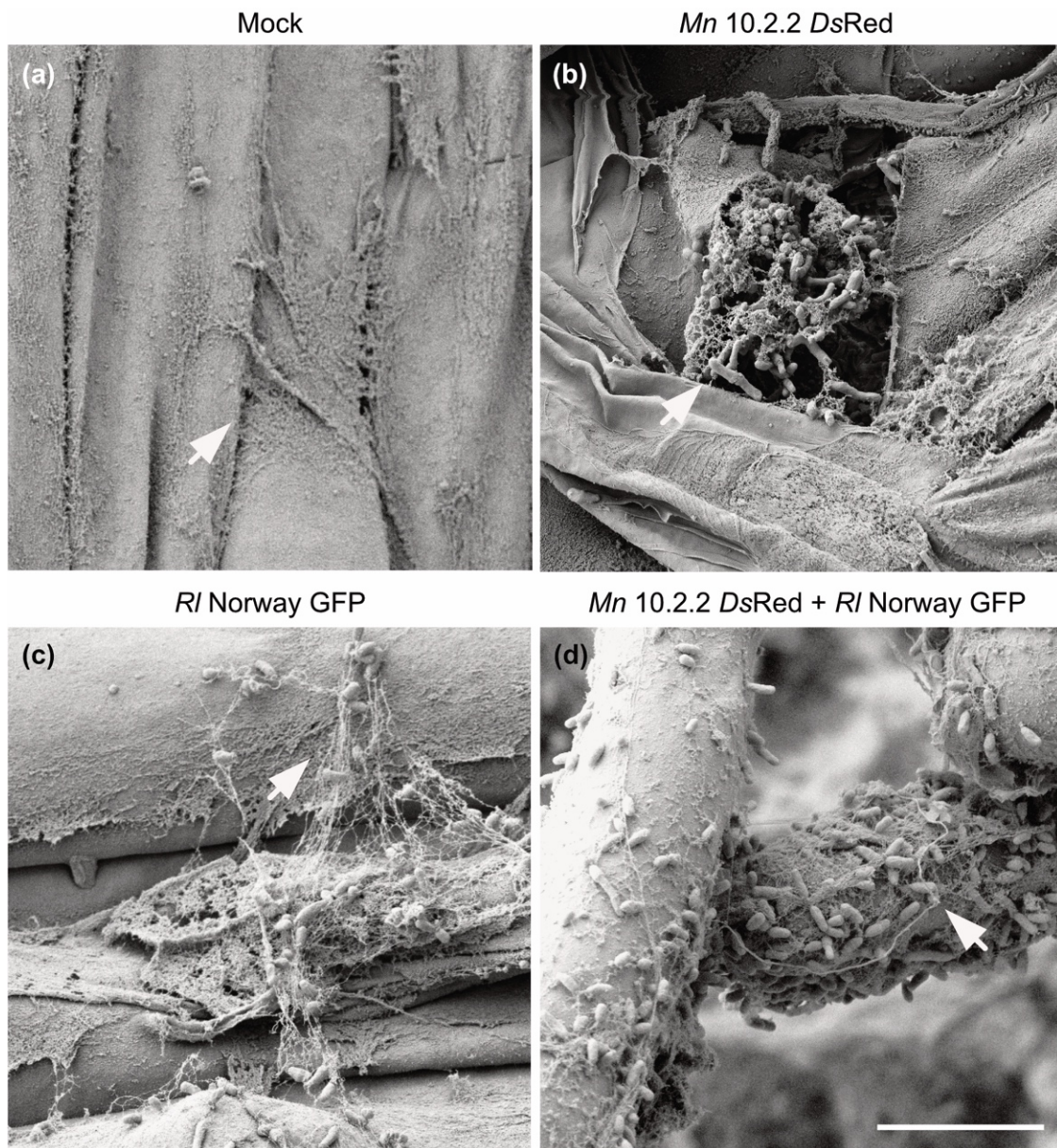


**Figure 9: Scanning electron microscopy (SEM) micrographs of root colonisation of rhizobia.**

Roots grown in 24-well plate were treated with a mock solution in the absence of bacteria (a), inoculated with *Mn 10.2.2 DsRed* (b), *RI Norway GFP* (c), or *Mn 10.2.2 DsRed + RI Norway GFP* (d) at  $OD_{600} = 0.1$  and harvested 11 dpi in the 24-well plate. The arrows indicate rod shaped bacteria surrounded by polymers. Scale bar: 10  $\mu\text{m}$ . Credit: A. Klingl.

To study the bacterial attachment to the root surface in a higher resolution, roots from plants grown in the same 24-well plate assay were inspected under scanning electron microscope (SEM) in collaboration with Prof. Andreas Klingl (LMU, Botany). The root surface and root hair of the root tips were examined. So far unidentified materials attached on the root surface have been observed under mock conditions (Fig. 9a, arrow). Upon *Mn* 10.2.2 *DsRed* inoculation, rod shaped bacteria were surrounded by net-like structures, which were short and dense (Fig. 9b). In the *R/* Norway single inoculation condition, longer and more loose filaments were detected surrounding the bacteria (Fig. 9c). Rhizobia surrounded by long filaments were detected in the *Mn* 10.2.2 *DsRed* and *R/* Norway GFP co-inoculation condition as well, but the structure was slightly more compact compared to that seen when *R/* Norway was inoculated alone (Fig. 9d). These results suggest that the materials surrounding *R/* Norway and *Mn* 10.2.2 display slightly different structures. There are still distinct, albeit slight, differences in the structure of the materials seen in the co-inoculation compared to that seen in the *R/* Norway inoculation (Fig. 9c, d).

## **5. Co-inoculation of *Mn* 10.2.2 and *R/* Norway promotes root colonisation of *L. japonicus* Gifu by both strains from a distal spot**

Motility is essential for rhizobia to migrate towards and colonise the plant root (Poole et al. 2018). Even though our 24-well plate liquid assay was a good alternative to regular substrate-based plant inoculation assays to quantify root colonisation, it does not allow for the role of motility in root colonisation to be studied. Therefore, to investigate whether the increased root colonisation observed upon co-inoculation with *Mn* 10.2.2 and *R/* Norway was influenced by their motility, we inoculated rhizobia on a ca. 5 cm distal spot from the closest plant in comparison with a proximal (regular) inoculation (Fig. 10a). As root colonisation can lead to nodulation, we further quantified the nodule number in each condition. Interestingly, nodule number under the co-inoculation condition was significantly higher than single inoculation at 11 dpi in both the distal and the proximal inoculation conditions (Fig. 10b). These results suggest a positive effect in nodulation under the co-inoculation condition. To further investigate the root colonisation, we inspected the root by microscopy to detect the presence of *R/* Norway GFP and *Mn* 10.2.2 *DsRed*. Upon proximal inoculation, all roots were colonised by rhizobia (Fig. 10c). Consistent with our previous results, *Mn* 10.2.2 *DsRed* induced the formation of nodules

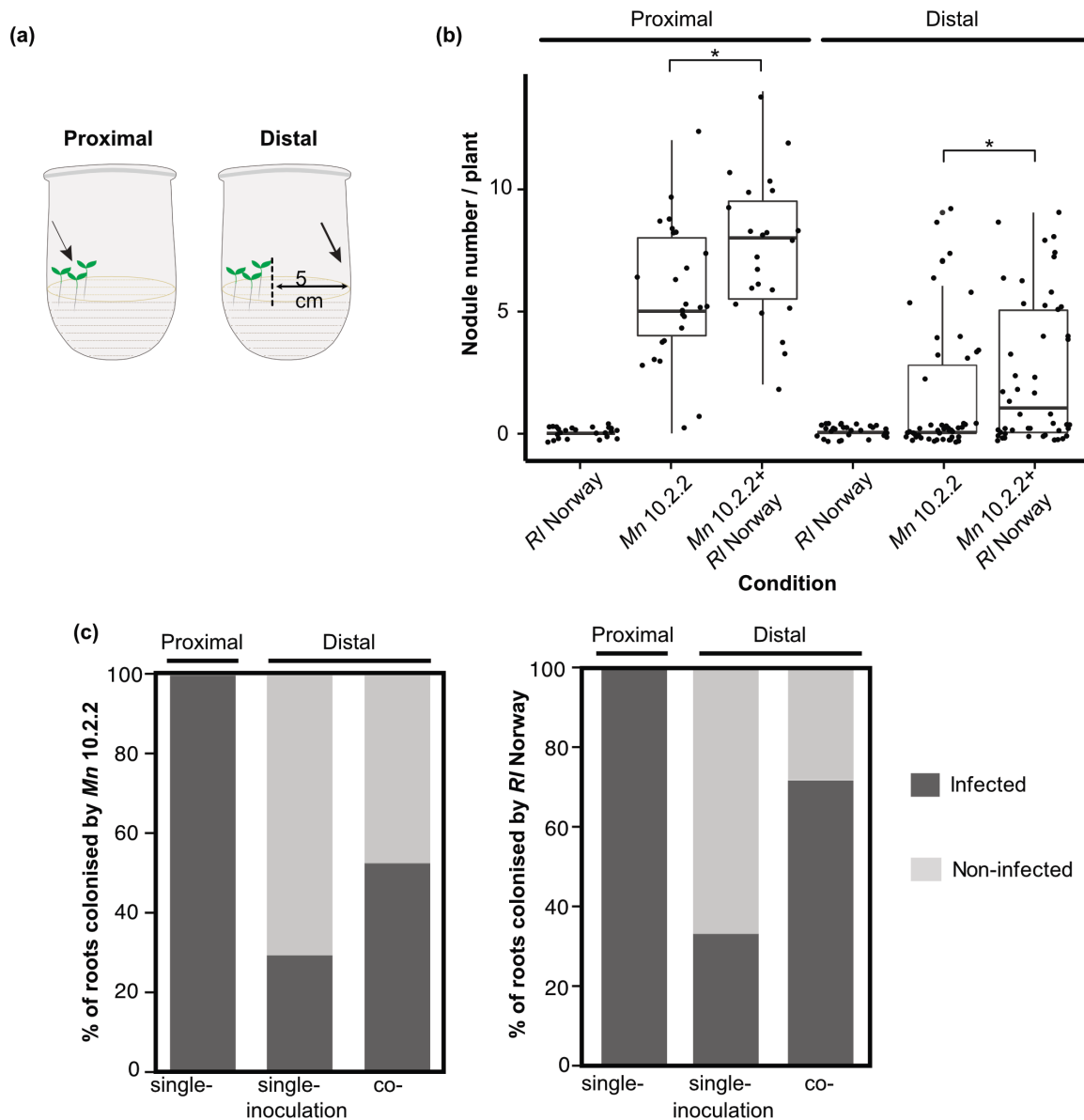


**Figure 10: Distal root colonisation is promoted by co-inoculation.**

(a) The scheme shows how rhizobia were inoculated from a “proximal” and a “distal” spot. In the “distal” spot the inoculation was located at approximately 5 cm distance from the plants. (b) Nodule number quantification on the roots of *L. japonicus* Gifu plants at 11 dpi. Each dot in the boxplot indicates the number of nodules per plant. *L. japonicus* Gifu roots were inoculated with *Mn* 10.2.2, *Ri* Norway GFP, and *Mn* 10.2.2 *DsRed* + *Ri* Norway GFP. At least 20 plants from each condition were quantified. \* indicate p-value < 0.05, which was analysed by t-test in proximal and wilcoxon test in distal conditions respectively. (c) Shows the percentage of roots colonised by *Mn* 10.2.2 *DsRed* and *Ri* Norway GFP. 40 plants per condition in the “distal” inoculation and 20 plants in the “proximal” condition were quantified by epifluorescence microscopy.

on all of the roots, while no nodules were observed upon inoculation with *R/ Norway GFP* (Fig. 10b). Under the distal inoculation conditions, microscopic examination showed that after single inoculation with *Mn 10.2.2 DsRed* only 28% of the total number of roots were colonised, while during co-inoculation conditions root colonisation by *Mn 10.2.2 DsRed* increased to 54% (Fig. 10c). Similar to *Mn 10.2.2 DsRed*, root colonisation by *R/ Norway GFP* was increased from 34% to 71% in the presence of *Mn 10.2.2 DsRed* (Fig. 10c). This experiment has been repeated twice with more than 40 roots in the “distal” inoculation and 25 roots in the “proximal” inoculation being quantified. These results suggest that the co-inoculation with *R/ Norway* and *Mn 10.2.2* promotes their root colonisation from a distal spot.

## **6. *R/ Norway* promotes motility of *Mn 10.2.2* on a surface polysaccharide-dependent manner**

To further investigate the root colonisation promotion observed in the distal inoculation experiments, we next studied whether *R/ Norway* could promote the swarming motility of *Mn 10.2.2 in vitro*, as swarming motility has been shown to allow bacteria to move rapidly on solid surfaces (Verstraeten et al. 2008, Tambalo et al. 2010). For this purpose, we spot-inoculated the rhizobia on swarming medium, which contains agar in a low concentration (0.7%) and incubated them for two weeks at 28 °C. *R/ Norway* migrated from the inoculation spot and formed a colony exhibiting a featureless mat pattern with approximately uniform cell density (Fig. 11). Swarming structures could only be observed at the edges of the colony (Fig. 11, arrow). In contrast, *Mn 10.2.2 DsRed* failed to migrate from the inoculation centre, and no swarming structures were observed, even after two weeks of incubation (Fig. 11). Interestingly, in the presence of *R/ Norway GFP*, *Mn 10.2.2 DsRed* was able to migrate and spike-like structures were observed in the mixed-colony (Fig. 11, arrow). Combined these results suggest that *R/ Norway* promotes the motility of *Mn 10.2.2 in vitro*.



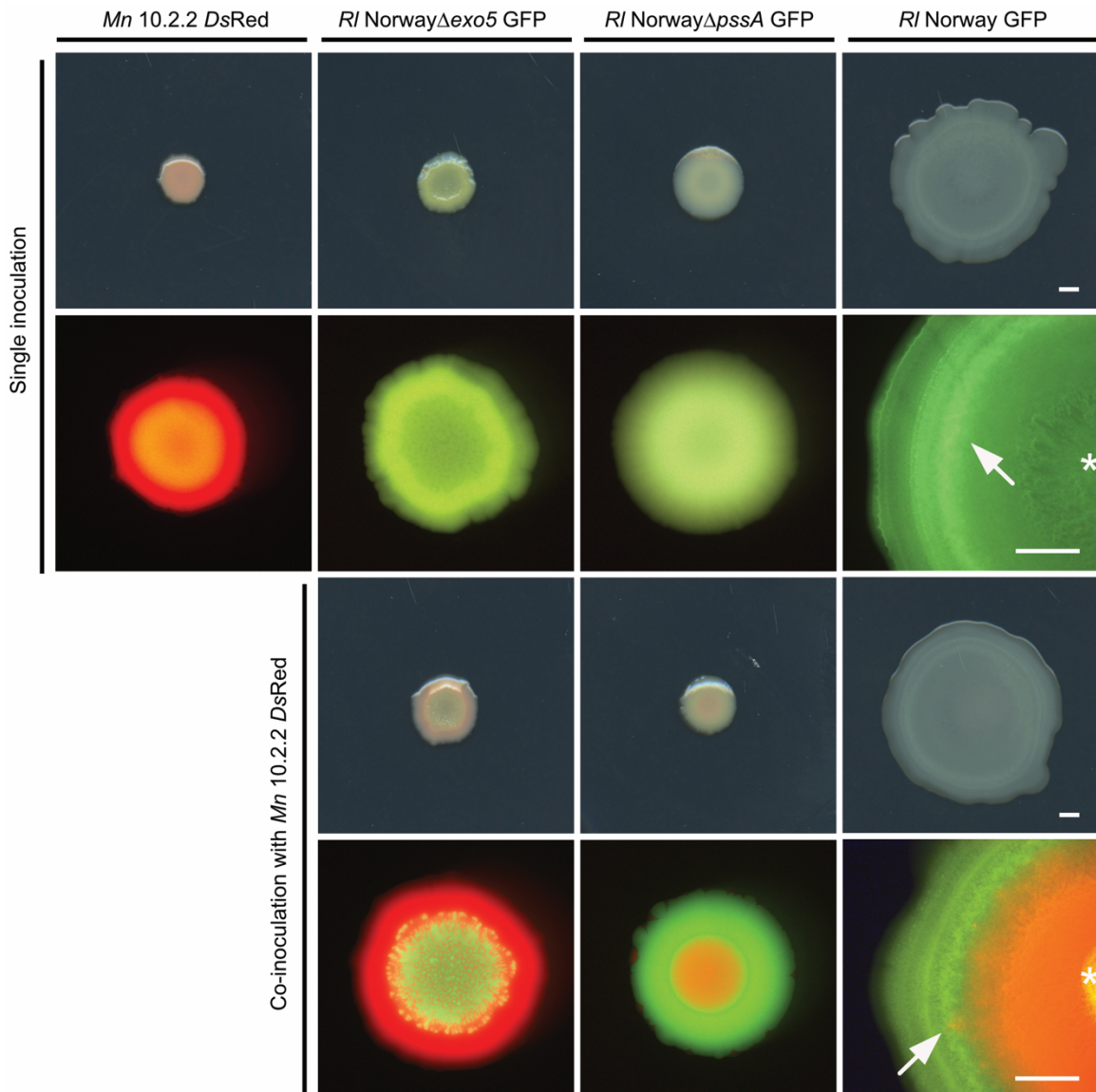


**Figure 11: *Rl* Norway GFP promotes the swarming motility of *Mn* 10.2.2 *DsRed*.**

Microscopic view of swarming colonies of *Mn* 10.2.2 *DsRed*, *Rl* Norway $\Delta$ *exo5* GFP, *Rl* Norway $\Delta$ *pssA* GFP, and *Rl* Norway GFP in single and co-inoculations at 2 wpi on the swarming medium. The arrows and asterisks indicate the swarming structures and inoculation centres, respectively. Micrographs taken from stereo microscope are representative of two independent experiments with three biological replicates each time. Scale bars: 2 mm.

Swarming movement is enabled by extracellular surfactants produced by bacteria (Partridge and Harshey 2013, Kearns 2010). Extracellular polysaccharides facilitate swarming by reducing the friction and the tension between the swarming colony and the agar interface (Partridge and Harshey 2013). To investigate whether the observed motility is influenced by the extracellular polysaccharides, we knocked out the *pssA* and *exo5* genes of *R/ Norway* by homologous recombination. The *pssA* and *exo5* genes are involved in the acidic EPS synthesis of *R/* in the early stage (Russo et al. 2006, Janczarek and Rachwal 2013). The *exo5* gene encoded enzyme is responsible for the synthesis of KPS and LPS as well (Laus et al. 2004, Kereszt et al. 1998, Muszynski et al. 2011). The swarming motility of *R/ Norway* $\Delta$ *pssA* GFP and *R/ Norway* $\Delta$ *exo5* GFP was largely impaired in comparison to that of the wild-type strain (Fig. 11). Interestingly, the swarming colony morphologies varied between the two mutants, which was probably due to the different structures of the surface polysaccharides. In the co-inoculation condition with the mutants, the migration of *Mn 10.2.2 DsRed* was not largely promoted (Fig. 11). This indicates that the extracellular polysaccharides are important for the swarming motility of *R/ Norway* and for its promotion of the motility of *Mn 10.2.2*.

## **7. *R/ Norway* and *Mn 10.2.2* can form mixed biofilms *in vitro***

The root colonisation by *R/ Norway* and *Mn 10.2.2* were both increased under co-inoculation conditions, on both the 24-well plate assay and the “distal” inoculation experiment. Previous studies have shown that biofilms are important for the root colonisation by rhizobia (Russo et al. 2006, Mongiardini et al. 2008), which raises the question of whether *R/ Norway* and *Mn 10.2.2* could form multispecies biofilms. To address this question, we quantified the ability of rhizobia to form biofilms *in vitro* in a tryptone yeast (TY) medium. Five-day old single and co-cultures of *R/ Norway* and *Mn 10.2.2* grown in 24-well plates were harshly washed with water. Afterwards, cells and other materials closely attached on the walls of the 24-well plates were quantified by crystal violet staining. The results showed that only *R/ Norway* formed biofilms under single inoculation conditions (Fig. 12). The similarity between the quantifications of *Mn 10.2.2* and that of the non-inoculated control indicated that the latter did not form biofilms (Fig. 12). In the co-culture condition, biofilms formation were not significantly different from that of *R/ Norway* single culture (Fig. 12). To investigate whether under co-culture conditions multispecies biofilms are formed, a glass chamber assay allowing visualisation of biofilms by microscopy was conducted. Rhizobia were cultured in glass chambers for four days in the minimal modified B medium. To inspect the structure of biofilms, CLSM was applied and samples were scanned from the top to the bottom in 1  $\mu$ m interval. Rhizobia attached on the

glass slide in one direction in all the inoculation conditions (Fig. 13). This observation is consistent with a previous study that described the attachment of rhizobia in the surface via a cell pole of rhizobia (Laus et al. 2005). The structures of biofilms in different conditions are shown as 3D views constructed from the CLSM z-stack micrographs in the orthographic view of Figure 13. *Mn* 10.2.2 *DsRed* alone did not form biofilms on the glass slides, as rhizobia were scattered on the glass surface and did not accumulate densely (Fig. 13). The lack of biofilms seen from *Mn* 10.2.2 is consistent with the well-plate assay (Fig. 12). *R/* Norway GFP formed densely populated clusters in the biofilms on the glass slide with the water channels (space between bacteria) (Fig. 13). In the co-culture condition, *Mn* 10.2.2 *DsRed* cells were mixed together with *R/* Norway GFP cells (Fig. 13). The mixed biofilms contain the water channels and a population density which were structurally similar with the *R/* Norway GFP alone (Fig. 13). Together, these results suggest that *R/* Norway and *Mn* 10.2.2 formed mixed biofilms on the glass slide, which present similar structure as *R/* Norway. Extracellular materials, such as extracellular polysaccharides and secreted proteins, are crucial for biofilm formation (Rinaudi and Giordano 2010). To address the impact of extracellular polysaccharides on biofilm formation, the biofilms of *R/* Norway $\Delta$ *exo5*, an extracellular polysaccharide impaired strain, were determined in both single and co-inoculation conditions. The biofilms formed by *R/* Norway $\Delta$ *exo5* were slightly higher than *R/* Norway alone in the 24-well plate (Fig. 12). In the glass chamber assay, *R/* Norway $\Delta$ *exo5* were evenly scattered on the glass surface with no water channels and attached homogeneously to the glass slide without clustering (Fig. 13). Interestingly, the biofilms formed in the co-culture of *R/* Norway $\Delta$ *exo5* with *Mn* 10.2.2 were decreased in the 24-well plate assay (Fig. 12). However, upon inspection of the glass chamber assay, there was no obvious structural alteration when compared with *R/* Norway $\Delta$ *exo5* alone (Fig. 13). This result suggests that the surface polysaccharides of *R/* Norway affect the biofilm formation in the single- and co- culture conditions.

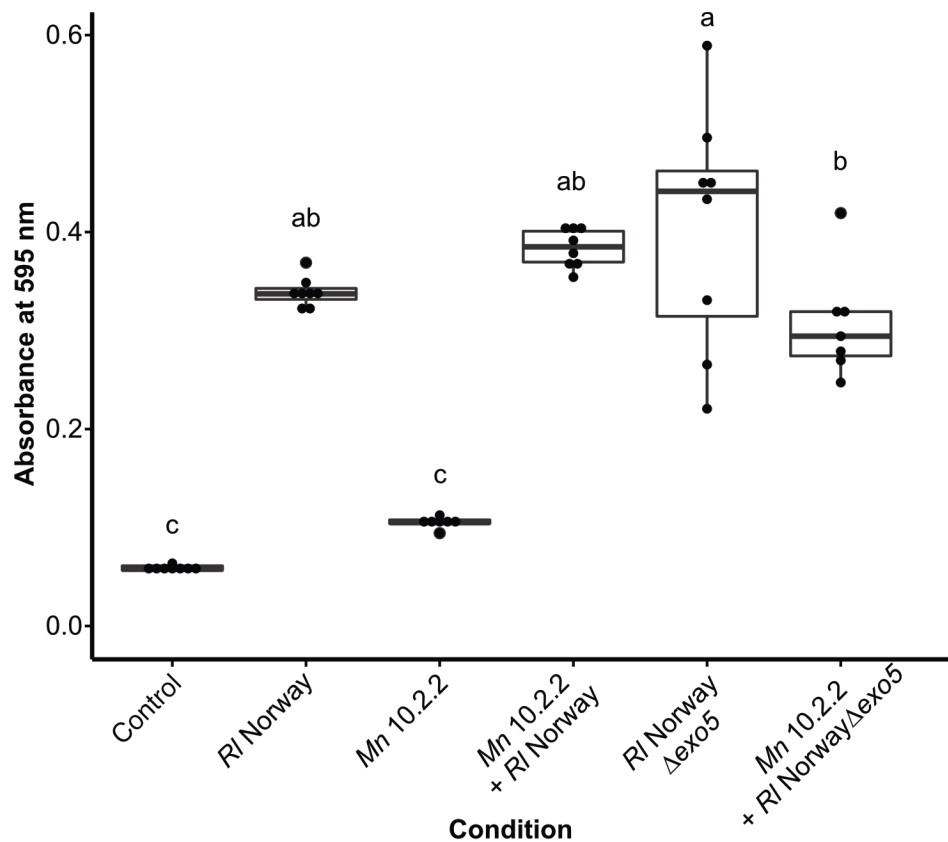


**Figure 12: *Mn 10.2.2* can form mixed biofilms with *RI Norway* *in vitro*.**

Boxplot showing biofilms quantification of *Mn 10.2.2 DsRed*, *RI Norway GFP*, and *Mn 10.2.2 DsRed + RI Norway GFP*, *RI Norway $\Delta$ exo5*, *Mn 10.2.2 + RI Norway $\Delta$ exo5* cultures grown on TY medium, and in TY medium only as control. After 5 dpi, biofilms of rhizobia grown in 24 well plate were quantified by crystal violet staining. Each dot represents one biological replicate. Three independent experiments were conducted. The statistical analysis was performed using ANOVA and TukeyHSD methods. Lower case letters indicate significance groups.

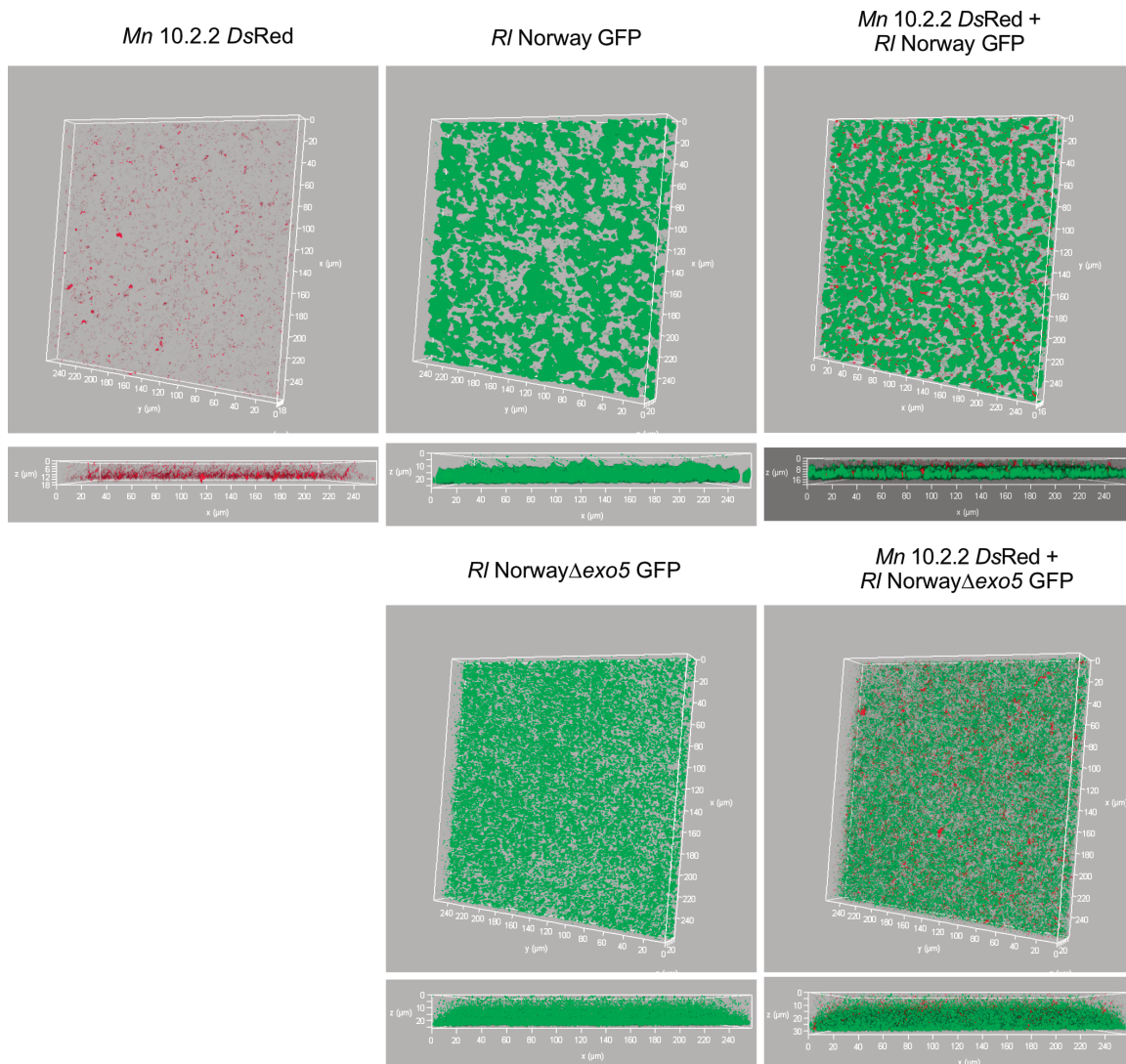


**Figure 13: *Mn* 10.2.2 can form mixed biofilms with *RI* Norway and *RI* Norway $\Delta$ exo5 on glass slides.**

CLSM micrographs of biofilms on glass slides upon rhizobia inoculation in the minimal modified B medium at 4 dpi in a static growth condition at 28 °C. Representative 3D view (upper panel) and orthographic view (lower panel) of biofilms formed by *Mn* 10.2.2 *DsRed*, *RI* Norway GFP, and *Mn* 10.2.2 *DsRed* + *RI* Norway GFP, *RI* Norway $\Delta$ exo5, *Mn* 10.2.2 *DsRed* + *RI* Norway $\Delta$ exo5 inoculation. 3D and orthographic view were constructed from CLSM z-stack micrographs. At least 6 replicates were inspected for each condition, and representative images are shown.

# Supplementary materials and methods

## 1. Bacterial strains and growth conditions

The bacterial strains and the specific antibiotics used in this work are listed in Table 2. Rhizobia from glycerol stocks stored at  $-80\text{ }^{\circ}\text{C}$  are first grown on the TY agar plate for 4-6 days before being grown in Tryptone Yeast (TY) broth (Beringer 1974) at  $28\text{ }^{\circ}\text{C}$  with 180 rpm for 2 days. The *Escherichia coli* (*E. coli*) ST18 strains used in the conjugation assay were grown for 1 day at  $37\text{ }^{\circ}\text{C}$  with 180 rpm in Luria Bertani (LB) broth. The following antibiotic concentrations were used for rhizobia: tetracycline (Tc,  $2\text{ }\mu\text{g ml}^{-1}$ ); neomycin (Nm,  $50\text{ }\mu\text{g ml}^{-1}$ ); streptomycin (Sm,  $500\text{ }\mu\text{g ml}^{-1}$ ); fosfomycin (Fm,  $15\text{ }\mu\text{g ml}^{-1}$ ). The antibiotic concentrations supplied for *E. coli* were kanamycin (Km  $50\text{ }\mu\text{g ml}^{-1}$ ) and tetracycline (Tc  $10\text{ }\mu\text{g ml}^{-1}$ ). The *E. coli* ST18 strain was additionally supplemented with  $50\text{ }\mu\text{g ml}^{-1}$  5-aminolevulinic acid (ALA).

## 2. Plant growth and inoculation conditions

*Lotus burtii* B-303 (seed bag number: 92873) and *Lotus japonicus* Gifu (seed bag number: 111249) seeds were germinated as previously described in (Liang et al. 2019). Different inoculation conditions were used for different experiments. For the nodulation and shoot growth assays, ten plants were grown in a jar containing 300 ml of dry sand:vermiculite (2:1 mixture) supplemented with 40 ml FAB medium. Rhizobia were grown and harvested in stationary phase and washed with sterile water by centrifugation at 4,000 g for 10 min. Bacteria were then resuspended in FAB medium, and the  $\text{OD}_{600}$  was adjusted to 0.005. Each plant was inoculated with 1 ml of bacterial suspension (contains approximately  $5 \times 10^6$  cells). The time course assay was done once, 20 plants per inoculation condition and 10 plants per mock condition were quantified. For the nodule infection assays, 25 plants in each condition were inspected in two independent experiments.

For the distal inoculation assay, five plants were grown in a jar containing ca. 250 ml of dried sand:vermiculite (2:1 mixture) supplemented with 40 ml FAB medium. Each plant was inoculated with 1 ml of the bacterial suspension ( $\text{OD}_{600} = 0.005$ ) as the “proximal” spot (Fig. 10a). For the distal-inoculation conditions, 5 ml of bacterial suspension at  $\text{OD}_{600} = 0.005$  was inoculated 5 cm away from the plant root. This assay was repeated twice with

**Table 2 Strains and plasmids**

Strain and plasmid	Derivation and relevant genotype	Reference
Strains		
<i>Rhizobium leguminosarum</i>		
Norway	Spontaneous Sm <sup>R</sup> mutation of <i>R/</i> Norway	(Liang et al. 2019)
Norway GFP	Spontaneous Sm <sup>R</sup> mutation of <i>R/</i> Norway containing pFAJ-GFP plasmid, Sm <sup>R</sup> , Tc <sup>R</sup>	(Liang et al. 2019)
Norway $\Delta$ <i>exo5</i> <i>DsRed</i>	<i>exo5</i> deletion of <i>R/</i> Norway containing pFAJ- <i>DsRed</i> plasmid, Sm <sup>R</sup> , Tc <sup>R</sup>	This work
Norway $\Delta$ <i>pssA</i> <i>DsRed</i>	<i>pssA</i> deletion of <i>R/</i> Norway containing pFAJ- <i>DsRed</i> plasmid, Sm <sup>R</sup> , Tc <sup>R</sup>	This work
<i>Mesorhizobium norvegicum</i>		
10.2.2	<i>Mn</i> 10.2.2 wild-type	(Gossmann et al. 2012, Kabdullayeva et al. 2020)
10.2.2 <i>DsRed</i>	<i>Mn</i> 10.2.2 containing the pFAJ- <i>DsRed</i> plasmid, Fm <sup>R</sup> , Tc <sup>R</sup>	This work
<i>Escherichia coli</i>		
TOP10	F- <i>mcrA</i> $\Delta$ ( <i>mrr-hsdRMS-mcrBC</i> ) $\Phi$ 80/ <i>lacZ</i> $\Delta$ M15 $\Delta$ <i>lacX74 recA1 araD139</i> $\Delta$ ( <i>araleu</i> )7697 <i>galU galK rpsL endA1 nupG</i> , Sm <sup>R</sup>	Invitrogen
ST18	S17 $\lambda$ pir $\Delta$ <i>hemA</i> , Tp <sup>R</sup> , Sm <sup>R</sup>	(Thoma and Schobert 2009)
Plasmids		
pFAJ-GFP	pFAJ1708 carries the GFP encoding gene, Tc <sup>R</sup>	(Kelly et al. 2013)
pFAJ- <i>DsRed</i>	pFAJ1708 carries the <i>DsRed</i> encoding gene, Tc <sup>R</sup>	(Kelly et al. 2013)
pK19 <i>mobsacB</i>	Integration vector with the ColE1 replication origin, <i>mob</i> , <i>sacB</i> , <i>lacZ</i> $\alpha$ , Km <sup>R</sup>	(Schäfer et al. 1994)
pK19 <i>mobsacB-pssA-AB</i>	pK19 <i>mobsacB</i> derivative carrying upstream 481bp and downstream 531bp flanking fragments of <i>pssA</i> regions, Km <sup>R</sup>	This work
pK19 <i>mobsacB-exo5-AB</i>	pK19 <i>mobsacB</i> derivative carrying upstream 481bp and downstream 531bp flanking fragments of <i>exo5</i> regions, Km <sup>R</sup>	This work

Tp, trimethoprim; Sm, streptomycin; Tc, tetracycline; Km, kanamycin; Fm, fosfomycin.

For the 24-well plate root colonisation assay, seven-day old seedlings were placed in a well and supplied with 1 ml of bacteria suspended in FAB medium ( $OD_{600} = 0.1$ ) and 1 ml of FAB medium for the mock control. This experiment was repeated three times and ca. 30 plants in total per condition were quantified. The bacteria were mixed in a 1:1 ratio in the co-inoculation condition. All inoculated plants were grown in a long day photoperiod at 24 °C (16 h:8 h, light:dark cycle).

### 3. Bacteria isolation from nodules

To isolate rhizobia from root nodules, nodules were cut from the root and surface sterilised with a 2% NaClO solution for two minutes and then washed for at least eight times using sterile water. Each nodule was crushed in an individual well of a 96-well plate containing a 10-20  $\mu$ l 10% glycerol solution. 3  $\mu$ l aliquots of the crushed suspensions were placed on TY agar plates supplemented with antibiotics. Plates were grown at 28 °C for 3-4 days. The isolation of rhizobia from *L. japonicus* Gifu nodules was repeated twice, with 50 nodules for each repetition.

### 4. Conjugation

Plasmids used in this work are listed in Table 2. To label rhizobia with fluorophores, pFAJ-GFP and pFAJ-DsRed plasmids were delivered into rhizobia by conjugation. The donor (*E. coli* ST18) and the acceptor (*R. lotum* Norway) were adjusted to  $OD_{600} = 1$  and mixed using a 1:10 (donor: acceptor) ratio. 2 ml of the mixed bacterial suspension was placed on TY agar and incubated for 24 h at 28 °C. Bacteria were then resuspended in 1 ml of a 10 mM  $MgSO_4$  solution. 100  $\mu$ l bacteria suspensions diluted 10, 100, and 1000 times were placed on selective medium for colony isolation.

### 5. Generation of the *pssA* and *exo5* gene deletion mutants

For the mutagenesis, a two-step homologous recombination method was used to delete *pssA* and *exo5* genes, as described in (Liang et al. 2019). To construct the plasmids for the mutagenesis, fragments flanking upstream and downstream of *pssA* and *exo5* genes (ca. 500 bp for each, detailed in Table 2) were amplified by using the primer combinations *pssA*\_FrA\_PstI\_F/ *pssA*\_FrA\_R; *pssA*\_FrB\_F/ *pssA*\_FrB\_BamHI\_R and *exo5*\_FraA\_HindIII\_F/*exo5*\_FraA\_R; *exo5*\_FraB\_F/ *exo5*\_FraB\_EcoRI\_R (see primers in Table 3). Overlapping PCR was used to overlay the amplified fragments following the protocol



Table 3). Overlapping PCR was used to overlay the amplified fragments following the protocol described by (Sant'Anna et al. 2011) Simultaneously, the restriction enzyme cutting sites *PstI/BamHI* and *HindIII/EcoRI* were added to the flanking fragments of *pssA* and *exo5*, respectively. The fragments were cloned into the suicide *pK19mobsacB* plasmid. The produced plasmids were transferred to *R/* Norway by conjugation and conjugants were selected on TY medium supplemented with neomycin. PCR amplification using primers M13\_Fwd and *pssA\_fraB\_BamHI\_R/exo5\_fraB\_EcoRI\_R* (Table 3) were used to confirm the insertion of the plasmid in the genome. The second selection step was conducted by growing rhizobia on TY medium supplemented with 10% sucrose. The neomycin sensitive colonies (having undergone a second recombination step leading to the loss of the *pK19mobsacB* suicide plasmid) were then selected as candidate mutants. The chromosomal deletion of the genes of interest were finally confirmed by PCR amplification and sanger sequencing using the primers listed in Table 3 (*pssA\_outer\_F/R*; *exo5\_outer\_F/R*).

## **6. Biofilms quantification by 24-well plate**

Bacteria were grown for two days in 10 ml TY medium supplemented with specific antibiotics. Cultures were harvested and washed with sterile water by centrifugation at 4,000 g for 10 minutes. For the 24-well plate biofilm quantification of rhizobia, the OD<sub>600</sub> of cultures was adjusted to 0.1 using TY medium, and 1 ml of the bacterial suspension was then inoculated into individual wells. Plates were incubated at 28 °C for five days in stationary conditions. Loosely attached bacteria were removed by rinsing plates vigorously 3-4 times by submerging in a container with distilled H<sub>2</sub>O water. Then, the wells were dried under a laminar flow hood. Dried wells were stained with a 0.1% crystal violet (Sigma-Aldrich) solution for 20 minutes and then washed vigorously with tap water as described above. Crystal violet that attached to the wells was dissolved with 1 ml of a 30% of acetic acid solution for 20 minutes. The dissolved crystal violet solutions were homogenised by gentle shaking or pipetting then diluted 10 times and quantified by a TECAN infinite M200 microplate reader at 595 nm.

## **7. Biofilms quantification by glass chamber slide**

For the glass chamber biofilm assay, cultures were adjusted to OD<sub>600</sub> = 0.2 by using a minimal Modified B medium (Liang et al. 2019, Spaink et al. 1992). A 300 µl aliquot of the culture was

**Table 3: PCR primer list**

Primers	Sequence (5'-3')	
M13_Rev	TGTAAAACGACCCCCAGT	Sanger sequencing
M13_Fwd	GGAAACAGCTATGACCAT	Sanger sequencing
pssA_FrA_PstI_F	AAA <u>ACTGCAGAGT</u> GATTCGCGTTATCGG	<i>pssA</i> gene upstream fragment amplification
pssA_FrA_R	<b>ATACGCATGTCCATCAAGAT</b> CTGTTGTCTTCGAGGGG	<i>pssA</i> gene upstream fragment amplification
pssA_FrB_F	TCTTGATGGACATGCGTAT	<i>pssA</i> gene downstream fragment amplification
pssA_FrB_BamHI_R	CGC <u>GATCC</u> CTTCTGGACAAGGTTTGG	<i>pssA</i> gene downstream fragment amplification
pssA_outer_F	CAACCCGAACTTCATCTCC	sanger sequencing
pssA_outer_R	AAACCGCAGACTCAACAC	sanger sequencing
exo5_FraA_HindIII_F	CCCA <u>AGCTT</u> GTCTGGAAGGTGAA	<i>exo5</i> gene upstream fragment amplification
exo5_FraA_R	<b>TGATAGAGATTGGTGCCG</b> CACATAGCCTGATCCAA	<i>exo5</i> gene upstream fragment amplification
exo5_FraB_F	CGGCACCAATCTCTATCA	<i>exo5</i> gene downstream fragment amplification
exo5_FraB_EcoRI_R	CCGGA <u>AATTCT</u> ACCCGAACGGCAT	<i>exo5</i> gene downstream fragment amplification
exo5_outer_F	GACCGAGAAAAAAGGCAA	Sanger sequencing
exo5_outer_R	GTGAAGCTCTATCGCAA	Sanger sequencing

Underline indicates restriction enzyme recognition sites. Bold letters indicate the overlapping regions used for the overlapping PCRs.

inoculated in each well of the Nunc™ Lab-Tek™ II glass chamber slide (Thermo Scientific). The glass chamber slide was incubated at 28 °C for four days under stationary conditions. A 100 µl culture of the upper phase was used to measure the OD<sub>600</sub> of cultures. Liquid culture in the glass chamber was gently poured out and rinsed twice with sterile water. The chamber was removed from the glass slide according to manufacturer's instructions and carefully covered with a cover slide. The GFP and DsRed labelled rhizobia on slides were inspected by CLSM (see histological staining and microscopy section for further details). The biofilms were scanned from the bottom to the top with 1 µm intervals.

## **8. Swarming assay**

25 ml of swarming medium in 0.7% agar (Tambalo et al. 2010) was poured in a 90 mm in diameter round Petri dish at 60 °C and dried overnight at room temperature after the agar become solidified. Rhizobia were harvested by centrifugation at 4,000 g for 10 minutes. Bacterial pellets were then washed with sterile water, and further centrifuged at 4,000 g for 10 minutes. 3 µl of the rhizobial suspension in sterile water (OD<sub>600</sub> = 1) was spot inoculated on the middle of the swarming medium agar plate and incubated at 28°C for two weeks. The colonies were scanned by a scanner and were inspected by a Leica MC165 FC stereo microscopy with GFP and DsRed filters (Leica Microsystems).

## **9. Histological staining and microscopy**

Freshly harvested roots were fixed in a 4% formaldehyde solution in 50 mM PIPES buffer with twice vacuum for 20 mins. Then the nodules were detached from the root with a razor blade and embedded in 5% agar. Once the agar solidified, nodules were sectioned using a VT1000S vibratome (Leica Biosystems) with thickness of 50 µm at frequency five and speed five. Finally, the nodule sections were counterstained with a fresh 0.01% calcofluor white solution by incubating at room temperature for 10 minutes.

To detect the root and nodule colonisation by fluorescently tagged rhizobia and the formation of biofilms on glass slides, a TCS SP5 confocal microscope (Leica Microsystems) equipped with a X20 HCX PL APO water immersion lens was used. Calcofluor white, GFP, and DsRed were excited by using the 405 Diode, Argon, and diode pumped solid-state lasers, respectively. Emissions were detected at 405-450 nm, 500-550 nm, and 600-650 nm respectively. To inspect root colonisation in the 24-well plate, an DMI 6000B inverted microscopy (Leica

Microsystems) was used to detect GFP and *DsRed* directly from the bottom of the plate using the GFP and Rho filter cubes, respectively. The swarming colony plates were inspected by a Leica M165 FC microscope (Leica Microsystems) with GFP and *DsRed* filters. For the SEM inspection, freshly harvested plant samples from 24-well plate were fixed with a 2.5% glutaraldehyde solution in 75 mM cacodylate buffer including 2 mM MgCl<sub>2</sub> at pH 7.0 for four days at 4°C. Then, the samples were applied to a glass slide, covered with a cover slip and frozen with liquid nitrogen. The cover slip was removed with a razor blade and the glass slide was washed four times with the fixation buffer (15, 30, 45, 90 minutes). Afterwards, post-fixation was performed with 1% OsO<sub>4</sub> in water for two hours. This was followed by two washing steps in buffer (first 15 minutes, then overnight) and three washing steps in double-distilled water (10, 30, 90 minutes). After dehydration in a graded acetone series (30 minutes with 10%, 20%, 40%, 60%, 80% respectively, and overnight, 80 and 90 minutes with 100% acetone), the samples were critical-point-dried and mounted on aluminium stubs. To enhance conductivity, the sample surface was sputter-coated with platinum for 60 seconds (SEM sample preparation and inspection were performed by Prof. Dr. Andreas Klingl, Botany, LMU).

## **10. Statistics and data visualisation**

All data plots and statistical analysis were performed with R studio (Version 0.99.903) with the packages “ggplot2”, “reshape2”, “car” and “multcompView”. The statistical analysis methods, including t-test, Wilcoxon test, ANOVA and TukeyHSD, were applied. Image J (Version 2.0.0-rc-46/1.50g) was used to process the image generated from the Leica LAS X software. LAS X software was employed to reconstruct all the three-dimensional micrographs.

# References

- Abdian, P. L., J. J. Caramelo, N. Ausmees & A. Zorreguieta (2013) RapA2 is a calcium-binding lectin composed of two highly conserved cadherin-like domains that specifically recognize *Rhizobium leguminosarum* acidic exopolysaccharides. *J Biol Chem*, 288, 2893-2904.
- Antolin-Llovera, M., E. K. Petutsching, M. K. Ried, V. Lipka, T. Nurnberger, S. Robatzek & M. Parniske (2014) Knowing your friends and foes--plant receptor-like kinases as initiators of symbiosis or defence. *New Phytol*, 204, 791-802.
- Ardourel, M., N. Demont, F. D. Debelle, F. Maillet, F. Debilly, J. C. Prome, J. Denarie & G. Truchet (1994) *Rhizobium-meliloti* lipooligosaccharide nodulation factors - different structural requirements for bacterial entry into target root hair-cells and induction of plant symbiotic developmental responses. *Plant Cell*, 6, 1357-1374.
- Arrighi, J. F., F. Cartieaux, S. C. Brown, M. Rodier-Goud, M. Boursot, J. Fardoux, D. Patrel, D. Gully, S. Fabre, C. Chaintreuil & E. Giraud (2012) *Aeschynomene evenia*, a model plant for studying the molecular genetics of the nod-independent *rhizobium*-legume symbiosis. *Mol Plant Microbe Interact*, 25, 851-861.
- Ausmees, N., K. Jacobsson & M. Lindberg (2001) A unipolarly located, cell-surface-associated agglutinin, RapA, belongs to a family of *Rhizobium*-adhering proteins (Rap) in *Rhizobium leguminosarum* bv. *trifolii*. *Microbiology*, 147, 11.
- Baetz, U. & E. Martinoia (2014) Root exudates: the hidden part of plant defense. *Trends Plant Sci*, 19, 90-98.
- Bauer, P., P. Ratet, M. D. Crespi, M. Schultze & A. Kondorosi (1996) Nod factors and cytokinins induce similar cortical cell division, amyloplast deposition and *MsEnod12A* expression patterns in alfalfa roots. *Plant J*, 10, 91-105.
- Becker, A., A. Kleickmann, M. Keller, W. Arnold & A. Puhler (1993) Identification and analysis of the *Rhizobium meliloti* *exoAMONP* genes involved in exopolysaccharide biosynthesis and mapping of promoters located on the *exoHKLAMONP* fragment. *Mol Gen Genet*, 241, 367-379.
- Becker, A., S. Ruberg, B. Baumgarth, P. A. Bertram-Drogatz, I. Quester & A. Puhler (2002) Regulation of succinoglycan and galactoglucan biosynthesis in *Sinorhizobium meliloti*. *J Mol Microbiol Biotechnol*, 4, 187-190.
- Begum, A. A., S. Leibovitch, P. Migner & F. Zhang (2001) Specific flavonoids induced *nod* gene expression and preactivated *nod* genes of *Rhizobium leguminosarum* increased pea (*Pisum sativum* L.) and lentil (*Lens culinaris* L.) nodulation in controlled growth chamber environments. *J Exp Bot*, 52, 1537-1543.
- Bellato, C., H. B. Krishnan, T. Cubo, F. Temprano & S. G. Pueppke (1997) The soybean cultivar specificity gene *noIX* is present, expressed in a *nodD*-dependent manner, and of symbiotic significance in cultivar-nonspecific strains of *Rhizobium* (*Sinorhizobium*) *fredii*. *Microbiology*, 143 ( Pt 4), 1381-1388.
- Beringer, J. E. (1974) R factor transfer in *Rhizobium leguminosarum*. *J Gen Microbiol*, 84, 188-198.
- Bladergroen, M. R., K. Badelt & H. P. Spaink (2003) Infection-blocking genes of a symbiotic *Rhizobium leguminosarum* strain that are involved in temperature-dependent protein secretion. *Mol Plant Microbe Interact*, 16, 53-64.
- Bolaños-Vásquez, M. C. & D. Werner (1997) Effects of *Rhizobium tropici*, *R. etli*, and *R. leguminosarum* bv. *phaseoli* on *nod* gene-inducing flavonoids in root exudates of *Phaseolus vulgaris*. *Mol Plant Microbe Interact*, 10, 339-346.
- Bonaldi, K., D. Gargani, Y. Prin, J. Fardoux, D. Gully, N. Nouwen, S. Goormachtig & E. Giraud (2011) Nodulation of *Aeschynomene afraspera* and *A. indica* by photosynthetic

- Bradyrhizobium* Sp. strain ORS285: the Nod-dependent versus the Nod-Independent symbiotic interaction. *Mol Plant Microbe Interact*, 24, 1359-1371.
- Boogerd, F. C. & D. van Rossum (1997) Nodulation of groundnut by *Bradyrhizobium*: a simple infection process by crack entry. *FEMS Microbiol Rev*, 21, 5-27.
- Braeken, K., R. Daniels, K. Vos, M. Fauvart, D. Bachaspatimayum, J. Vanderleyden & J. Michiels (2008) Genetic determinants of swarming in *Rhizobium etli*. *Microbial Ecology*, 55, 54-64.
- Burén, S. & L. M. Rubio (2018) State of the art in eukaryotic nitrogenase engineering. *FEMS Microbiol Lett*, 365.
- Burmølle, M., D. Ren, T. Bjarnsholt & S. J. Sørensen (2014) Interactions in multispecies biofilms: do they actually matter? *Trends Microbiol*, 22, 84-91.
- Burmølle, M., J. S. Webb, D. Rao, L. H. Hansen, S. J. Sorensen & S. Kjelleberg (2006) Enhanced biofilm formation and increased resistance to antimicrobial agents and bacterial invasion are caused by synergistic interactions in multispecies biofilms. *Appl Environ Microbiol*, 72, 3916-3923.
- Canarini, A., C. Kaiser, A. Merchant, A. Richter & W. Wanek (2019) Root exudation of primary metabolites: mechanisms and their roles in plant responses to environmental stimuli. *Front Plant Sci*, 10, 157.
- Canter Cremers, H. C., M. Batley, J. W. Redmond, L. Eydem, M. W. Breedveld, L. P. Zevehuizen, E. Pees, C. A. Wijffelman & B. J. Lugtenberg (1990) *Rhizobium leguminosarum exoB* mutants are deficient in the synthesis of UDP-glucose 4'-epimerase. *J Biol Chem*, 265, 21122-21127.
- Capoen, W., J. Den Herder, J. Sun, C. Verplancke, A. De Keyser, R. De Rycke, S. Goormachtig, G. Oldroyd & M. Holsters (2009) Calcium spiking patterns and the role of the calcium/calmodulin-dependent kinase CCaMK in lateral root base nodulation of *Sesbania rostrata*. *Plant Cell*, 21, 1526-1540.
- Cárdenas, L., A. Martínez, F. Sánchez & C. Quinto (2008) Fast, transient and specific intracellular ROS changes in living root hair cells responding to Nod factors (NFs). *Plant J*, 56, 802-813.
- Cerri, M. R., Q. H. Wang, P. Stolz, J. Folgmann, L. Frances, K. Katzer, X. L. Li, A. B. Heckmann, T. L. Wang, J. A. Downie, A. Klingl, F. de Carvalho-Niebel, F. Xie & M. Parniske (2017) The *ERN1* transcription factor gene is a target of the CCaMK/CYCLOPS complex and controls rhizobial infection in *Lotus japonicus*. *New Phytol*, 215, 323-337.
- Chandler, M. (1978) Some observations on infection of *Arachis hypogaea* L. by *Rhizobium*. *J Exp Bot*, 29, 749-755.
- Chandler, M., R. A. Date & R. J. Roughley (1982) Infection and root-nodule development in *Stylosanthes* species by *Rhizobium*. *J Exp Bot*, 33, 47-57.
- Charpentier, M., R. Bredemeier, G. Wanner, N. Takeda, E. Schleiff & M. Parniske (2008) *Lotus japonicus* CASTOR and POLLUX are ion channels essential for perinuclear calcium spiking in legume root endosymbiosis. *Plant Cell*, 20, 3467-3479.
- Checucci, A., E. Azzarello, M. Bazzicalupo, M. Galardini, A. Lagomarsino, S. Mancuso, L. Marti, M. C. Marzano, S. Mocali, A. Squartini, M. Zanardo & A. Mengoni (2016) Mixed nodule infection in *Sinorhizobium meliloti*-*Medicago sativa* symbiosis suggest the presence of cheating behavior. *Front Plant Sci*, 7.
- Considine, M. J., K. H. M. Siddique & C. H. Foyer (2017) Nature's pulse power: legumes, food security and climate change. *J Exp Bot*, 68, 1815-1818.
- Cooper, J. E. 2004. Multiple responses of rhizobia to flavonoids during legume root infection. 1-62. Elsevier.
- Costa, T. R. D., C. Felisberto-Rodrigues, A. Meir, M. S. Prevost, A. Redzej, M. Trokter & G. Waksman (2015) Secretion systems in Gram-negative bacteria: structural and mechanistic insights. *Nat Rev Microbiol*, 13, 343-359.

- Crespi, B. J. (2001) The evolution of social behavior in microorganisms. *Trends Ecol. Evol.*, 16, 6.
- Currier, W. W. & G. A. Strobel (1976) Chemotaxis of *Rhizobium spp.* to plant root exudates. *Plant Physiol*, 57, 820-823.
- D'Haese, W. & M. Holsters (2002) Nod factor structures, responses, and perception during initiation of nodule development. *Glycobiology*, 12, 79-105.
- Dai, W. J., Y. Zeng, Z. P. Xie & C. Staehelin (2008) Symbiosis-promoting and deleterious effects of NopT, a novel type 3 effector of *Rhizobium sp.* strain NGR234. *J Bacteriol*, 190, 5101-5110.
- Damiani, I., N. Pauly, A. Puppo, R. Brouquisse & A. Boscari (2016) Reactive oxygen species and nitric oxide control early steps of the legume - *rhizobium* symbiotic interaction. *Front Plant Sci*, 7, 454.
- de Faria, S. M., G. T. Hay & J. I. Sprent (1988) Entry of rhizobia into roots of *Mimosa scabrella* bentham occurs between epidermal cells. *J Gen Microbiol*, 143, 2291-2296.
- de Ruijter, N. C. A., T. Bisseling & A. M. C. Emons (1999) *Rhizobium* Nod factors induce an increase in sub-apical fine bundles of actin filaments in *Vicia sativa* root hairs within minutes. *Mol Plant Microbe Interact*, 12, 829-832.
- Debelle, F., C. Plazanet, P. Roche, C. Pujol, A. Savagnac, C. Rosenberg, J. C. Prome & J. Denarie (1996) The NodA proteins of *Rhizobium meliloti* and *Rhizobium tropici* specify the N-acylation of Nod factors by different fatty acids. *Mol Microbiol*, 22, 303-314.
- Downie, J. A. 1998. Functions of rhizobial nodulation genes. In *The Rhizobiaceae: Molecular Biology of Model Plant-Associated Bacteria*, eds. H. P. Spaink, A. Kondorosi & P. J. J. Hooykaas, 387-402. Dordrecht: Springer Netherlands.
- Downie, J. A. (2010) The roles of extracellular proteins, polysaccharides and signals in the interactions of rhizobia with legume roots. *FEMS Microbiol Rev*, 34, 150-170.
- Downie, J. A. (2014) Legume nodulation. *Curr Biol*, 24, 184-190.
- Ehrhardt, D. W., E. M. Atkinson & S. R. Long (1992) Depolarization of alfalfa root hair membrane potential by *Rhizobium meliloti* Nod Factors. *Science*, 256, 998-1000.
- Ehrhardt, D. W., R. Wais & S. R. Long (1996) Calcium spiking in plant root hairs responding to *Rhizobium* nodulation signals. *Cell*, 85, 673-681.
- Elias, S. & E. Banin (2012) Multi-species biofilms: living with friendly neighbors. *FEMS Microbiol Rev*, 36, 990-1004.
- Endre, G., A. Kereszt, Z. Kevei, S. Mihacea, P. Kaló & G. B. Kiss (2002) A receptor kinase gene regulating symbiotic nodule development. *Nature*, 417, 962-962.
- Faruque, O. M., H. Miwa, M. Yasuda, Y. Fujii, T. Kaneko, S. Sato & S. Okazaki (2015) Identification of *Bradyrhizobium elkanii* genes involved in incompatibility with soybean plants carrying the *Rj4* allele. *Appl Environ Microbiol*, 81, 6710-6717.
- Fauvert, M. & J. Michiels (2008) Rhizobial secreted proteins as determinants of host specificity in the *rhizobium*-legume symbiosis. *FEMS Microbiol Lett*, 285, 1-9.
- Fisher, R. F., T. T. Egelhoff, J. T. Mulligan & S. R. Long (1988) Specific binding of proteins from *Rhizobium meliloti* cell-free extracts containing NodD to DNA sequences upstream of inducible nodulation genes. *Genes Dev*, 2, 282-293.
- Flemming, H.-C. & J. Wingender (2010) The biofilm matrix. *Nat Rev Microbiol*, 8, 623-633.
- Fotiadis, C. T., M. Dimou, D. G. Georgakopoulos, P. Katinakis & A. P. Tampakaki (2012) Functional characterization of NopT1 and NopT2, two type III effectors of *Bradyrhizobium japonicum*. *FEMS Microbiol Lett*, 327, 66-77.
- Foyer, C. H., H.-M. Lam, H. T. Nguyen, K. H. M. Siddique, R. K. Varshney, T. D. Colmer, W. Cowling, H. Bramley, T. A. Mori, J. M. Hodgson, J. W. Cooper, A. J. Miller, K. Kunert, J. Vorster, C. Cullis, J. A. Ozga, M. L. Wahlqvist, Y. Liang, H. Shou, K. Shi, J. Yu, N. Fodor, B. N. Kaiser, F.-L. Wong, B. Valliyodan & M. J. Consideine (2016) Neglecting legumes has compromised human health and sustainable food production. *Nature Plants*, 2.

- Frankow-Lindberg, B. E. & A. S. Dahlin (2013) N<sub>2</sub> fixation, N transfer, and yield in grassland communities including a deep-rooted legume or non-legume species. *Plant and Soil*, 370, 567-581.
- Freiberg, C., R. Fellay, A. Bairoch, W. J. Broughton, A. Rosenthal & X. Perret (1997) Molecular basis of symbiosis between *Rhizobium* and legumes. *Nature*, 387, 394-401.
- Friesen, M. L. & A. Mathias (2010) Mixed infections may promote diversification of mutualistic symbionts: why are there ineffective rhizobia? *J Evol Biol*, 23, 323-334.
- Fujishige, N. A., N. N. Kapadia, P. L. De Hoff & A. M. Hirsch (2006) Investigations of *Rhizobium* biofilm formation. *FEMS Microbiol Ecol*, 56, 195-206.
- Gage, D. J. (2002) Analysis of infection thread development using Gfp- and DsRed-expressing *Sinorhizobium meliloti*. *J Bacteriol*, 184, 7042-7046.
- Gage, J. D. (2004) Infection and invasion of roots by symbiotic, nitrogen-fixing rhizobia during nodulation of temperate legumes. *Microbiol Mol Biol Rev*, 68, 280-300.
- Gil-Serrano, A. M., G. Franco-Rodríguez, P. Tejero-Mateo, J. Thomas-Oates, H. P. Spaink, J. Ruiz-Sainz, M. Megías & Y. Lamrabet (1997) Structural determination of the lipo-chitin oligosaccharide nodulation signals produced by *Rhizobium fredii* HH103. *Carbohydr Res*, 303, 435-443.
- Gilchrist, M. & N. Benjamin. 2017. From atmospheric nitrogen to bioactive nitrogen oxides. In *Nitrite and Nitrate in Human Health and Disease*, eds. N. S. Bryan & J. Loscalzo, 11-19. Cham: Springer International Publishing.
- Giraud, E., L. Moulin, D. Vallenet, V. Barbe, E. Cytryn, J.-C. Avarre, M. Jaubert, D. Simon, F. Cartieaux, Y. Prin, G. Bena, L. Hannibal, J. Fardoux, M. Kojadinovic, L. Vuillet, A. Lajus, S. Cruveiller, Z. Rouy, S. Mangenot, B. Segurens, C. Dossat, W. L. Franck, W.-S. Chang, E. Saunders, D. Bruce, P. Richardson, P. Normand, B. Dreyfus, D. Pignol, G. Stacey, D. Emerich, A. Verméglio, C. Médigue & M. Sadowsky (2007) Legumes symbioses: absence of *Nod* genes in photosynthetic bradyrhizobia. *Science*, 316, 1307-1312.
- Goethals, K., M. Van Montagu & M. Holsters (1992) Conserved motifs in a divergent *nod* box of *Azorhizobium caulinodans* ORS571 reveal a common structure in promoters regulated by LysR-type proteins. *Proc Natl Acad Sci U S A*, 89, 1646-1650.
- Gonzalez-Rizzo, S., M. Crespi & F. Frugier (2006) The *Medicago truncatula* CRE1 cytokinin receptor regulates lateral root development and early symbiotic interaction with *Sinorhizobium meliloti*. *Plant Cell*, 18, 2680-2693.
- Gonzalez-Sama, A., M. M. Lucas, M. R. de Felipe & J. J. Pueyo (2004) An unusual infection mechanism and nodule morphogenesis in white lupin (*Lupinus albus*). *New Phytol*, 163, 371-380.
- Goodchild, D. J. & F. J. Bergersen (1966) Electron microscopy of the infection and subsequent development of soybean nodule cells. *J Bacteriol*, 96, 204-213.
- Goormachtig, S., W. Capoen, E. K. James & M. Holsters (2004) Switch from intracellular to intercellular invasion during water stress-tolerant legume nodulation. *Proc Natl Acad Sci U S A*, 6303-6308.
- Gordon, V. D. & L. Wang (2019) Bacterial mechanosensing: the force will be with you, always. *J Cell Sci*, 132, jcs227694.
- Gossmann, J. A., K. Markmann, A. Brachmann, L. E. Rose & M. Parniske (2012) Polymorphic infection and organogenesis patterns induced by a *Rhizobium leguminosarum* isolate from *Lotus* root nodules are determined by the host genotype. *New Phytol*, 196, 561-573.
- Gottfert, M., S. Rothlisberger, C. Kundig, C. Beck, R. Marty & H. Hennecke (2001) Potential symbiosis-specific genes uncovered by sequencing a 410-kilobase DNA region of the *Bradyrhizobium japonicum* chromosome. *J Bacteriol*, 183, 1405-1412.
- Groth, M., N. Takeda, J. Perry, H. Uchida, S. Draxl, A. Brachmann, S. Sato, S. Tabata, M. Kawaguchi, T. L. Wang & M. Parniske (2010) NENA, a *Lotus japonicus* homolog of



- Sec13*, is required for rhizodermal infection by arbuscular mycorrhiza fungi and rhizobia but dispensable for cortical endosymbiotic development. *Plant Cell*, 22, 2509-2526.
- Heckmann, A. B., F. Lombardo, H. Miwa, J. A. Perry, S. Bunnewell, M. Parniske, T. L. Wang & J. A. Downie (2006) *Lotus japonicus* nodulation requires two GRAS domain regulators, one of which is functionally conserved in a non-legume. *Plant Physiol*, 142, 1739-1750.
- Heidstra, R., R. Geurts, H. Franssen, H. P. Spaink, A. B. Van Kammen & T. Bisseling (1994) Root hair deformation activity of nodulation factors and their fate on *Vicia sativa*. *Plant Physiol*, 105, 787-797.
- Held, M., H. Hou, M. Miri, C. Huynh, L. Ross, M. S. Hossain, S. Sato, S. Tabata, J. Perry, T. L. Wang & K. Szczyglowski (2014) *Lotus japonicus* cytokinin receptors work partially redundantly to mediate nodule formation. *Plant Cell*, 26, 678-694.
- Henderson, I. R., F. Navarro-Garcia, M. Desvaux, R. C. Fernandez & D. Ala'Aldeen (2004) Type V protein secretion pathway: the autotransporter story. *Microbiol Mol Biol Rev*, 68, 692-744.
- Hirsch, A. M. (1992) Developmental biology of legume nodulation. *New Phytol*, 122, 211-237.
- Hölscher, T. & Á. T. Kovács (2017) Sliding on the surface: bacterial spreading without an active motor. *Environ Microbiol*, 19, 2537-2545.
- Hubber, A., A. C. Vergunst, J. T. Sullivan, P. J. Hooykaas & C. W. Ronson (2004) Symbiotic phenotypes and translocated effector proteins of the *Mesorhizobium loti* strain R7A VirB/D4 type IV secretion system. *Mol Microbiol*, 54, 561-574.
- Hubber, A. M., J. T. Sullivan & C. W. Ronson (2007) Symbiosis-induced cascade regulation of the *Mesorhizobium loti* R7A VirB/D4 type IV secretion system. *Mol Plant Microbe Interact*, 20, 255-261.
- Ibanez, F., L. Wall & A. Fabra (2017) Starting points in plant-bacteria nitrogen-fixing symbioses: intercellular invasion of the roots. *J Exp Bot*, 68, 1905-1918.
- Jacob-Dubuisson, F., J. Guérin, S. Baelen & B. Clantin (2013) Two-partner secretion: as simple as it sounds? *Res Microbiol*, 164, 583-595.
- James, E. K., J. I. Sprent, J. M. Stuhlerland, S. G. Mcinroy & F. R. Minchin (1992) The structure of nitrogen fixing root nodule on the aquatic mimosoid legume *Neptunia plena*. *Ann Bot*, 69, 173-180.
- Janczarek, M. (2011) Environmental signals and regulatory pathways that influence exopolysaccharide production in rhizobia. *Int J Mol Sci*, 12, 7898-7933.
- Janczarek, M. & K. Rachwal (2013) Mutation in the *pssA* gene involved in exopolysaccharide synthesis leads to several physiological and symbiotic defects in *Rhizobium leguminosarum* bv. *trifolii*. *Int J Mol Sci*, 14, 23711-23735.
- John, M., H. Röhrig, J. Schmidt, U. Wieneke & J. Schell (1993) *Rhizobium* NodB protein involved in nodulation signal synthesis is a chitooligosaccharide deacetylase. *Proc Natl Acad Sci U S A*, 90, 625-629.
- Jordan, D. C., I. Grinyer & W. H. Coulter (1963) Electron microscopy of infection threads and bacteria in young root nodules of *Medicago Sativa*. *J Bacteriol*, 86, 125-137.
- Kabdullayeva, T., D. B. Crosbie & M. Marín (2020) *Mesorhizobium norvegicum* sp. nov., a rhizobium isolated from a *Lotus corniculatus* root nodule in Norway. *Int J Syst Evol Microbiol*, 70, 388-396.
- Kamst, E., J. Pilling, L. M. Raamsdonk, B. J. Lugtenberg & H. P. Spaink (1997) *Rhizobium* nodulation protein NodC is an important determinant of chitin oligosaccharide chain length in Nod factor biosynthesis. *J Bacteriol*, 179, 2103-2108.
- Kanamori, N., L. H. Madsen, S. Radutoiu, M. Frantescu, E. M. H. Quistgaard, H. Miwa, J. A. Downie, E. K. James, H. H. Felle & L. L. Haaning (2006) A nucleoporin is required for induction of Ca<sup>2+</sup> spiking in legume nodule development and essential for rhizobial and fungal symbiosis. *Proc Natl Acad Sci U S A*, 103, 359-364.

- Kaneko, T., Y. Nakamura, S. Sato, E. Asamizu, T. Kato, S. Sasamoto, A. Watanabe, K. Idesawa, A. Ishikawa, K. Kawashima, T. Kimura, Y. Kishida, C. Kiyokawa, M. Kohara, M. Matsumoto, A. Matsuno, Y. Mochizuki, S. Nakayama, N. Nakazaki, S. Shimpo, M. Sugimoto, C. Takeuchi, M. Yamada & S. Tabata (2000) Complete genome structure of the nitrogen-fixing symbiotic bacterium *Mesorhizobium loti*. *DNA Res*, 7, 331-338.
- Kawaharada, Y., S. Kelly, M. W. Nielsen, C. T. Hjuler, K. Gysel, A. Muszyński, R. W. Carlson, M. B. Thygesen, N. Sandal & M. H. Asmussen (2015) Receptor-mediated exopolysaccharide perception controls bacterial infection. *Nature*, 523, 308-308.
- Kawaharada, Y., M. W. Nielsen, S. Kelly, E. K. James, K. R. Andersen, S. R. Rasmussen, W. Fuchtbauer, L. H. Madsen, A. B. Heckmann, S. Radutoiu & J. Stougaard (2017) Differential regulation of the *Epr3* receptor coordinates membrane-restricted rhizobial colonization of root nodule primordia. *Nat Commun*, 8, 14534.
- Kearns, D. B. (2010) A field guide to bacterial swarming motility. *Nat Rev Microbiol*, 8, 634-644.
- Keating, D. H., M. G. Willits & S. R. Long (2002) A *Sinorhizobium meliloti* lipopolysaccharide mutant altered in cell surface sulfation. *J Bacteriol*, 184, 6681-6689.
- Kelly, S. J., A. Muszynski, Y. Kawaharada, A. M. Hubber, J. T. Sullivan, N. Sandal, R. W. Carlson, J. Stougaard & C. W. Ronson (2013) Conditional requirement for exopolysaccharide in the *Mesorhizobium-Lotus* symbiosis. *Mol Plant Microbe Interact*, 26, 319-329.
- Kennedy, A. C. & L. Z. de Luna. 2005. Rhizosphere. In *Encyclopedia of Soils in the Environment*, ed. D. Hillel, 399-406. Oxford: Elsevier.
- Kereszt, A., E. Kiss, B. L. Reuhs, R. W. Carlson, A. Kondorosi & P. Putnoky (1998) Novel *rkp* gene clusters of *Sinorhizobium meliloti* involved in capsular polysaccharide production and invasion of the symbiotic nodule: the *rkpK* gene encodes a UDP-glucose dehydrogenase. *J Bacteriol*, 180, 5426-5431.
- Kieber, J. J. & G. E. Schaller (2018) Cytokinin signaling in plant development. *Development*, 145, dev149344.
- Kim, S., W. Zeng, S. Bernard, J. Liao, M. Venkateshwaran, J.-M. Ane & Y. Jiang (2019) Ca<sup>2+</sup>-regulated Ca<sup>2+</sup> channels with an RCK gating ring control plant symbiotic associations. *Nat Commun*, 10, 3703.
- Kimbrel, J. A., W. J. Thomas, Y. Jiang, A. L. Creason, C. A. Thireault, J. L. Sachs & J. H. Chang (2013) Mutualistic co-evolution of type III effector genes in *Sinorhizobium fredii* and *Bradyrhizobium japonicum*. *PLoS Pathog*, 9, e1003204.
- Kitaeva, A. B., K. N. Demchenko, I. A. Tikhonovich, A. C. Timmers & V. E. Tsyganov (2016) Comparative analysis of the tubulin cytoskeleton organization in nodules of *Medicago truncatula* and *Pisum sativum*: bacterial release and bacteroid positioning correlate with characteristic microtubule rearrangements. *New Phytol*, 210, 168-183.
- Knight, C. D., L. Rossen, J. G. Robertson, B. Wells & J. A. Downie (1986) Nodulation inhibition by *Rhizobium leguminosarum* multicopy *nodABC* genes and analysis of early stages of plant infection. *J Bacteriol*, 166, 552-558.
- Kohlen, W., J. L. P. Ng, E. E. Deinum & U. Mathesius (2018) Auxin transport, metabolism, and signalling during nodule initiation: indeterminate and determinate nodules. *J Exp Bot*, 69, 229-244.
- Krehenbrink, M. & J. A. Downie (2008) Identification of protein secretion systems and novel secreted proteins in *Rhizobium leguminosarum* bv. *viciae*. *BMC Genomics*, 9, 55.
- Król, J., J. Wielbo, A. Mazur, J. Kopcinska, B. Lotocka, W. Golinowski & A. Skorupska (1998) Molecular characterization of *pssCDE* genes of *Rhizobium leguminosarum* bv. *trifolii* strain TA1: *pssD* mutant is affected in exopolysaccharide synthesis and endocytosis of bacteria. *Mol Plant Microbe Interact*, 11, 1142-1148.
- Laranjo, M., A. Alexandre & S. Oliveira (2014) Legume growth-promoting rhizobia: an overview on the *Mesorhizobium* genus. *Microbiol Res*, 169, 2-17.

- Latchford, J. W., D. Borthakur & A. W. Johnston (1991) The products of *Rhizobium* genes, *psi* and *pss*, which affect exopolysaccharide production, are associated with the bacterial cell surface. *Mol Microbiol*, 5, 2107-2114.
- Laus, M. C., T. J. Logman, A. A. N. van Brussel, R. W. Carlson, P. Azadi, M. Y. Gao & J. W. Kijne (2004) Involvement of *exo5* in production of surface polysaccharides in *Rhizobium leguminosarum* and its role in nodulation of *Vicia sativa* subsp *nigra*. *J Bacteriol*, 186, 6617-6625.
- Laus, M. C., A. A. N. van Brussel & J. W. Kijne (2005) Roles of cellulose fibrils and exopolysaccharides of *Rhizobium leguminosarum* in attachment to an infection of *Vicia sativa* root hairs. *Mol Plant Microbe Interact*, 18, 6.
- Lee, K. W., S. Periasamy, M. Mukherjee, C. Xie, S. Kjelleberg & S. A. Rice (2014) Biofilm development and enhanced stress resistance of a model, mixed-species community biofilm. *ISME J*, 8, 894-907.
- Lefebvre, B., T. Timmers, M. Mbengue, S. Moreau, C. Hervé, K. Tóth, J. Bittencourt-Silvestre, D. Klaus, L. Deslandes & L. Godiard (2010) A remorin protein interacts with symbiotic receptors and regulates bacterial infection. *Proc Natl Acad Sci U S A*, 107, 2343-2348.
- Lerouge, P., P. Roche, C. Faucher, F. Mailliet, G. Truchet, J. C. Promé & J. Dénarié (1990) Symbiotic host-specificity of *Rhizobium meliloti* is determined by a sulphated and acylated glucosamine oligosaccharide signal. *Nature*, 344, 781-781.
- Lévy, J., C. Bres, R. Geurts, B. Chalhoub, O. Kulikova, G. Duc, E. P. Journet, J. M. Ané, E. Lauber & T. Bisseling (2004) A putative Ca<sup>2+</sup> and calmodulin-dependent protein kinase required for bacterial and fungal symbioses. *Science*, 303, 1361-1364.
- Liang, J., A. Hoffrichter, A. Brachmann & M. Marín (2018a) Complete genome of *Rhizobium leguminosarum* Norway, an ineffective *Lotus* micro-symbiont. *Stand Genomic Sci* 13, 36.
- Liang, J., A. Klingl, Y. Y. Lin, E. Boul, J. Thomas-Oates & M. Marín (2019) A sub-compatible rhizobium strain reveals infection duality in *Lotus*. *J Exp Bot*, 70, 1903-1913.
- Liang, P., T. F. Stratil, C. Popp, M. Marin, J. Folgmann, K. S. Mysore, J. Wen & T. Ott (2018b) Symbiotic root infections in *Medicago truncatula* require remorin-mediated receptor stabilization in membrane nanodomains. *Proc Natl Acad Sci U S A*, 115, 5289-5294.
- Limpens, E., S. Moling, G. Hooiveld, P. A. Pereira, T. Bisseling, J. D. Becker & H. Küster (2013) cell- and tissue-specific transcriptome analyses of *Medicago truncatula* root nodules. *PLoS One*, 8, e64377.
- Lipa, P., J. M. Vinardell, J. Kopcinska, A. Zdybicka-Barabas & M. Janczarek (2018) Mutation in the *pssZ* gene negatively impacts exopolysaccharide synthesis, surface properties, and symbiosis of *Rhizobium leguminosarum* bv. *trifolii* with clover. *Genes (Basel)*, 9.
- Liu, C.-W., A. Breakspear, D. Guan, M. R. Cerri, K. Abbs, S. Jiang, F. C. Robson, G. Radhakrishnan, S. Roy & C. Bone (2019a) NIN acts as a network hub controlling a growth module required for rhizobial infection. *Plant Physiol*, 1704-1722.
- Liu, C.-W. & J. D. Murray (2016) The role of flavonoids in nodulation host-range specificity: an update. *Plants (Basel)*, 5.
- Liu, J., L. Rutten, E. Limpens, T. van der Molen, R. van Velzen, R. Chen, Y. Chen, R. Geurts, W. Kohlen, O. Kulikova & T. Bisseling (2019b) A remote *cis*-regulatory region is required for *NIN* expression in the pericycle to initiate nodule primordium formation in *Medicago truncatula*. *Plant Cell*, 31, 68.
- Liu, Y., X. Jiang, D. Guan, W. Zhou, M. Ma, B. Zhao, F. Cao, L. Li & J. Li (2017) Transcriptional analysis of genes involved in competitive nodulation in *Bradyrhizobium diazoefficiens* at the presence of soybean root exudates. *Sci Rep*, 7, 10946.
- Locht, C., P. Bertin, F. D. Menozzi & G. Renaud (1993) The filamentous haemagglutinin, a multifaceted adhesion produced by virulent *Bordetella spp*. *Mol Microbiol*, 9, 653-660.

- Lopes, S. P., H. Ceri, N. F. Azevedo & M. O. Pereira (2012) Antibiotic resistance of mixed biofilms in cystic fibrosis: impact of emerging microorganisms on treatment of infection. *Int J Antimicrob Agents*, 40, 260-263.
- López-Lara, I. M., L. Blok-Tip, C. Quinto, M. L. Garcia, G. Stacey, G. V. Bloemberg, G. E. M. Lamers, B. J. J. Lugtenberg, J. E. Thomas-Oates & H. P. Spaik (1996) *nodZ* of *Bradyrhizobium* extends the nodulation host range of *Rhizobium* by adding a fucosyl residue to nodulation signals. *Mol Microbiol*, 21, 397-408.
- Loureiro, M. F., E. K. James, J. I. Sprent & A. A. Franco (1995) Stem and root nodules on the tropical wetland legume *Aeschynomene fluminensis*. *New Phytol*, 130, 531-544.
- Lowe, G., M. Meister & H. C. Berg (1987) Rapid rotation of flagellar bundles in swimming bacteria. *Nature*, 325, 637-640.
- LPWG (2017) A new subfamily classification of the Leguminosae based on a taxonomically comprehensive phylogeny – The Legume Phylogeny Working Group (LPWG). *Taxon*, 66, 44-77.
- Madsen, E. B., L. H. Madsen, S. Radutoiu, M. Olbryt, M. Rakwalska, K. Szczyglowski, S. Sato, T. Kaneko, S. Tabata & N. Sandal (2003) A receptor kinase gene of the LysM type is involved in legume perception of rhizobial signals. *Nature*, 425, 637-637.
- Madsen, L. H., L. Tirichine, A. Jurkiewicz, J. T. Sullivan, A. B. Heckmann, A. S. Bek, C. W. Ronson, E. K. James & J. Stougaard (2010) The molecular network governing nodule organogenesis and infection in the model legume *Lotus japonicus*. *Nat Commun*, 1, 10.
- Maillet, F., J. Fournier, H. C. Mendis, M. Tadege, J. Wen, P. Ratet, K. S. Mysore, C. Gough & K. M. Jones (2020) *Sinorhizobium meliloti* succinylated high-molecular-weight succinoglycan and the *Medicago truncatula* LysM receptor-like kinase MtLYK10 participate independently in symbiotic infection. *Plant J*, 102, 311-326.
- Marczak, M., A. Mazur, P. Koper, K. Żebracki & A. Skorupska (2017) Synthesis of rhizobial exopolysaccharides and their importance for symbiosis with legume plants. *Genes*, 8, 360.
- Marie, C., W. J. Broughton & W. J. Deakin (2001) *Rhizobium* type III secretion systems: legume charmer or alarmer. *Curr Opin Plant Biol*, 4, 336-342.
- Marlovits, T. C., T. Kubori, A. Sukhan, D. R. Thomas, J. E. Galan & V. M. Unger (2004) Structural insights into the assembly of the type III secretion needle complex. *Science*, 306, 1040-1042.
- Meinhardt, L. W., H. B. Krishnan, P. A. Balatti & S. G. Pueppke (1993) Molecular cloning and characterization of a sym plasmid locus that regulates cultivar-specific nodulation of soybean by *Rhizobium fredii* USDA257. *Mol Microbiol*, 9, 17-29.
- Mendoza-Suárez, M. A., B. A. Geddes, C. Sánchez-Cañizares, R. H. Ramírez-González, C. Kirchhelle, B. Jorin & P. S. Poole (2020) Optimizing *Rhizobium* legume symbioses by simultaneous measurement of rhizobial competitiveness and N<sub>2</sub> fixation in nodules. *Proc Natl Acad Sci U S A*, 117, 9822.
- Meneses, N., G. Mendoza-Hernández & S. Encarnación (2010) The extracellular proteome of *Rhizobium etli* CE3 in exponential and stationary growth phase. *Proteome Sci*, 8, 51.
- Mergaert, P., W. D'Haese, M. Fernández-López, D. Geelen, K. Goethals, J.-C. Promé, M. Van Montagu & M. Holsters (1996) Fucosylation and arabinosylation of Nod factors in *Azorhizobium caulinodans*: involvement of *nolKnodZ* as well as *noeC* and/or downstream genes. *Mol Microbiol*, 21, 409-419.
- Merz, A. J., M. So & M. P. Sheetz (2000) Pilus retraction powers bacterial twitching motility. *Nature*, 407, 98-102.
- Meuskens, I., A. Saragliadis, J. C. Leo & D. Linke (2019) Type V secretion systems: an overview of passenger domain functions. *Front Microbiol*, 10.
- Mitchell, J. G. & K. Kogure (2006) Bacterial motility: links to the environment and a driving force for microbial physics. *FEMS Microbiol Ecol*, 55, 3-16.

- Miwa, H. & S. Okazaki (2017) How effectors promote beneficial interactions. *Curr Opin Plant Biol*, 38, 148-154.
- Miwa, H., J. Sun, G. E. Oldroyd & J. A. Downie (2006) Analysis of Nod-factor-induced calcium signaling in root hairs of symbiotically defective mutants of *Lotus japonicus*. *Mol Plant Microbe Interact*, 19, 914-923.
- Moling, S., A. Pietraszewska-Bogiel, M. Postma, E. Fedorova, M. A. Hink, E. Limpens, T. W. J. Gadella & T. Bisseling (2014) Nod factor receptors form heteromeric complexes and are essential for intracellular infection in *Medicago* nodules. *Plant Cell*, 26, 4188-4199.
- Monahan-Giovanelli, H., C. A. Pinedo & D. J. Gage (2006) Architecture of infection thread networks in developing root nodules induced by the symbiotic bacterium *Sinorhizobium meliloti* on *Medicago truncatula*. *Plant Physiol*, 140, 661-670.
- Mongiardini, E. J., N. Ausmees, J. Perez-Gimenez, M. Julia Althabegoiti, J. Ignacio Quelas, S. L. Lopez-Garcia & A. R. Lodeiro (2008) The rhizobial adhesion protein RapA1 is involved in adsorption of rhizobia to plant roots but not in nodulation. *FEMS Microbiol Ecol*, 65, 279-288.
- Montiel Gonzalez, J., M. K. Arthikala, L. Cárdenas & C. Quinto (2016) Legume NADPH oxidases have crucial roles at different stages of nodulation. *Int J Mol Sci*, 17, 680.
- Murray, J. D. (2011) Invasion by invitation: rhizobial infection in legumes. *Mol Plant Microbe Interact*, 24, 631-639.
- Murray, J. D., B. J. Karas, S. Sato, S. Tabata, L. Amyot & K. Szczyglowski (2007) A cytokinin perception mutant colonized by *Rhizobium* in the absence of nodule organogenesis. *Science*, 315, 101-104.
- Muszyński, A., C. Heiss, C. T. Hjuler, J. T. Sullivan, S. J. Kelly, M. B. Thygesen, J. Stougaard, P. Azadi, R. W. Carlson & C. W. Ronson (2016) Structures of exopolysaccharides involved in receptor-mediated perception of *Mesorhizobium loti* by *Lotus japonicus*. *J Biol Chem*, 291, 20946-20961.
- Muszynski, A., M. Laus, J. W. Kijne & R. W. Carlson (2011) Structures of the lipopolysaccharides from *Rhizobium leguminosarum* RBL5523 and its UDP-glucose dehydrogenase mutant (*exo5*). *Glycobiology*, 21, 55-68.
- Ndoye, I., F. de Billy, J. Vasse, B. Dreyfus & G. Truchet (1994) Root Nodulation of *Sesbania rostrata*. *J Bacteriol*, 176, 1060-1068.
- O'Neill, M. A., A. G. Darvill & P. Albersheim (1991) The degree of esterification and points of substitution by O-acetyl and O-(3-hydroxybutanoyl) groups in the acidic extracellular polysaccharides secreted by *Rhizobium leguminosarum* biovars *viciae*, *trifolii*, and *phaseoli* are not related to host range. *J Biol Chem*, 266, 9549-9555.
- Okazaki, S., S. Okabe, M. Higashi, Y. Shimoda, S. Sato, S. Tabata, M. Hashiguchi, R. Akashi, M. Gottfert & K. Saeki (2010) Identification and functional analysis of type III effector proteins in *Mesorhizobium loti*. *Mol Plant Microbe Interact*, 23, 223-234.
- Okazaki, S., P. Tittabutr, A. Teulet, J. Thouin, J. Fardoux, C. Chaintreuil, D. Gully, J. F. Arrighi, N. Furuta, H. Miwa, M. Yasuda, N. Nouwen, N. Teaumroong & E. Giraud (2015) *Rhizobium*-legume symbiosis in the absence of Nod factors: two possible scenarios with or without the T3SS. *ISME J*, 10, 64-74.
- Okazaki, S., S. Zehner, J. Hempel, K. Lang & M. Gottfert (2009) Genetic organization and functional analysis of the type III secretion system of *Bradyrhizobium elkanii*. *FEMS Microbiol Lett*, 295, 88-95.
- Oldroyd, G. E. (2013) Speak, friend, and enter: signalling systems that promote beneficial symbiotic associations in plants. *Nat Rev Microbiol*, 11, 252-263.
- Oldroyd, G. E., J. D. Murray, P. S. Poole & J. A. Downie (2011) The rules of engagement in the legume-rhizobial symbiosis. *Annu Rev Genet*, 45, 119-144.
- Oldroyd, G. E. D. & J. A. Downie (2006) Nuclear calcium changes at the core of symbiosis signalling. *Curr Opin Plant Biol*, 9, 351-357.

- Ormeño-Orrillo, E., M. Rosenblueth, E. Luyten, J. Vanderleyden & E. Martínez-Romero (2008) Mutations in lipopolysaccharide biosynthetic genes impair maize rhizosphere and root colonization of *Rhizobium tropici* CIAT899. *Environ Microbiol*, 10, 1271-1284.
- Ott, T. (2017) Membrane nanodomains and microdomains in plant–microbe interactions. *Curr Opin Plant Biol*, 40, 82-88.
- Parniske, M. (2018) Uptake of bacteria into living plant cells, the unifying and distinct feature of the nitrogen-fixing root nodule symbiosis. *Curr Opin Plant Biol*, 44, 164-174.
- Parniske, M., B. Ahlborn & D. Werner (1991) Isoflavonoid-inducible resistance to the phytoalexin glyceollin in soybean rhizobia. *J Bacteriol*, 173, 3432-3439.
- Partridge, J. D. & R. M. Harshey (2013) Swarming: flexible roaming plans. *J Bacteriol*, 195, 909-918.
- Patriarca, E. J., R. Tate, S. Ferraioli & M. Iaccarino (2004) Organogenesis of legume root nodules. *Int Rev Cytol*, 234, 201-262.
- Pawlowski, K. & K. N. Demchenko (2012) The diversity of actinorhizal symbiosis. *Protoplasma*, 249, 967-979.
- Peck, M. C., R. F. Fisher & S. R. Long (2006) Diverse flavonoids stimulate NodD1 binding to *nod* gene promoters in *Sinorhizobium meliloti*. *J Bacteriol*, 188, 5417-5427.
- Perret, X., C. Staehelin & W. J. Broughton (2000) Molecular basis of symbiotic promiscuity. *Microbiol Mol Biol Rev*, 64, 180-201.
- Perry, B. J. & C. K. Yost (2014) Construction of a mariner-based transposon vector for use in insertion sequence mutagenesis in selected members of the Rhizobiaceae. *BMC Microbiol*, 14, 298.
- Poinsot, V., E. Bélanger, S. Laberge, G. P. Yang, H. Antoun, J. Cloutier, M. Treilhou, J. Dénarié, J. C. Promé & F. Debellé (2001) Unusual methyl-branched alpha,beta-unsaturated acyl chain substitutions in the Nod Factors of an arctic *rhizobium*, *Mesorhizobium* sp. strain N33 (*Oxytropis arctobia*). *J Bacteriol*, 183, 3721-3728.
- Poole, P., V. Ramachandran & J. Terpolilli (2018) Rhizobia: from saprophytes to endosymbionts. *Nat Rev Microbiol*, 16, 291-303.
- Quesada-Vincens, D., R. Fellay, T. Nasim, V. Viprey, U. Burger, J. C. Prome, W. J. Broughton & S. Jabbouri (1997) *Rhizobium* sp. strain NGR234 NodZ protein is a fucosyltransferase. *J Bacteriol*, 179, 5087-5093.
- Radutoiu, S., L. H. Madsen, E. B. Madsen, H. H. Felle, Y. Umehara, M. Grønland, S. Sato, Y. Nakamura, S. Tabata & N. Sandal (2003) Plant recognition of symbiotic bacteria requires two LysM receptor-like kinases. *Nature*, 425, 585-585.
- Rae, A. L., P. Bonfante - Fasolo & N. J. Brewin (1992) Structure and growth of infection threads in the legume symbiosis with *Rhizobium leguminosarum*. *Plant J*, 2, 385-395.
- Recourt, K., A. A. van Brussel, A. J. Driessen & B. J. Lugtenberg (1989) Accumulation of a *nod* gene inducer, the flavonoid naringenin, in the cytoplasmic membrane of *Rhizobium leguminosarum* biovar *viciae* is caused by the pH-dependent hydrophobicity of naringenin. *J Bacteriol*, 171, 4370-4377.
- Reddy, P., M. Rendón-Anaya, M. D. Río & S. Khandual (2007) Flavonoids as signalling molecules and regulators of root nodule development. *Dynamic Soil, Dynamic Plant*, 1, 83-94.
- Ried, M. K., M. Antolin-Llovera & M. Parniske (2014) Spontaneous symbiotic reprogramming of plant roots triggered by receptor-like kinases. *Elife*, 3, e03891.
- Rinaudi, L. V. & W. Giordano (2010) An integrated view of biofilm formation in rhizobia. *FEMS Microbiol Lett*, 304, 1-11.
- Rinaudi, L. V. & J. E. González (2009) The low-molecular-weight fraction of exopolysaccharide II from *Sinorhizobium meliloti* is a crucial determinant of biofilm formation. *J Bacteriol*, 191, 7216-7224.

- Robertsen, B. K., P. Aman, A. G. Darvill, M. McNeil & P. Albersheim (1981) Host-Symbiont Interactions : V. The structure of acidic extracellular polysaccharides secreted by *Rhizobium leguminosarum* and *Rhizobium trifolii* *Plant Physiol*, 67, 389-400.
- Robledo, M., L. Rivera, J. I. Jiménez-Zurdo, R. Rivas, F. Dazzo, E. Velázquez, E. Martínez-Molina, A. M. Hirsch & P. F. Mateos (2012) Role of *rhizobium* endoglucanase CelC2 in cellulose biosynthesis and biofilm formation on plant roots and abiotic surfaces. *Microb Cell Fact*, 11, 12.
- Rodpohong, P., J. T. Sullivan, K. Songsrirote, D. Sumpton, K. W. J. T. Cheung, J. Thomas-Oates, S. Radutoiu, J. Stougaard & C. W. Ronson (2009) Nodulation gene mutants of *Mesorhizobium loti* R7A-*nodZ* and *nolL* mutants have host-specific phenotypes on *Lotus* spp. *Mol Plant Microbe Interact*, 22, 1546-1554.
- Roux, B., N. Rodde, M. F. Jardinaud, T. Timmers, L. Sauviac, L. Cottret, S. Carrere, E. Sallet, E. Courcelle, S. Moreau, F. Debelle, D. Capela, F. de Carvalho-Niebel, J. Gouzy, C. Bruand & P. Gamas (2014) An integrated analysis of plant and bacterial gene expression in symbiotic root nodules using laser-capture microdissection coupled to RNA sequencing. *Plant J*, 77, 817-837.
- Roux, B., N. Rodde, S. Moreau, M. F. Jardinaud & P. Gamas (2018) Laser capture microdissection coupled to RNA sequencing: a powerful approach applied to the model legume *Medicago truncatula* in interaction with *Sinorhizobium meliloti*. *Methods Mol Biol*, 1830, 191-224.
- Roy, S., W. Liu, R. S. Nandety, A. Crook, K. S. Mysore, C. I. Pislariu, J. Frugoli, R. Dickstein & M. K. Udvardi (2020) Celebrating 20 years of genetic discoveries in legume nodulation and symbiotic nitrogen fixation. *Plant Cell*, 32, 15-41.
- Russo, D. M., A. Williams, A. Edwards, D. M. Posadas, C. Finnie, M. Dankert, J. A. Downie & A. Zorreguieta (2006) Proteins exported via the PrsD-PrsE type I secretion system and the acidic exopolysaccharide are involved in biofilm formation by *Rhizobium leguminosarum*. *J Bacteriol*, 188, 4474-4486.
- Saito, K., M. Yoshikawa, K. Yano, H. Miwa, H. Uchida, E. Asamizu, S. Sato, S. Tabata, H. Imaizumi-Anraku & Y. Umehara (2007) NUCLEOPORIN85 is required for calcium spiking, fungal and bacterial symbioses, and seed production in *Lotus japonicus*. *Plant Cell*, 19, 610-624.
- Salinero-Lanzarote, A., A. Pacheco-Moreno, L. Domingo-Serrano, D. Durán, E. Ormeño-Orrillo, E. Martínez-Romero, M. Albareda, J. M. Palacios & L. Rey (2019) The Type VI secretion system of *Rhizobium etli* Mim1 has a positive effect in symbiosis. *FEMS Microbiol Ecol*, 95.
- Sánchez-Andújar, B., C. Coronado, S. Philip-Hollingsworth, F. B. Dazzo & A. J. Palomares (1997) Structure and role in symbiosis of the *exoB* gene of *Rhizobium leguminosarum* bv *trifolii*. *Mol Gen Genet*, 255, 131-140.
- Sant'Anna, F. H., D. S. Andrade, D. B. Trentini, S. S. Weber & I. S. Schrank (2011) Tools for genetic manipulation of the plant growth-promoting bacterium *Azospirillum amazonense*. *BMC Microbiol*, 11, 107.
- Schäfer, A., A. Tauch, W. Jäger, J. Kalinowski, G. Thierbach & A. Pühler (1994) Small mobilizable multi-purpose cloning vectors derived from the *Escherichia coli* plasmids pK18 and pK19: selection of defined deletions in the chromosome of *Corynebacterium glutamicum*. *Gene*, 145, 69-73.
- Schiessl, K., J. L. S. Lilley, T. Lee, I. Tamvakis, W. Kohlen, P. C. Bailey, A. Thomas, J. Luptak, K. Ramakrishnan, M. D. Carpenter, K. S. Mysore, J. Wen, S. Ahnert, V. A. Grieneisen & G. E. D. Oldroyd (2019) NODULE INCEPTION recruits the lateral root developmental program for symbiotic nodule organogenesis in *Medicago truncatula*. *Curr Biol*, 29, 3657-3668.

- Sharma, S. B. & E. R. Signer (1990) Temporal and spatial regulation of the symbiotic genes of *Rhizobium meliloti* in planta revealed by transposon Tn5-gusA. *Genes Dev*, 4, 344-356.
- Shaw, S. L. & S. R. Long (2003) Nod factor elicits two separable calcium responses in root hair cells. *Plant physiol*, 131, 976-984.
- Shen, D., T. T. Xiao, R. v. Velzen, O. Kulikova, X. Gong, R. Geurts, K. Pawlowski & T. Bisseling (2020) A homeotic mutation changes legume nodule ontogeny into actinorhizal-type ontogeny. *Plant Cell*, 32, 1868-1885.
- Singh, S., K. Katzer, J. Lambert, M. Cerri & M. Parniske (2014) CYCLOPS, a DNA-binding transcriptional activator, orchestrates symbiotic root nodule development. *Cell host & microbe*, 15, 139-152.
- Skorupska, A., M. Janczarek, M. Marczak, A. Mazur & J. Król (2006) Rhizobial exopolysaccharides: genetic control and symbiotic functions. *Microbial cell factories*, 5.
- Smit, G., J. W. Kijne & B. J. Lugtenberg (1987) Involvement of both cellulose fibrils and a Ca<sup>2+</sup>-dependent adhesin in the attachment of *Rhizobium leguminosarum* to pea root hair tips. *J Bacteriol*, 169, 4294-4301.
- Smit, G., D. M. J. Tubbing, J. W. Kijne & B. J. J. Lugtenberg (1991) Role of Ca<sup>2+</sup> in the activity of rhicadhesin from *Rhizobium leguminosarum* biovar *viciae*, which mediates the first step in attachment of *Rhizobiaceae* cells to plant root hair tips. *Arch Microbiol*, 155, 5.
- Soyano, T., H. Kouchi, A. Hirota & M. Hayashi (2013) Nodule inception directly targets NF-Y subunit genes to regulate essential processes of root nodule development in *Lotus japonicus*. *PLoS Genetics*, 9.
- Soyano, T., Y. Shimoda, M. Kawaguchi & M. Hayashi (2019) A shared gene drives lateral root development and root nodule symbiosis pathways in *Lotus*. *Science*, 366, 1021-1023.
- Spaink, H. P., A. Aarts, G. Stacey, G. V. Bloemberg, B. J. J. Lugtenberg & E. P. Kennedy (1992) Detection and separation of *Rhizobium* and *Bradyrhizobium* Nod metabolites using thin-layer chromatography. *Mol Plant Microbe Interact*, 5, 72-80.
- Spaink, H. P., D. M. Sheeley, A. A. van Brussel, J. Glushka, W. S. York, T. Tak, O. Geiger, E. P. Kennedy, V. N. Reinhold & B. J. Lugtenberg (1991) A novel highly unsaturated fatty acid moiety of lipo-oligosaccharide signals determines host specificity of *Rhizobium*. *Nature*, 354, 125-130.
- Sprent, J. I. (2007) Evolving ideas of legume evolution and diversity: a taxonomic perspective on the occurrence of nodulation. *New Phytol*, 174, 11-25.
- Sprent, J. I., J. Ardley & E. K. James (2017) Biogeography of nodulated legumes and their nitrogen-fixing symbionts. *New Phytol*, 215, 40-56.
- Stacey, G., S. Luka, J. Sanjuan, Z. Banfalvi, A. J. Nieuwkoop, J. Y. Chun, L. S. Forsberg & R. Carlson (1994) *nodZ*, a unique host-specific nodulation gene, is involved in the fucosylation of the lipooligosaccharide nodulation signal of *Bradyrhizobium japonicum*. *J Bacteriol*, 176, 620-633.
- Stracke, S., C. Kistner, S. Yoshida, L. Mulder, S. Sato, T. Kaneko, S. Tabata, N. Sandal, J. Stougaard & K. Szczyglowski (2002) A plant receptor-like kinase required for both bacterial and fungal symbiosis. *Nature*, 417, 959-962.
- Subbarao, N. S., P. F. Mateos, D. Baker, H. S. Pankratz, J. Palma, F. B. Dazzo & J. I. Sprent (1995) The unique root-nodule symbiosis between *Rhizobium* and the aquatic legume, *Neptunia Natans* (L-F) Druce. *Planta*, 196, 311-320.
- Sugawara, M., S. Takahashi, Y. Umehara, H. Iwano, H. Tsurumaru, H. Odake, Y. Suzuki, H. Kondo, Y. Konno, T. Yamakawa, S. Sato, H. Mitsui & K. Minamisawa (2018) Variation in bradyrhizobial NopP effector determines symbiotic incompatibility with *Rj2*-soybeans via effector-triggered immunity. *Nat Commun*, 9, 3139.
- Sullivan, J. T., J. R. Trzebiatowski, R. W. Cruickshank, J. Gouzy, S. D. Brown, R. M. Elliot, D. J. Fleetwood, N. G. McCallum, U. Rossbach, G. S. Stuart, J. E. Weaver, R. J. Webby,



- F. J. De Bruijn & C. W. Ronson (2002) Comparative sequence analysis of the symbiosis island of *Mesorhizobium loti* strain R7A. *J Bacteriol*, 184, 3086-3095.
- Tambalo, D. D., C. K. Yost & M. F. Hynes (2010) Characterization of swarming motility in *Rhizobium leguminosarum* bv. *viciae*. *FEMS Microbiol Lett*, 307, 165-174.
- Teulet, A., N. Busset, J. Fardoux, D. Gully, C. Chaintreuil, F. Cartieaux, A. Jauneau, V. Comorge, S. Okazaki, T. Kaneko, F. Gressent, N. Nouwen, J. F. Arrighi, R. Koebnik, P. Mergaert, L. Deslandes & E. Giraud (2019) The rhizobial type III effector ErnA confers the ability to form nodules in legumes. *Proc Natl Acad Sci U S A*, 116, 21758-21768.
- Thoma, S. & M. Schobert (2009) An improved *Escherichia coli* donor strain for diparental mating. *FEMS Microbiol Lett*, 294, 127-132.
- Tielen, P., M. Strathmann, K.-E. Jaeger, H.-C. Flemming & J. Wingender (2005) Alginate acetylation influences initial surface colonization by mucoid *Pseudomonas aeruginosa*. *Microbio Res*, 160, 165-176.
- Timmers, A. C., M. C. Auriac, F. de Billy & G. Truchet (1998) Nod factor internalization and microtubular cytoskeleton changes occur concomitantly during nodule differentiation in alfalfa. *Development*, 125, 339-349.
- Tirichine, L., H. Imaizumi-Anraku, S. Yoshida, Y. Murakami, L. H. Madsen, H. Miwa, T. Nakagawa, N. Sandal, A. S. Albrektsen, M. Kawaguchi, A. Downie, S. Sato, S. Tabata, H. Kouchi, M. Parniske, S. Kawasaki & J. Stougaard (2006a) Deregulation of a Ca<sup>2+</sup>/calmodulin-dependent kinase leads to spontaneous nodule development. *Nature*, 441, 1153-1156.
- Tirichine, L., E. K. James, N. Sandal & J. Stougaard (2006b) Spontaneous root-nodule formation in the model legume *Lotus japonicus*: a novel class of mutants nodulates in the absence of rhizobia. *Mol Plant Microbe Interact*, 19, 373-382.
- Tirichine, L., N. Sandal, L. H. Madsen, S. Radutoiu, A. S. Albrektsen, S. Sato, E. Asamizu, S. Tabata & J. Stougaard (2007) A gain-of-function mutation in a cytokinin receptor triggers spontaneous root nodule organogenesis. *Science*, 315, 104-107.
- Truchet, G., P. Roche, P. Lerouge, J. Vasse, S. Camut, F. de Billy, J.-C. Promé & J. Dénarié (1991) Sulphated lipo-oligosaccharide signals of *Rhizobium meliloti* elicit root nodule organogenesis in alfalfa. *Nature*, 351, 670-673.
- Uheda, E., H. Daimon & F. Yoshizako (2001) Colonization and invasion of peanut (*Arachis hypogaea* L.) roots by *gusA*-marked *Bradyrhizobium* sp. *Can J Microbiol*, 79, 733-738.
- Ulanowska, K., A. Tkaczyk, G. Konopa & G. Wegrzyn (2006) Differential antibacterial activity of genistein arising from global inhibition of DNA, RNA and protein synthesis in some bacterial strains. *Arch Microbiol*, 184, 271-278.
- van Brussel, A. A. N., R. Bakhuizen, P. C. van Spronsen, H. P. Spaink, T. Tak, B. J. J. Lugtenberg & J. W. Kijne (1992) Induction of pre-infection thread structures in the leguminous host plant by mitogenic lipo-Oligosaccharides of *Rhizobium*. *Science*, 257, 70-72.
- van der Drift, K. M., H. P. Spaink, G. V. Bloemberg, A. A. van Brussel, B. J. Lugtenberg, J. Haverkamp & J. E. Thomas-Oates (1996) *Rhizobium leguminosarum* bv. *trifolii* produces lipo-chitin oligosaccharides with *nodE*-dependent highly unsaturated fatty acyl moieties. An electrospray ionization and collision-induced dissociation tandem mass spectrometric study. *J Biol Chem*, 271, 22563-22569.
- van Spronsen, P. C., R. Bakhuizen, A. A. van Brussel & J. W. Kijne (1994) Cell wall degradation during infection thread formation by the root nodule bacterium *Rhizobium leguminosarum* is a two-step process. *Eur J Cell Biol*, 64, 88-94.
- van Spronsen, P. C., M. Gronlund, C. P. Bras, H. P. Spaink & J. W. Kijne (2001) Cell biological changes of outer cortical root cells in early determinate nodulation. *Mol Plant Microbe Interact*, 14, 839-847.

- van Zeijl, A., R. H. Op den Camp, E. E. Deinum, T. Charnikhova, H. Franssen, H. J. Op den Camp, H. Bouwmeester, W. Kohlen, T. Bisseling & R. Geurts (2015) *Rhizobium* lipochitooligosaccharide signaling triggers accumulation of cytokinins in *Medicago truncatula* Roots. *Mol Plant*, 8, 1213-1226.
- Vanderlinde, E. M., A. Muszynski, J. J. Harrison, S. F. Koval, D. L. Foreman, H. Ceri, E. L. Kannenberg, R. W. Carlson & C. K. Yost (2009) *Rhizobium leguminosarum* biovar *viciae* 3841, deficient in 27-hydroxyoctacosanoate-modified lipopolysaccharide, is impaired in desiccation tolerance, biofilm formation and motility. *Microbiology*, 155, 3055-3069.
- Vázquez, M., O. Santana & C. Quinto (1993) The NodI and NodJ proteins from *Rhizobium* and *Bradyrhizobium* strains are similar to capsular polysaccharide secretion proteins from Gram-negative bacteria. *Mol Microbiol*, 8, 369-377.
- Vega-Hernández, M. C., R. Pérez-Galdona, F. B. Dazzo, A. Jarabo-Lorenzo, M. C. Alfayate & M. León-Barrios (2000) Novel infection process in the indeterminate root nodule symbiosis between *Chamaecytisus proliferus* (tagasaste) and *Bradyrhizobium* sp. *New Phytol*, 707-721.
- Venado, R., J. Liang & M. Marín. 2020. Chapter Four - Rhizobia infection, a journey to the inside of plant cells. In *Adv Bot Res*, eds. P. Frendo, F. Frugier & C. Masson-Boivin. Academic Press.
- Verstraeten, N., K. Braeken, B. Debkumari, M. Fauvart, J. Fransaer, J. Vermant & J. Michiels (2008) Living on a surface: swarming and biofilm formation. *Trends Microbiol*, 16, 496-506.
- Vicario, J. C., M. S. Dardanelli & W. Giordano (2015) Swimming and swarming motility properties of peanut-nodulating rhizobia. *FEMS Microbiol Lett*, 362, 1-6.
- Vozza, N. F., P. L. Abdian, D. M. Russo, E. J. Mongiardini, A. R. Lodeiro, S. Molin & A. Zorreguieta (2016) A *Rhizobium leguminosarum* CHDL- (Cadherin-Like-) lectin participates in assembly and remodeling of the biofilm matrix. *Front Microbiol*, 7, 1608.
- Walker, T. S., H. P. Bais, E. Grotewold & J. M. Vivanco (2003) Root exudation and rhizosphere biology. *Plant Physiol*, 132, 44.
- Walley, F. L., G. O. Tomm, A. Matus, A. E. Slinkard & C. van Kessel (1996) Allocation and cycling of nitrogen in an alfalfa-bromegrass sward. *Agron J*, 88, 834-843.
- Wang, D., F. Couderc, C. F. Tian, W. Gu, L. X. Liu & V. Poinso (2018) Conserved Composition of nod factors and exopolysaccharides produced by different phylogenetic lineage *Sinorhizobium* strains nodulating soybean. *Front Microbiol*, 9, 2852-2852.
- Webb, K. J., L. Skot, M. N. Nicholson, B. Jorgensen & S. Mizen (2000) *Mesorhizobium loti* increases root-specific expression of a calcium-binding protein homologue identified by promoter tagging in *Lotus japonicus*. *Mol Plant Microbe Interact*, 13, 606-616.
- Wenzel, M., L. Friedrich, M. Gottfert & S. Zehner (2010) The type III-secreted protein NopE1 affects symbiosis and exhibits a calcium-dependent autocleavage activity. *Mol Plant Microbe Interact*, 23, 124-129.
- Westhoek, A., E. Field, F. Rehling, G. Mulley, I. Webb, P. S. Poole & L. A. Turnbull (2017) Policing the legume-Rhizobium symbiosis: a critical test of partner choice. *Sci Rep*, 7, 1419.
- Wheatley, R. M. & P. S. Poole (2018) Mechanisms of bacterial attachment to roots. *FEMS Microbiol Rev*, 42, 448-461.
- Williams, A., A. Wilkinson, M. Krehenbrink, D. M. Russo, A. Zorreguieta & J. A. Downie (2008) Glucomannan-mediated attachment of *Rhizobium leguminosarum* to pea root hairs is required for competitive nodule infection. *J Bacteriol*, 190, 4706-4715.
- Xiao, T. T., S. Schilderink, S. Moling, E. E. Deinum, E. Kondorosi, H. Franssen, O. Kulikova, A. Niebel & T. Bisseling (2014) Fate map of *Medicago truncatula* root nodules. *Development*, 141, 3517-3528.

- Xie, F., J. D. Murray, J. Kim, A. B. Heckmann, A. Edwards, G. E. D. Oldroyd & A. Downie (2012) Legume pectate lyase required for root infection by rhizobia. *Proc Natl Acad Sci U S A*, 109, 633-638.
- Xin, D.-W., S. Liao, Z.-P. Xie, D. R. Hann, L. Steinle, T. Boller & C. Staehelin (2012) Functional analysis of NopM, a novel E3 ubiquitin ligase (NEL) domain effector of *Rhizobium* sp. strain NGR234. *PLoS pathogens*, 8, e1002707-e1002707.
- Yang, G. P., F. Debelle, A. Savagnac, M. Ferro, O. Schiltz, F. Maillet, D. Prome, M. Treilhou, C. Vialas, K. Lindstrom, J. Denarie & J. C. Prome (1999) Structure of the *Mesorhizobium huakuii* and *Rhizobium galegae* Nod factors: a cluster of phylogenetically related legumes are nodulated by rhizobia producing Nod factors with alpha,beta-unsaturated N-acyl substitutions. *Mol Microbiol*, 34, 227-337.
- Yang, S., F. Tang, M. Gao, H. B. Krishnan & H. Zhu (2010) R gene-controlled host specificity in the legume–rhizobia symbiosis. *Proc Natl Acad Sci U S A*, 107, 18735-18740
- Yano, K., S. Yoshida, J. Muller, S. Singh, M. Banba, K. Vickers, K. Markmann, C. White, B. Schuller, S. Sato, E. Asamizu, S. Tabata, Y. Murooka, J. Perry, T. L. Wang, M. Kawaguchi, H. Imaizumi-Anraku, M. Hayashi & M. Parniske (2008) CYCLOPS, a mediator of symbiotic intracellular accommodation. *Proc Natl Acad Sci U S A*, 105, 20540-20545.
- Yokota, K., E. Fukai, L. H. Madsen, A. Jurkiewicz, P. Rueda, S. Radutoiu, M. Held, M. S. Hossain, K. Szczyglowski & G. Morieri (2009) Rearrangement of actin cytoskeleton mediates invasion of *Lotus japonicus* roots by *Mesorhizobium loti*. *Plant Cell*, 21, 267-284.
- York, L. M., A. Carminati, S. J. Mooney, K. Ritz & M. J. Bennett (2016) The holistic rhizosphere: integrating zones, processes, and semantics in the soil influenced by roots. *J Exp Bot*, 67, 3629-3643.
- Young, J. P., L. C. Crossman, A. W. Johnston, N. R. Thomson, Z. F. Ghazoui, K. H. Hull, M. Wexler, A. R. Curson, J. D. Todd, P. S. Poole, T. H. Mauchline, A. K. East, M. A. Quail, C. Churcher, C. Arrowsmith, I. Cherevach, T. Chillingworth, K. Clarke, A. Cronin, P. Davis, A. Fraser, Z. Hance, H. Hauser, K. Jagels, S. Moule, K. Mungall, H. Norbertczak, E. Rabinowitsch, M. Sanders, M. Simmonds, S. Whitehead & J. Parkhill (2006) The genome of *Rhizobium leguminosarum* has recognizable core and accessory components. *Genome Biol*, 7, R34.
- Zheng, H., Y. Mao, J. Teng, Q. Zhu, J. Ling & Z. Zhong (2015) Flagellar-dependent motility in *Mesorhizobium tianshanense* is involved in the early stage of plant host interaction: study of an *flgE* mutant. *Curr Microbiol*, 70, 219-227.

# List of figures

Figure 1: Overview of the different steps in the root nodule symbiosis.....	8
Figure 2: Chemical structures of the repeating units of rhizobia exopolysaccharides. .....	15
Figure 3: Nodule phenotypes of <i>Lotus</i> upon <i>R/</i> Norway inoculation at 6 wpi. ....	76
Figure 4: Plant growth phenotypes upon rhizobia inoculation.....	78
Figure 5: Co-inoculation with <i>R/</i> Norway and <i>Mn</i> 10.2.2 induced no growth defects on the host.....	79
Figure 6: <i>L. japonicus</i> Gifu colonisation by rhizobia. ....	81
Figure 7: <i>R/</i> Norway GFP colonises mixed nodules inter- and intra- cellularly.....	82
Figure 8: Co-inoculation with <i>Mn</i> 10.2.2 and <i>R/</i> Norway increases root colonisation. .....	84
Figure 9: Scanning electron microscopy (SEM) micrographs of root colonisation of rhizobia.....	85
Figure 10: Distal root colonisation is promoted by co-inoculation. ....	87
Figure 11: <i>R/</i> Norway GFP promotes the swarming motility of <i>Mn</i> 10.2.2 <i>DsRed</i> . .	89
Figure 12: <i>Mn</i> 10.2.2 can form mixed biofilms with <i>R/</i> Norway <i>in vitro</i> . ....	92
Figure 13: <i>Mn</i> 10.2.2 can form mixed biofilms with <i>R/</i> Norway and <i>R/</i> Norway $\Delta$ <i>exo5</i> on glass slides. ....	93

# Acknowledgements

First, greatest thanks go to my supervisor Dr. Macarena Marín. Thanks for guiding me through my master thesis and my doctoral studies. I am always grateful that she accepted me as her student even when I was not experienced at all. She taught me almost from zero in the lab and gave me the scientific training. She always has time for me to answer my questions and for the insightful discussion.

I would also like to thank our collaborators Anne Hoffrichter and Dr. Andreas Brachmann for the genome project, Prof. Dr. Andreas Klingl with electron microscopy pictures and Prof. Jane Thomas-Oates for the Nod factors structure analysis. Thanks to Rafael Venado for writing the book chapter together. It was not possible to make it work without them.

I also thank all my thesis advisory committees: Prof. Wolfgang Enard, Prof. Thomas Ott, and Prof. Heinrich Jung for the insightful discussions and all the suggestions during my TAC meetings.

I would like to thank Prof. Heinrich Jung, Prof. Andreas Klingl, Prof. Wolfgang Enard, Prof. Silke Werth and Prof. Nicolas Gompel for their time and effort to evaluate this work.

Many thanks go to “3rd Floor genetics” for the good atmosphere. Many thanks to Philipp Bellon and Chloé Cathebras for maintaining the microscopes. They have solved my problems whenever I needed their help. Thanks to Chloé Cathebras for bouldering together. We had so much fun in the boulderwelt. Thanks to Dr. Marion Cerri for teaching me how to do nodule sections and answer my countless questions. Thanks to Florian Dunker for organising the “movie night” and “werewolf night”.

Many thanks for my office mate Rosa Elena Andrade Aguirre and Isabel Seidler.

Many thanks to Dr. Sara Masachis for working together on the “mixed nodule” project in the last months of my doctoral study. It was very insightful to discuss with her about science. Also thank her for the Yoga course during my thesis writing, which gave me a lot of power.

Thanks for Dr. Sara Masachis and Florian Dunker for critical reading my thesis and giving all the useful comments, Duncan Crosbie for correcting my English mistakes.

Special thanks to all the members in AG Marín. I would be the lonely only PhD student in the lab without you. Thanks for all the moment that we spent together in the prep lab.

Special thanks to my asian lunch group: Xiaoyun Gong, Fang-Yu Hwu and Yen-Yu Lin, who have companied with me for almost everyday lunch and discussed difficult experiments.

Xiaoyun always shared me her delicious lunch when I am starving. They also gave great suggestions for my experiments.

In the end, I greatly thank my family, especially Kai, without their support and love I would not have come this far.

# Curriculum vitae

Juan Liang

## Personal Data

---

Date of Birth	Nov.13.1989
Place of Birth	Shangqiu China

## Higher Education

---

2016.06 - 2020.11	Doctoral studies (Ludwig-Maximilians-Universität München, Graduate School Life Science Munich; Dr. Macarena Marín)
2013.10 - 2016.03	Master thesis (Ludwig-Maximilians-Universität München, Genetics; Dr. Macarena Marín) Master study (Ludwig-Maximilians-Universität München)
2009.09 - 2013.07	Bachelor thesis (Henan Normal University, Xinxiang, China) Bachelor study (Henan Normal University, Xinxiang, China)

## Further Education

---

Soft skills	Optimising writing strategies
Methods courses	Statistical Literacy, Bioinformatics, Adobe illustrator

## International Conferences

---

2019.10	21th International Congress on Nitrogen Fixation (Wuhan, China; poster presentation)
2016.08	12th European Nitrogen Fixation Conference (Budapest, Hungary)